ASSESSING POTENTIAL DIFFERENCES OF DIESEL FUEL EFFECTS ON COMBUSTION AND ENGINE BEHAVIOR BETWEEN DIFFERENTLY-SIZED ENGINES

A Dissertation

by

JUE LI

Submitted to the Office of Graduate and Professional Studies of
Texas A&M University
in partial fulfillment of the requirements for the degree of

DOCTOR OF PHILOSOPHY

Chair of Committee,	Timothy Jacobs
Committee Members,	Jerald Caton
	Kalyan Annamalai
	Mark Holtzapple
Head of Department,	Andreas A. Polycarpou

December 2017

Major Subject: Mechanical Engineering

ABSTRACT

Fuel properties impact the combustion and emissions behavior of diesel engines through their influence on the physical process associated with fuel injection, entrainment and fuel-air mixing, as well as by changes to the combustion chemistry associated with fuel properties. In addition, these influences are also impacted strongly by various engine sizes. Thus, to find fuel effects on engine behavior between two engines, the research is conducted through a series of experimental tests at 1500 rev/min and two loads for commercial diesel and Fuels for Advanced Combustion Engines fuels between two engines.

First, baseline testing and simulation was aimed at using experiment and a simulation model of two differently sized engines to identify the effects of engine size on combustion characteristics and emissions. The results are compared for the same brake mean effective pressure and show that engine size has a significant impact on indicated efficiency, with the larger displaced engine having a higher indicated efficiency than the smaller displaced engine.

Second, the effects of cetane number (CN) on combustion and emissions between differently sized engines were investigated using a fuel matrix with each variable having a base value as well as a lower and higher level. The results show that CN significantly affects combustion phasing and emissions of the two engines in similar ways. As CN increases, the magnitude of heat release rate (HRR) increases and its peak location advances as CN increases.

Moreover, the effects of distillation temperature (T90) on engine efficiency and emissions are performed. The results show comparing with medium-duty (MD) engine performance, increasing T90 shows relative stronger effects on HRR for light-duty (LD) engine, especially for the low-load condition.

Finally, the effects of aromatic content on engine efficiency and emissions are discussed. The results show increasing aromatic content increases the magnitude of the peak HRR, and delays its location for both engines at the low-load condition. At the medium-load condition, increasing aromatic content has similar effect on LD engine, but does not show obvious effect on MD engines.

ACKNOWLEDGEMENTS

First and foremost, I would like to express my deep appreciation to my advisor, Dr.Timothy Jacobs, for his long-time patience and enthusiastic support and guidance during the entire period of my schooling in TAMU. He has motivated me a lot during my research presented here. I am honored that he is able to serve as my chair of advisory committee.

My committee members – Dr. Jerald Caton, Dr. Kalyan Annamalai, and Dr. Mark Holtzapple – are thanked for their involvement in the successful completion and scientific validity of this dissertation. Each committee member has provided helpful comments and suggestions which I greatly appreciate.

I want to express my gratitude to my lab mates for their camaraderie, friendship, and help: Dr. Jiafeng Sun, Dr. Josh Bittle, Dr. Tingting Li, Dr. Alireza Mashayekh, Jacob Hedrick, Abdullah Bajwa, Timothy Kroeger, Ben McKeathen, Kelsey Fieseler and Cole Frazier.

I would like to thank Shell Global Solutions, Inc. for their generous support of this research project. Especially I want to thank Dr. Michael.Parkes and Dr. Tushar.Bera for their helpful comments and suggestions.

Finally, I wish to thank my parents and my wife for their love and support. They have always encouraged and supported me along the way. They always influenced me a lot in my life. I am grateful to them for what they did for me. I promise I will always be with them no matter what we are facing in the future.

CONTRIBUTORS AND FUNDING SOURCES

Contributors

This work was supervised by a dissertation committee consisting of Professor Timothy Jacobs, Jerald Caton, and Kalyan Annamalai of the Department of Mechanical Engineering and Professor Mark Holtzapple of the Department of Chemical Engineering.

All work conducted for the thesis (or) dissertation was completed by the student independently.

Funding Sources

The project is funded and supported by Shell Global Solutions, Inc.

NOMENCLATURE

S/B	Stroke-to-bore
IVC	Intake valve close
EVO	Exhaust valve open
BMEP	Brake mean effective pressure
BSFC	Brake specific fuel consumption
IMEP	(Net) Indicated mean effective pressure
BS	Brake Specific
TDC	Top dead center
BTDC	Before top dead center
ATDC	After top dead center
CA50	Mass burnt 50 percent timing
DC	Direct current
EGR	Exhaust gas recirculation
Exp	Experiment data
LD	Light duty
MD	Medium duty
SAE	Society of Automobile Engineers
ASME	American Society for Testing and Materials
Sim	Simulation data
°CA	Degree crank angle

CO	Carbon Monoxide
HC	Hydrocarbon
NO	Nitrous Oxide
FID	Flame ionization detection
DI-Pulse model	Direct-injection diesel multi-pulse combustion model
CN	Cetane number
T90	90% Distillation temperature
AC	Aromatic content

TABLE OF CONTENTS

Page

LIST OF FIGURES

Page

LIST OF TABLES

Page

1. INTRODUCTION

1.1 Background

In the commercial transportation sector, the increasingly stringent regulations for tailpipe pollutants and greenhouse gas emissions have motivated the development of high efficiency, clean diesel engines. Conventional diesel combustion is intrinsically dominated by mixing-controlled combustion, thereby posing challenges to control NOx and soot emissions.

To meet the US EPA 2010 heavy-duty NOx and particulate matter (PM) standards, engine OEMs have chosen to implement urea-based selective catalytic reduction (SCR) and diesel particulate filter (DPF) devices. This not only makes the engine system more expensive, but also increases vehicle total fluid consumption (i.e., additional fluid consumption from urea and hydrocarbon dosing in the exhaust). Moreover, the continuous demand for lower tailpipe emissions puts increasing stress on the after-treatment system and requires further reduction in engine-out NOx emissions. Consequently, this drives the need to develop combustion systems that control soot while maintaining high fuel efficiency.

In general, engine size strongly impacts engine combustion and emissions behavior. Different combustion characteristics such as peak temperature, peak pressure, combustion duration, and heat release rate can change as engine size changes, in spite of similar control and operating parameters. Consequently, engine performance and emissions will also change as engine size changes (at similar control parameters).

Moreover, fuel physical and chemical properties play an important role in diesel combustion. Some studies have suggested that fuels with medium octane number (ON) and gasoline-like distillation range [1] or a blend of gasoline and diesel fuel enhances diesel combustion [2]. However, there are still questions about what is the optimal fuel for diesel combustion among different-sized engines. Therefore, detailed studies on how different fuel properties affect diesel combustion and emissions among different-sized engines are of great interest to the engine community.

The distillation characteristics of a fuel affect fuel-air mixture formation, as well as the ignition and combustion processes inside an engine. A real fuel consists of many components and thus exhibits a wide boiling range, with lighter fractions boiling at lower temperatures and heavier components boiling at higher temperatures. The temperature at which 90% of the fuel volume is vaporized (T90) is specified for commercial diesel fuels in North America. Fuels with a higher T90 temperature are less volatile. Diesel fuel contains a large selection of hydrocarbons ranging from 10 to 22 carbon atoms per molecule. There are three major classes of molecules in diesel fuels: alkanes, cycloalkanes, and aromatics. Aromatics are known to increase oxides of nitrogen (NOx) emissions in conventional diesel combustion as they produce higher combustion temperatures. Because aromatics generally have a low CN, they may also affect the cold start performance of an engine.

Cetane number (CN) is a measure of the auto-ignition quality of diesel fuels used for conventional compression ignition engines. Higher CN fuels have shorter ignition delays. Because CN is derived from the ignition delay in conventional diesel

combustion, it contains information related to both physical delays (atomization, vaporization, mixing) and chemical delays (reactivity). Hence, it also has a strong influence on diesel combustion phasing [3-5]. For example, Risberg et al. [4] found a strong correlation between CN and CA50 (the crank angle cycle where 50% of the total heat is released) for experimental and commercial diesel fuels.

1.2 Objectives

The project goals are identifying potential of fuel effects on combustion and engine behavior between light- and medium-duty diesel engines. The fundamental research question being addressed in this work is as follows: Do the design criteria for optimal fuel properties, as determined by desired combustion and engine behavior, change as size (bore diameter and stroke length) of a compression ignition (i.e., diesel) engine changes? Although combustion is fundamentally the same among different compression ignition platforms, certain phenomena (e.g., fuel injection, penetration, breakup, atomization, and vaporization) are strongly influenced by the engine bore diameter and stroke. These same phenomena are fundamentally dependent on fuel properties (e.g., viscosity, density, surface tension) and the subsequent combustion correspondingly is strongly dependent on fuel properties (e.g., cetane number). Thus, an optimal fuel for combustion and engine behavior of a light-duty (small displacement) engine may not necessarily be the optimal fuel for combustion and engine behavior of a medium-duty (larger displacement) engine. In this context, “engine behavior” is meant to include the engine’s performance (power), efficiency, and emissions, which of course

all strongly depend on combustion (characterized by ignition delay, combustion duration, and locations of combustion such as 50% mass fraction burned location). Therefore, the final objectives of the project are to clarify the following items:

1) With increasing engine size, explain the changing trend (if any) of a higher CN on engine combustion (heat transfer, combustion duration) and emissions (smoke, NOx),

2) With increasing engine size, explain the effect of aromatic content (AC) on engine combustion and emissions,

3) With changing operating conditions, explain the effect that AC has on emissions for differently sized engines,

4) With changing engine size, explain the effect that distillation temperature (T90) has on combustion and emissions.

5) With changing operating parameters (i.e., load condition and injection timing) explain the impact of the studied fuel properties (CN, AC, T90) on combustion and emissions

To clarify the five items, the whole project has four steps. First, the baseline testing is performed on both of engines. In the baseline testing, two nearly identical engines – differently only by displaced volume and stroke to bore (S/B) ratio – are tested at 1500 RPM and nominally 1.88 bar BMEP(low load)/5.65 BMEP (medium load) with injection timing changing from 3° BTDC to 15° BTDC. Through analysis of baseline testing results, effects of engine size on combustion and emissions are explained. Moreover, an idea of the two engines' characteristics, which is helpful for FACE fuel

testing points design and results analysis, will be clarified. The second step is engine simulation development. In this step, the two engines' models are established by using GT-Power and simulated at the same operation points of baseline testing. Deeper analysis on effect of engine size on combustion and emissions can be performed through simulation work and both of models are helpful for FACE fuel simulation step. The third step is FACE fuel testing on both of engines. Eight FACE fuels are designed around three properties of primary importance: cetane number (measure of ignition quality), aromatic content (affects fuel constituent composition), and distillation (measure of volatility). All of fuels are tested with a single shot injection strategy, the timing of which was switched from 15 BTDC to 6 BTDC and controlled to maintain a constant combustion phasing (CA 50 –10deg ATDC) at both of loads (low load/medium load) either. Then, the first five gaps about effects of fuel properties on combustion and emissions between different sized engines will be clarified through the first three steps. In the final step, FACE fuel simulation will be performed, including changing operating conditions and NOx sweep simulation. The first simulation work (changing operation conditions) is helpful for deeper research on the first five gaps and the NOx sweep simulation will clarify the final gap from literature review.

2. LITERATURE REVIEW

Fuel properties impact the combustion and emissions behavior of diesel engines through their influence on the physical process associated with fuel injection, jet penetration, entrainment and fuel-air mixing, as well as by changes to the combustion chemistry associated with fuel chemistry, aromatics, molecular weight, and additive concentrations. Continued focus on ultra-low NOx engine-out targets and variation of the available fuel on the worldwide market drives the need for a deeper understanding of the changes to the engine behavior caused by fuel property variations. In addition, these influences are also impacted strongly by various engine sizes. Thus, to find fuel effects on combustion and engine behavior between light- and medium-duty diesel engines, the literature review was done.

The literature review mostly involves 58 relevant papers, most of which study the effects of different engine sizes and fuel properties. Papers about GT-Power, a computational simulation software package specialized for engines, are reviewed recently. Within the 58 reviewed papers, 39 (68%) were published since 2005; 14 papers (24%) are about study of effect of injection timings and injection pressure; 17 papers (29%) are about study of effect of different engine sizes; 25 papers (43%) are about study of effect of fuel properties; three papers (5%) are about study of GT-power model. The general conclusions can be divided into: diesel engine combustion and emissions behavior, effect of engine size, effect of various fuel properties, and GT-Power diesel model. The literature review is correspondingly organized in this fashion.

2.1 Diesel combustion

Combustion

In a diesel engine, diesel fuel is injected into the cylinder toward the end of the compression stroke. The fuel then atomizes into small drops, penetrates through the combustion chamber, and mixes with the charge (mixture of air, residual gas, and/or recirculated exhaust gas) in the cylinder. Because the charge high temperature and pressure are above the fuel ignition point, spontaneous ignition of portions of the charge occurs after an ignition delay of a few crank angles. The combustion causes pressure and temperature to increase significantly, reducing the evaporation time of the remaining liquid fuel and improving the mixing of air and fuel vapor.

Therefore, the fuel/air mixture within combustible limits then burns rapidly. Essentially all the fuel has to pass through the atomization, vaporization, fuel-air mixing, and combustion processes. Moreover, mixing of the air with burning and burned gases continues throughout the combustion and expansion processes [6].

The combustion process can be divided into four stages: ignition delay, premixed combustion, mixing-controlled combustion, and late combustion. Ignition delay is the period between start of fuel injection (SOI) and start of combustion (SOC). In premixed combustion stage, the mixture within flammability limits prepared in the ignition delay stage burns rapidly in a few crank angle degrees, featuring high heat release rate. In mixing-controlled combustion stage, the burning is controlled primarily by the air/fuel mixing process.

Several studies investigate the effect of the injection pressure in different engines. Benajes et al. [7] investigated the effect of injection pressure and boosting pressure on combustion process and pollutant emission in the medium-duty diesel engine. The research shows that the increasing boosting pressure and injection pressure caused NOx emissions to increase as a result of intense combustion from faster air-fuel mixing process. On the other hand, soot emissions and fuel consumption at higher injection pressure and boosting pressure were reduced by improved mixing process. Similar trends were observed in another study investigating the effect of the injection pressure on a light-duty engine [8]. The effect of injection pressure on emissions, however, is also impacted by other conditions, such as EGR rate and load conditions. In Hideyuki's [9] research, using high EGR rate (60% EGR rate), the effect of injection pressure on soot emissions is very little. Tie's [10] research of injection pressure on engine performance shows that combustion efficiency is increased by injection pressure increasing on a light-duty engine. Many researchers focused the effect of injection pressure on the engine performance and exhaust emissions for one engine. There is little research, however, comparing the effects of injection pressure among differently sized engines. This is an area of needed future work.

2.2 Effect of engine size

In general, engine size impacts the engine combustion and emissions behavior strongly. Different combustion characteristics such as peak temperature, peak pressure, combustion duration, and heat release rate can change as engine size changes, in spite of similar control and operating parameters. Consequently, engine performance and

emissions will also change as engine size changes (at similar control parameters). Research on the effect of engine size on combustion and emissions can be divided into three parts: effect of stroke to bore ratio, engine displacement, and diesel engine size-scaling relationships.

Effect of stroke to bore ratio

The stroke-to-bore (S/B) ratio has a fundamental impact on engine design because it determines the overall dimensions of the power plant for a given displacement. In addition, stroke to bore ratio determines the geometric proportions of the combustion chamber which impacts the combustion and emissions strongly. Therefore, the effect of S/B ratio on combustion, heat transfer and efficiency is analyzed through simulation [11-13] and experiment [14-17]. The engine displacements are the same in most of the cited research evaluating S/B ratio. Thus, all the comparisons are made on the same assumption: running the engines at the same operating condition. The conclusions are summarized in Table 1.

Table 1 Effect of increasing S/B ratio on various in-cylinder parameters

Rapid burning phase	Decrease
Brake torque output	Increase
Flame propagation	Increase
Dimensionless flame areas	Increase
Surface areas in contact with burned gases	Decrease

Table 1 indicates that the duration of the rapid burning phase decreases with increased S/B ratio and the effect is non-linear, being more dramatic when the S/B ratio is increasing from below 1 to 1. The reason is that with the increased S/B ratio, there are more favorable flame front area characteristics and higher turbulence intensity which enhance the rate of entrainment in the engine. For heat transfer rate, the total heat transfer rate (i.e., heat loss) decreases with decreasing S/B ratio. Specifically, the heat transfer rate to cylinder wall decreases [11, 13] with decreasing S/B, with mitigating increases of heat transfer through the piston top and cylinder head. Further, short stroke engines (lower S/B ratio) cause earlier piston contact to burned gases, which causes steep gradient of the heat transfer rate profile to occur earlier. The influence of turbulence rate on combustion of different S/B ratios is discussed [11] using simulation techniques; the conclusions follow: the dimensionless flame areas are larger in the long-stroke engine (high S/B ratio), where surface areas in contact with burned gases (wall-wetted-area / volume) are much larger in the short-stroke engine (low S/B ratio) when the piston is close to the TDC position.

Effect of displacement

The engine displacement is another important factor that affects combustion and emissions. It is difficult to separate the effects of displacement and S/B ratio from each other. Further, compression ratio is often different among differently sized engines; compression ratio also strongly impacts combustion and emissions. Thus, there are only a few studies that focus solely on the effect of engine displacement. The general effect of engine displacement on various parameters is described in Table 2 [17-21].

Table 2 Effect of increasing engine displacement on various engine parameters

Mechanical efficiency	Decrease
Combustion efficiency	Decrease
Thermodynamic efficiency	Same
Brake fuel conversion efficiency	Decrease

The combustion chamber area-to-volume ratio increases as displaced volume increases, which causes an increase in friction. Further, the boundary layer volume to bulk gas volume ratio increases which affects the emission of CO from the engine and consequently the combustion efficiency [18]. Typically, CO originates from mass in the cylinder that reaches a peak temperature between 1000 and 1400 K, characteristic of partial combustion. This mass is typically located in the crevice and boundary layer. Thus, the emission of CO increases with increasing of boundary layer volume. Related, trapped unburned hydrocarbons increase as crevice volume increases with increased displacement. The effects of displacement on various engine efficiencies, such as brake fuel conversion, combustion, thermal, volumetric, and mechanical efficiencies, have also been studied. Because of higher friction losses in larger displacement engine, the mechanical efficiency is decreased with increased displacement. Similarly, and as explained above with differences in HC and CO emissions, combustion efficiency decreases slightly with an increase in displacement. Thermal efficiency (the ratio of indicated output of an engine to the quantity of energy released during combustion) and the gas exchange efficiency (i.e., “pumping efficiency) seem to be mostly unaffected by

engine displacement [21]. The net result of these various efficiencies is captured in what is called the brake fuel conversion efficiency, summarized by this equation: $\eta_{b,\,fc} = \eta_{thermal} * \eta_{com} * \eta_{mech} * \eta_{gas}$. In general, brake fuel conversion efficiency decreases with the increase in displacement. The trend is dependent, however, on engine speed and load. For low-and mid-load conditions, the brake fuel conversion efficiency seems to always decrease with an increase in displacement. The trend can also be impacted by other operating parameters such as injection timing in high load condition [19, 20].

Diesel engine size-scaling relationships

This section describes the relationships between large diesel engines (e.g., off-road heavy-duty engines) and small diesel engines (e.g., high speed automotive engines) as determined from CFD simulation results [22-25]. Firstly, the researchers used some theoretical equations, such as spray penetration equation, flame lift-off length equation, swirl ratio equation and other equations to establish some reasonable relationships between different engine displacements and other various engine parameters. CFD simulation models include numerical mesh dependency, turbulence, and heat transfer effects. Different scaling behaviors related to turbulence and chemistry timescales and their effects on combustion and emissions in engines of different size were considered [22, 26-29]. From the results, the pressure and heat release rates are well scaled using the established relationships. NOx and soot emissions, however, do not scale well, especially under medium and high load conditions. Table 3 summarizes the scaling relationships between engine displacement (V) and other engine parameters.

Table 3 Scaling relationships between engine displacement (V) and other engine parameters

Parameter	Scaling Relationship
Mass of fuel injected	V
Spray penetration tip length	$V^{1/3}$
Flame lift-off length	$V^{1/3}$
Injection velocity	$V^{2/9}$
Injection duration	$V^{1/9}$
Engine speed	$V^{-1/9}$
Valve-lifts	$V^{1/3}$

In Luke's [24] research, the scaled engines were compared in a conventional diesel combustion regime. The test variables included start of injection (SOI), intake temperature, engine speed, and swirl ratio. Overall engine performances including IMEP and ISFC between the two engines were nearly the same (good agreement) in the operating conditions designed by the relationships from Table 3. This agreement persists with changes in engine speed, SOI, and intake temperature. Differences in the fuel spray characteristics or relative air entrainment rate were not captured with the scaling models. Moreover, the smaller engine exhibits higher heat release rates during the initial stages of the combustion which means there is an increase in the available combustible mixture during the initial stages of combustion in the smaller engine.

2.3 Effect of fuel properties

Fuel properties impact the performance and emissions behavior of diesel engines through their influence on the physical process associated with fuel injection, jet penetration, entrainment and fuel-air mixing, as well as by changes to the combustion chemistry associated with fuel chemistry, aromatics, molecular weight, and additive concentrations. Continued focus on ultra-low NOx engine-out targets and variation of available fuel drive the need for a deeper understanding of the changes to the engine behavior caused by fuel property variations.

Literature suggests there are three fuel properties of primary importance to the performance of advanced combustion engines: cetane number (measure of ignition quality), aromatic content (affects fuel constituent composition), and distillation (measure of volatility). From the reference papers, cetane number varies from 7 to 80; most studies are in the range 0f 30-55. Aromatic content varies from 0-55%; most studies are in the range of 15-40%. Distillation temperature (T90) varies from 220 to 400˚C; most studies are in the range of 300-320˚C. In some papers, the three parameters change simultaneously and the conclusions are drawn for one parameter often combined with others. Takahashi et al. [30] and Kumar, et al. [31], however, change fuel properties in a matrix such that that each could be isolated.

Simple calculations based on Gallant, et al. [32] and involving select fuel properties (distillation temperature, cetane number, mono-aromatic content, poly-aromatic content, total aromatic content, density, and heating value) show some correlations. For example, it is shown that the three distillation temperatures (T10, T50,

and T90) are all correlated to one another and with the poly-aromatic content. The cetane number is correlated with the mono- and the total aromatic content. The poly-aromatic content impacts fuel density and heating value indicating that heavy fuels tend to have a greater fraction of poly-aromatic components and lower heating values.

FACE fuels

The mission of the Fuels for Advanced Combustion Engines (FACE) Group is to recommend sets of test fuels well suited for advanced combustion engine research so there is a common platform of fuels. The FACE group creates both diesel fuels matrix and gasoline fuels matrix [33]. The matrix of diesel fuels for advanced combustion engine research is introduced in Gallant, et al. [32]; the FACE diesel fuels matrix includes nine fuels and is designed around three properties of primary importance: cetane number (measure of ignition quality), aromatic content (affects fuel constituent composition), and distillation (measure of volatility). The details are shown in **Figure 1** [33] and target properties are shown as center points in the figure. Specifically, the target properties are: cetane number of 42.5, aromatics content of 32.5%, and T90 of 305°C. Additionally, Gallant, et al.'s report [32] documents an overview of the comparison between the details of the actual results of the fuel chemical and physical properties and the design values by using ASTM analyses, GC/MS analyses, and thermodynamic characterizations. In the report, CN, aromatic content and T90 for each fuel are measured by Southwest Research Institute (SwRI), Chevron-Phillips Chemical Company's Specialty Chemicals Group (CPChem) and NRCan's National Centre for Upgrading Technology (NCUT)) using ASTM engine method and the actual values for

most of points are close to target value. Other fuel properties, such as viscosity, heating value, spec gravity are determined by the three laboratories either. Besides traditional ASTM analysis, fuel molecular composition and molecular structure are quantified by GC-FIMS and 1H/13C NMR analyses.

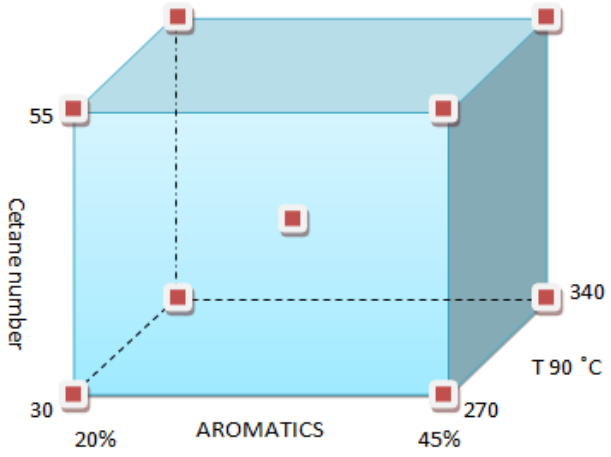

Figure 1 FACE diesel fuels matrix [33]

Mikhail's [34] report provides detailed results from a variety of standard ASTM International-type analyses and advanced characterization techniques conducted to measure the chemical and physical properties of the FACE diesel fuels. From the report, based on standard ASTM tests, most of the FACE diesel fuels are able to meet the target value of cetane number, aromatic content and T90. When the derived cetane number is measured by the Ignition Quality Tester (IQT) instrument, the IQT values are up to 6.6 points higher for the fuels having a low nominal cetane number of 30. The possible reason is the ASTM equations for correlating the engine and IQT test results are usually

used for diesel fuels whose cetane numbers are in the range of 40 to 60. Moreover, those diesel fuels are also analyed on other advanced characterization techniques to obtain more details about chemical and structural composition information. The results show that some components in most of FACE fuels, such as n-paraffins, isoparaffins, cycloparaffins, and aromatics, have a good agreement with commercial fuels. The low cetane number FACE fuels (CN 30) contain more than 20% of light (C8–C10) monoaromatics, which is not typical of commercial diesel fuels.

Recently, many researchers investigate the effects of various FACE diesel fuels. In Hosseini, et al.'s [35] research, cetane number and T90 distillation temperature in FACE fuels matrix are discovered to affect combustion phasing. Based on comparison of effects, cetane number clearly has the stronger effect. An increase in cetane number or a decrease in the T90 distillation temperature advances the combustion phasing. The effect of cetane number is linked to increased low temperature heat release (LTHR) with increasing cetane number. The T90 effect is primarily due to a change in the physical delay period associated with preparation of the fuel-air mixture. William et al. [36] make analysis of effect of FACE diesel fuels on low temperature combustion on various load conditions of a 0.75-L engine. In his research, at low load condition, the high CN is good for reducing THC and CO from incomplete reactions by shorting ignition delay and the highest level for THC and CO is generated at the fuel with lowest CN and highest aromatic content. It indicates that the aromatic contents also contribute to the products of the incomplete oxidization. At medium and high load conditions, low CN is good for reducing soot emissions by increasing ignition delay to decrease the part of diffusion

combustion which is the main period for soot formation. There is not any obvious benefit on reducing THC and CO as their absolute values are typically very low (e.g., less than 200 ppm for HC) for conventional diesel combustion. Although higher aromatic content shows an extended ignition delay, soot is not necessarily decreased by the extended ignition delay because the aromatics are considered as precursors of the soot production. Bonsack et al. [37] investigates the effects of FACE diesel fuels on low temperature combustion, focusing on the nanoparticle emissions from a GM 1.9-L diesel engine. The particle number concentrations and mean particle diameter increase simultaneously an increasing CN of the FACE fuels. The effects of distillation temperature (T90) on particle diameter are not consistent: the count mode diameter is found to be lower with higher T90 in the low CN condition; the diameter is found to be lower with lower T90 in the high CN condition.

Spray Penetration

Fuel sprays in diesel engine cylinders are extensively studied and reported on in the literature. Schweitzer [38] and Wakuri et al. [39] observe the influence of injection pressure and ambient temperature on spray behavior and provide simple correlations describing the behavior. Wakuri et al. [39] report that the distance of spray penetration is proportional to the square root of injector diameter, time, and injection velocity. Further, it is influenced by mixture density and pressure. Dent [40] studied spray behavior further and determined the spray penetration distance equation ($S = 13.6 * [(\frac{\Delta P}{\rho_g})^{\frac{1}{2}} * t * d_0]^{\frac{1}{2}} * (\frac{530}{T_g})^{1/4}$) from momentum conservation applied to two phase jets. Further, Dent [41]

verified the model by comparing calculation results with experimental data for cold bomb and hot bomb. The equation shows that the penetration distance is impacted by fuels' density, injection pressure, injector diameter, and gas temperature in the cylinder and also indicates that spray penetration is proportional to the square root of time after the start of injection. Hiroyasu and Arai [42] study the spray at the beginning of injection and observe that spray penetration is initially linearly proportional to time. At later stages, it is proportional to the square root of time, in agreement with Dent [40]. The time transition between the two "regions" (i.e., early spray formation and later spray formation) corresponds to the beginning of the breakup process, ($0 \le t \le t_b \;\; S = 0.39 * \sqrt{\frac{2\Delta P}{\rho_f}} t \qquad t_b \le t \;\; S = 2.95 * \left(\frac{\Delta P}{\rho_a}\right)^{0.25} * \sqrt{d_0 t} \qquad t_b = 28.65 * \frac{\rho_{f*d_0}}{\sqrt{\rho_a \Delta P}}$).

Bao, et al. [43] compare spray penetration for different fuels (Ethanol, Gasoline, Iso-Octane) under various injection pressures (4, 7, 11 and 15 MPa) and found similar conclusions with Hiroyasu's work on low injection pressure. The results show that under low injection pressure (4 MPa), a lower fuel density causes longer penetration length, due to higher injection velocity and decreased nozzle loss. As the injection pressure increases, droplet size conditions become the primary factor of penetration distance. Because the penetration is impacted by aerodynamic drag force applied to fuel droplets, instead of the injection velocity or nozzle loss of the liquid jet. The lower aerodynamic drag force with larger droplet size leads to longer penetration distance.

Combustion

In Lucas, et al. [44], the effects of jet fuel properties on compression ignition engine operation are investigated under high-load conditions for jet fuels with varying

cetane number. They find fuel cetane number could impact the pressure rise rate for the range of conditions tested. Cetane number indicates the quality of ignition of diesel fuel and reveals its effect in an engine with the ignition delay between start of injection and start of combustion. Ignition delay decreases as cetane number increases for moderate cetane numbers [32, 44, 45]. The correlation is not as strong, however with high cetane number fuels. In Hosseini, et al.'s [35] research, cetane number and T90 distillation temperature are changed separately; both are discovered to affect combustion phasing. Based on comparison of effects, cetane number clearly has the stronger effect. An increase in cetane number or a decrease in the T90 distillation temperature advances the combustion phasing. The effect of cetane number is linked to increased low temperature heat release (LTHR) with increasing cetane number. The T90 effect is primarily due to a change in the physical delay period associated with preparation of the fuel-air mixture. At a similar 50% mass fraction burned location, the high CN fuels exhibited significantly longer combustion duration than the low CN fuels. Butts, et al. [46] report similar conclusions as Hosseini's work: the magnitude of LTHR increases and its peak value location advances as CN increases. Aromatics content in fuels seems to have little impact on ignition delay and combustion period; however, it has a significant effect on flame temperature: higher aromatic content causes higher flame temperature, especially for poly-aromatic content [47].

Emissions

Several studies have been conducted in the past to assess the effect of diesel fuel property changes on engine-out emissions. Many of these suggest conflicting results on the directional influences of critical fuel properties on engine behavior, some of which are explained by the significant differences in NOx levels and engine operating conditions under which the data are gathered. The problem is complicated by the typically high degree of confounding between fuel properties, which makes it difficult to isolate individual effects.

In one of the early works on this subject, based on 7 various fuels, Rosenthal and Bendinsky [48] independently changed the fuels by cetane number from 20 to 60, aromatic contents from 0% to 70%, and T90 from 220 to 400˚C. The fuels were studied with transient and steady-state experiments on two heavy duty diesel engines to conclude that aromatic content is the primary fuel parameter influencing NOx and particulate emissions. Later, Ullman, et al. [49] reported that increasing CN (42-60) decreased all regulated emissions (HC, CO, NOx and PM) on a heavy-duty engine. In an effort to distinguish the effect of cetane improved fuels versus naturally high-cetane fuels, Green, et al. [50] study three commercial fuels of cetane number (CN) of 40-42, the same fuels raised to CN 48-50 with a cetane improver additive, and three commercial fuels of base CN 47-50. The study reports that the cetane improved fuels show benefits with respect to both power and fuel efficiency, owing to their higher volumetric energy content while generating the same emissions as fuels which are naturally high in cetane. Using laser elastic scatter imaging on a heavy-duty engine to characterize fuel volatility

effects, Canaan, et al. [51] describe a strong, linear correlation between the fuel's mid-boiling point and maximum liquid-phase jet penetration with the penetration increasing with higher boiling point temperatures. In contrast to previous studies, based on fuel matrix where the cetane number was varied from 40 to 55 (naturally and cetane improved) and aromatic content was varied from 10 to 30%, Ryan, et al. [52] found no significant differences that could be related to changes in the targeted fuel properties. Tamanouchi, et al. [53] tested fuels with T90 varying from 277 to 336°C and poly-aromatic content varying from 3.2 to 9.6% while maintaining constant cetane number (at approximately 50) and total aromatic content (at approximately17%). They found that total hydrocarbon emissions and particulate matter (PM) decreased with lowering 90% distillation temperature (T90) or lower poly-aromatic content in the fuel and the effects are impacted by various engines. In general, T90 has similar performance with aromatic content on PM, better performance on THC emissions.

Kidoguchi et al. [54] analyze the separate influences of cetane number (varying from 43 to 56) and aromatic content (varying from 0% to 38%). The study finds that higher cetane number increases NOx and decreases PM with constant aromatic content. When CN is constant, increasing aromatic content has little effect on combustion characteristics but increases PM and NOx. At retarded injection timing (from 5° before top dead center, or BTDC, to 2° after top dead center, or ATDC), total hydrocarbon emissions increase dramatically at low load with low cetane number fuels due to the over leaning caused by long ignition delay. Further, for low cetane number fuels, total hydrocarbon emissions and soluble organic fraction of particulate emissions increase at

low load with increases in aromatic content. The U.S. Environmental Protection Agency (EPA) published a technical document detailing the issues specific to relating engine-out emissions as a function of diesel fuel properties covering multiple data sources, test cycles, engine platforms and modeling strategies. Their results pointed to some improvements in PM with reducing poly-aromatic content for light-duty engines, but a wide variation in diesel fuel effects on NOx emissions dependent heavily on engine design, operating conditions, drive cycles and other factors. Kee, et al. [55] use rapid compression machine experiments to compare two fuels which varied significantly in their aromatic content (0% to 20%) and found that aromatic-containing fuels produce higher NOx due to longer formation durations. Azetsu [47] shows the flame temperature and soot formation increase with higher aromatic content by changing it from 0 to 20 at various injection pressures (60 MPa and 100 MPa). Sluder et al. [56] suggest that diesel-range fuels with higher volatility in the top 50% of the distillation curve exhibited improved emissions. Recently, Eckerle et al. [57] and Li et al. [58] used fuel matrix to quantify the influence of aromatic content on NOx emissions at various speed-load conditions. The results show that the NOx emissions increase when total aromatic content increases in fuels. The correlation between NOx emissions and total aromatic content was more obvious at medium and high load conditions. At these conditions, major portion of fuel was burned at fuel-rich locations where the chemical composition of fuel impacts the local gas temperature more strongly. Specifically, for fuels with higher total aromatic content, the adiabatic temperature of the hydrocarbons with ring

structures tend to be higher which could generate higher temperature in fuel-rich region, ultimately causing higher NOx emissions.

Kumar et al. [31] investigate experimentally the combustion and emissions performance of various diesel fuels on an advanced diesel engine. The study reveals that NOx is impacted by cetane number and distillation characteristics under high EGR, diffusion burn dominated conditions. Lower T50 (mid-distillation temperature) results in simultaneous reductions in both NOx and smoke while higher cetane number provides a small NOx benefit through reducing ignition delay and improving combustion quality. Warey et al. [59] observed similar results. Nishiumi's [60] research on PM emissions show that fuel cetane number affects the insoluble organic fraction (ISOF) in PM emissions. Further, the total hydrocarbon and PM emissions decrease with lowering T90. A narrow distillation range that eliminates high boiling point components is effective in reducing the SOF at low speed/low load and high speed/high load conditions. Furthermore, the narrow distillation fuel results in lower ISOF under the high speed / high load conditions. Takahashi [30], however, shows that excessively high cetane (e.g., 78) increases ISOF fraction in PM emissions, due to poor mixing of injected fuel and air. He also shows increasing cetane number (35-58) by lowering mono-aromatic content provides a small NOx benefit at medium load condition.

Summary

Pressure rise rate and ignition delay is decreased with increasing cetane number. An increased CN advances the combustion phasing. For PM emissions, the higher fuel cetane number increases the insoluble organic fraction (ISOF). Increasing cetane number

via the lowering of mono-aromatic content marginally decreases NOx; at high load, however, the effect of cetane is negligible compared to other parameters such as injection timing. For CO and HC, there are some benefits when the cetane number is increasing.

Aromatics content in fuels seems to have little impact on ignition delay and combustion period; however, it has a significant effect on flame temperature and soot formation. Moreover, the effects of aromatic content on emissions also depend on the engine operating conditions.

Total hydrocarbon emissions and PM decrease with the lowering of the 90% distillation temperature (T90) and rising of the 50% distillation temperature (T50). Creating a narrow distillation range by eliminating high boiling point components is effective in reducing SOF. Furthermore, a narrow distillation fuel results in lower ISOF under high speed / high load conditions.

2.4 Combining Fuel Property Effects and Engine Size Effects

Based on the above discussions, some connections between observed fuel property effects on performance, efficiency, and emissions and engine size effects on the same can be drawn. There are more than 25 papers about effect of fuel properties and 17 papers about effect of engine size. In those papers, 8 papers are about engine sizes bigger than 4L; 12 papers are about engine sizes in range of 1 L to 4 L; 3 papers are about engine sizes smaller than 1L; 11 of them are about cetane number, 10 of them are about distillation temperature; five of them are about aromatic content.

Net apparent heat release rate (AHRR) shows a decrease in the premixed burn magnitude as cetane number increases. Low cetane number fuels have longer ignition delays, which cause the amount of energy converted during the premixed burn to be relatively higher (compared to shorter ignition delays), resulting in increased pressure rise rates in various sizes of engines. The changing trend of combustion characteristics are not impacted by changing engine sizes. Increasing cetane number decreases NOx, THC and CO emissions and this trend increases as engine displacement increases. Increasing cetane number increases soot emissions but the effect of increasing soot emissions with increasing cetane diminishes as size increases.

Higher aromatics content in fuels has little impact on ignition delay and combustion period, especially in small size engine (in a 0.8 L diesel engine, higher aromatics content in fuels has little impact on heat release rate and cylinder pressure [54]); it has a significant effect, however, on flame temperature. Moreover, the effect of aromatic content on emissions is impacted strongly by other factors, such as injection timing, EGR rate and load conditions. In general, lowering aromatics in fuel, especially lower poly-aromatic contents provide benefits of lower particulate emissions [36, 47].

Changes to distillation temperature have little impact on heat release rate and cylinder pressure, but lower T90 decreases penetration distance [51] and advances the combustion phasing [35] under various sizes of engines. Total hydrocarbon emissions and PM decrease with lowering T90 for all engines and the effect of T50 on emissions becomes important as engine size decreases. In small size engines, lower T50 (mid-distillation temperature) results in simultaneous reductions in both NOx and smoke [31].

These connections are made from comparison of reference papers, none of which had the specific objective of identifying the different effect of fuel properties on engine combustion and emissions of differently sized engines. Thus, no real conclusions on the effect of fuel properties and engine sizes on engine performance, efficiencies, and emissions can be made. Moreover, the conclusions of the effect of fuel properties and engine sizes on combustion and emissions are not detailed and accurate enough. This will continue to be a focus of study.

3. SIMULATING DIESEL ENGINE IN GT-POWER

3.1 Purpose of GT-Power

In the project, medium-duty and light-duty engines will be operated at 1500 rpm, low load and medium load conditions by changing injection timings from -15° ATDC to 6° ATDC and rail pressure from 400 bar to 600 bar in both engines. The project will study 8 kinds of fuels which will be changed by cetane number (30-55) and distillation temperature (T90) (270-340) similar with FACE fuels. In this arrangement, the total testing points will approach 800, which is impractical to do all experimentally. Thus, the popular engine simulation software, GT-Power, is used to simulate engine performance after baseline testing to identify the critical points and conditions to study experimentally. After baseline testing, experiments with various fuels (of different properties) will provide validation data to the GT-Power simulation.

Fuel properties, injection timing, and rail pressure will be adjusted using the GT-Power simulation. For fuel properties, due to different cetane number or distillation temperature, properties such as premixed/diffusion combustion rate multiplier, ignition delay multiplier, convection multiplier, entrainment rate multiplier will be adjusted in the GT-Power combustion section. The injection timing and rail pressure can be adjusted in the "injector" object.

GT-Power is a popular engine simulation tool designed for steady-state and transient simulations. It is applicable to many types of internal combustion engines and provides the user with many components to model any advanced concept. GT-Power

uses several physics-based models to calculate engine performance and emissions; the relevant models for the current study are described here.

3.2 Combustion Model

In order to obtain more accurate simulation results on combustion and emissions area, the applicability of GT-Power's predictive combustion model (DI-Jet combustion model) is investigated.

The combustion model (DI-Jet Model) is a quasi-dimensional multi-zone combustion model for direct injection compression ignition engine. It is primarily used to predict burn rate and NOx emissions. Soot is also predicted, but the predicted concentrations are not particularly meaningful and should be used to study only trends in the results.

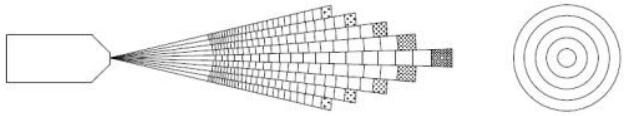

Figure 2 GT-Power's DI-Jet model divides the injected fuel mass into many radial zones issuing axially at a given angle from the injector tip.

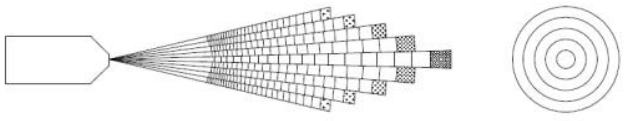

Figure 3 Numbering rule of the zones

As shown in **Figure 2**, GT-Power creates a computational region by dividing the injected fuel mass is divided into several radial zones issuing axially at a given angle from the injector. Five radial zones and a maximum of 80 axial zones (depending on the value specified in the 'EngCylCombDIJet' model) [61]. **Figure 3** shows how the zones are numbered. At each time step taken by the code during the injection period, an axial "slice" (five radial zones) is injected into the cylinder (if the time steps are very small, the fuel may be injected at only every other time step). The total mass of fuel in all of the zones will be equal to the specified injection rate (mg/stroke) divided by the specified number of nozzle holes; the DI-Jet model really models the plume from only one nozzle hole. The mass of fuel in each axial "slice" is determined by the injection pressure at that time step and the elapsed time since the last zones were injected. This mass injected at each time step is divided equally among the five radial zones. The instantaneous injection pressure is also used to calculate the injection velocity of each axial slice. Each zone additionally contains subzones for liquid fuel, unburned vapor fuel and entrained air, and burned gas. Immediately after a zone is injected, the zone is 100% liquid fuel. As the zone moves into the cylinder, it "entrains" air and the fuel begins to evaporate, thus forming the unburned subzone. The mass of the entrained air causes the velocity of the zone to decrease because momentum of the zone is conserved. The outer zones entrain air more quickly than the inner zones, thus decreasing their velocity more quickly and resulting in less penetration distance as can be seen in **Figure 1**. From the mass of vapor fuel and entrained air in each unburned subzone, the zonal fuel to air ratio

is known. The zonal temperature is calculated taking into account the temperature of the injected fuel, entrained air temperature, and the effects of the fuel evaporation. When the combination of cylinder pressure, zonal temperature, and fuel-to-air ratio becomes combustible, the fuel in the zone ignites, further changing the temperature and composition. All products of combustion will be moved to the burned subzone. NOx and soot are calculated independently in each burned subzone taking into account the fuel/air ratio and temperature. The total cylinder NOx and soot are the integrated total of all of the individual burned subzones.

3.3 Model Description and Validation

The sub-combustion model in GT-Power for the two engines is DI-PULSE model. It includes: Entrainment Rate Multiplier, Ignition Delay Multiplier, Premixed Combustion Rate Multiplier, Diffusion Combustion Rate Multiplier. The simulation parameters is kept the same for varying operating conditions (such as injection timing) at the same load condition, but changed between different two loads. The comparisons of measured and predicted pressure traces and heat release rates as functions of crank angle for the medium-duty and light-duty engines are shown in Figure 4 and Figure 5, including low load and medium load condition. The simulation results are reasonably close to experimental data. Additionally, the comparisons of engine performance are shown in Table 4 and 5. The percent differences in brake torque between the simulation and experiment for low load and medium load conditions are 0.9% and 2.8%, respectively. The percent differences in brake specific fuel consumption (BSFC) are

3.7% and 2.6%. The percent differences in CA50 location are 1.9% and 0.99%, respectively. Light duty engine model has similar accuracy.

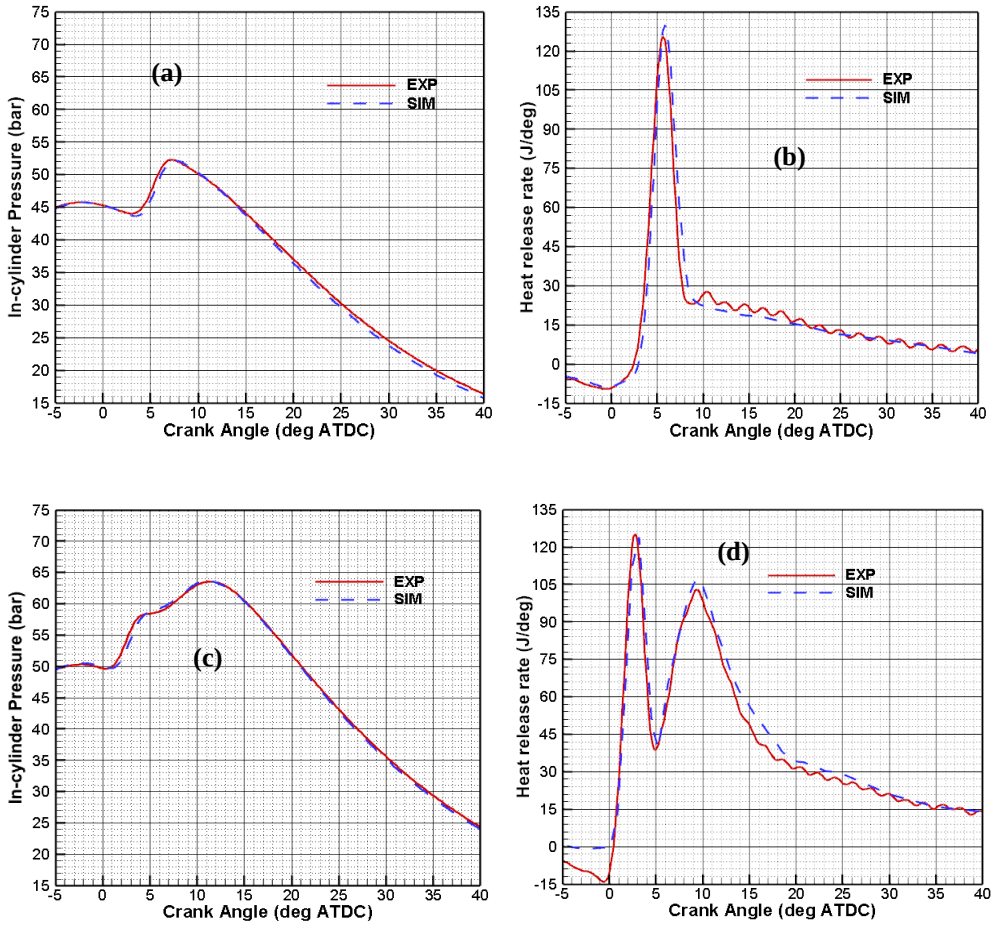

Figure 4 (a) In-cylinder pressure and (b) heat release rate at low load condition and (c) in-cylinder pressure and (d) heat release rate at medium load condition as functions of engine crank angle for experimental and simulated data of medium-duty engine. Each condition is at 1500 rpm engine speed and injection timing = -9°CA ATDC

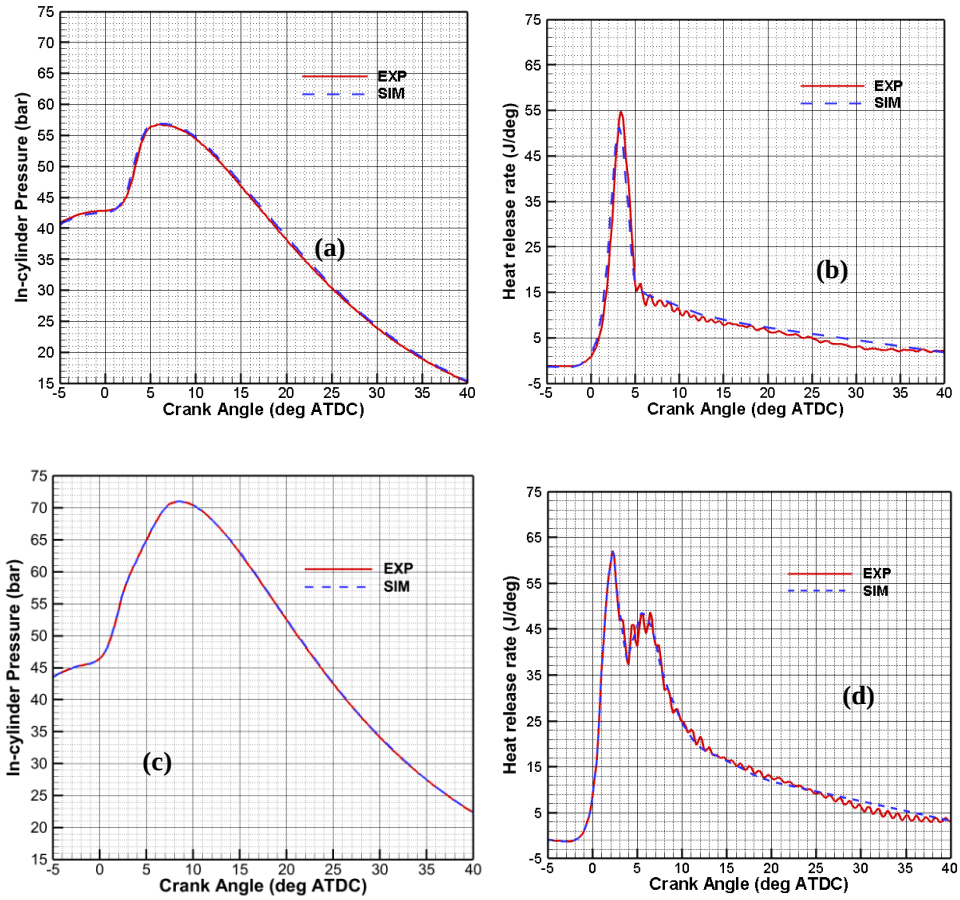

Figure 5 (a) In-cylinder pressure and (b) heat release rate at low load condition and (c) in-cylinder pressure and (d) heat release rate at medium load condition as functions of engine crank angle for experimental and simulated data of light-duty engine. Each condition is at 1500 rpm engine speed and injection timing = -9°CA ATDC

Table 4 Comparison between experiment and simulation of various engine performance parameters of the medium-duty engine at the chosen validation condition

	Low-Load			Medium-Load		
	Experiment	Simulation	Difference (%)	Experiment	Simulation	Difference (%)
Speed (RPM)	1500	1500		1500	1500	
Torque (N-m)	67	68	0.9	203	207	2.8
BMEP (bar)	1.87	1.9	0.9	5.65	5.75	2.8
Peak pressure (bar)	55.9	56.1	0.4	63.8	64	0.3
Location of Peak pressure (deg)	8.8	8.7	1.13	8.6	8.5	1.1
BSFC (g/kWh)	345.5	332.4	3.7	243	237.5	2.6
CA50 location (deg)	7.6	7.45	1.9	10.1	10	0.99
Ignition Delay (°CA)	14.3	14.1	0.14	9.1	9.1	0

Table 5 Comparison between experiment and simulation of various engine performance parameters of the light-duty engine at the chosen validation condition

	Low-Load			Medium-Load		
	Experiment	Simulation	Difference (%)	Experiment	Simulation	Difference (%)

Table 5 Continued

Location of Peak pressure (deg)	6.8	7.2	5.8	7.4	7.4	0
BSFC (g/kWh)	373	376	0.8	272.3	281.2	3.2
CA50 location (deg)	5.375	5.4	0.4	10.1	10	0.99
Ignition Delay (deg)	11.7	11.8	0.85	8.7	8.7	0
Speed (RPM)	1500	1500		1500	1500	
Torque (N-m)	29	29.05	1.7	86	86.3	0.3
BMEP (bar)	1.908	1.9118	1.6	5.65	5.67	0.3
Peak pressure (bar)	60.7	61.3	0.9	70.7	71	0.4

Based on these comparisons, the two simulations are believed to be an appropriate representation of the engines for calculating reaction temperature and turbulence intensity.

3.4 Relationship between GT-Power parameter and fuel properties

For diesel fuel, the composition of diesel varies by location in the world, time of the year, and even the engine which will consume the fuel. GT-Power's fuel library (GT-ISE library) provides multiple diesel fuels and is named using the following convention: diesel-XXXkg-m3. The XXX represents the density of the fuel at 1 bar and 20°C. The library includes diesel fuels with the following densities: 770, 785, 810, 812, 818, 845, and 858. Information about enthalpy, density, and transport properties in those fuels are

different; they are just distinguished by their densities at a reference condition. Thus, for the current project, certain properties such as cetane number or distillation temperature cannot be directly adjusted as a fuel property in GT-power; other property-dependent parameters (e.g., ignition delay with CN), however, can change as a result of changing fuel property.

Effect of fuel properties on engine combustion

An increase in cetane number decreases ignition delay to advance the combustion phasing. At a similar 50% mass fraction burned location, the high CN fuels exhibited significantly longer combustion duration than the low CN fuels. The effect of cetane number is linked to increased low temperature heat release (LTHR) with increasing cetane number and decreases the premixed heat release fraction. Because of the decreased premixed heat release fraction, an increase in cetane number also generally decreases the pressure rise rate.

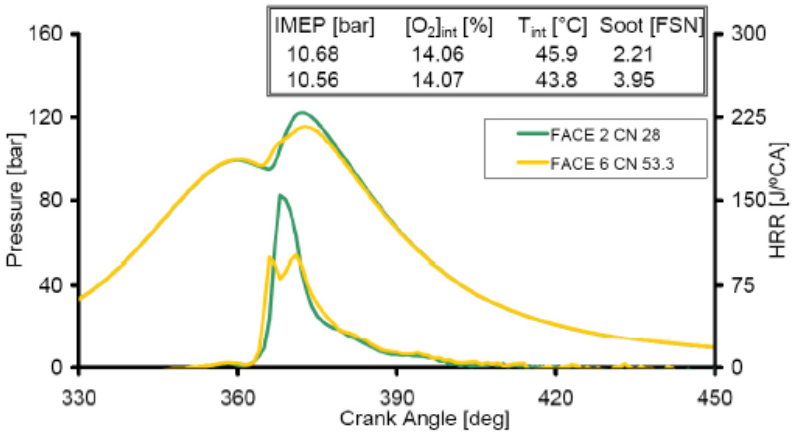

Figure 6 Effect of cetane number on in-cylinder pressure and heat release rate [36]

Higher AC causes higher flame temperature. AC in fuels seems to have little impact on ignition delay and combustion period; it has a significant effect, however, on flame temperature and soot formation. The specific effects of AC on emissions seem to depend on the engine operating conditions.

Although AC has little impact on combustion characteristics, it seems to have a general relationship with density. The poly-aromatic content impacts fuel density and heating value indicating that heavy fuels tend to have a greater fraction of poly-aromatic components and lower heating values. This relationship is concluded by Jeihouni Y et al [62]. Figure 7 illustrates this relationship [62].

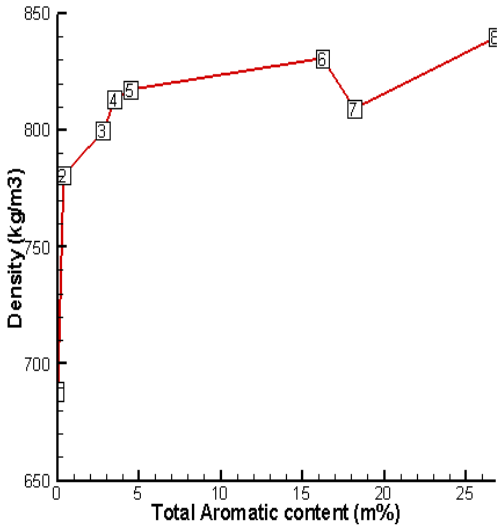

Figure 7 Density under various aromatic content [62]

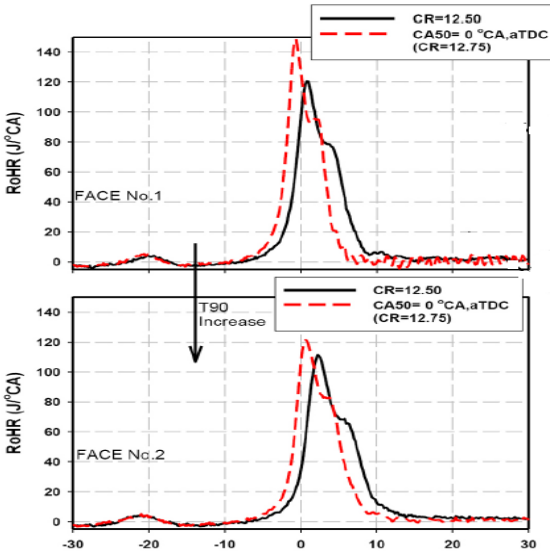

Figure 8 Heat release rate under various T90

A decrease in the T90 distillation temperature advances the combustion phasing and increases the combustion duration. The T90 effect is primarily due to a change in the

physical delay period associated with preparation of the fuel-air mixture. Moreover, higher T90 has higher flame temperature. The relationship [35] between distillation temperature (T90) and heat release rate is shown in **Figure 8**.

Table 6 Effects of CN, Aromatic content and T90 on combustion characteristics

Parameter ↑	Pressure	Heat release rate	Ignition Delay	Combustion duration	Location B50	Flame temperature
Cetane number	Decrease	Decrease in the premixed burn magnitude	Decrease	Increase	Postpone	
Aromatic content						Increase
Distillation temperature (T90)		Increase	Increase	Decrease	Advance	Decrease

Capture Fuel Effects in GT-POWER

There are several parameters that can be used in GT-Power to achieve the effect of differing fuel properties on combustion. These parameters include: Entrainment Rate Multiplier, Ignition Delay Multiplier, Premixed Combustion Rate Multiplier, Diffusion Combustion Rate Multiplier, fuel density, fuel lower heating value, and fuel enthalpy of vaporization.

Density and Heating value

Increasing density with other parameters being held constant, including total fuel injection quantity, causes lower rates of heat release as shown in **Figure 9** and 10 and summarized in Table 7. This is likely caused by differences in spray penetration,

breakup, and vaporization. Lowering the fuel's heating value has a similar effect on rates of heat release; but in that case, less energy is available for release.

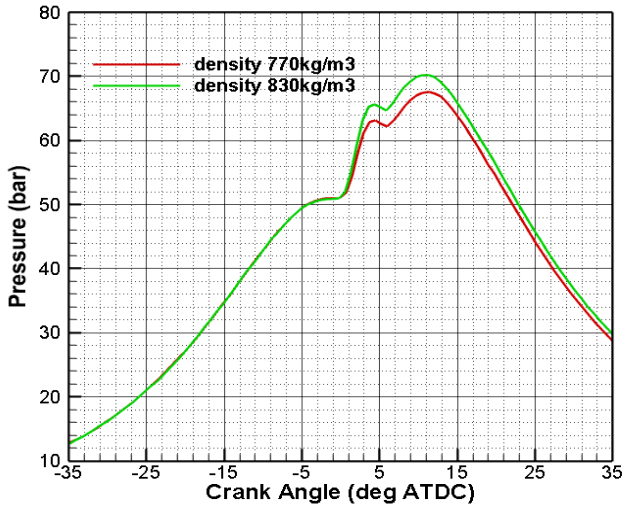

Figure 9 In-cylinder pressure sensitivity to fuel density

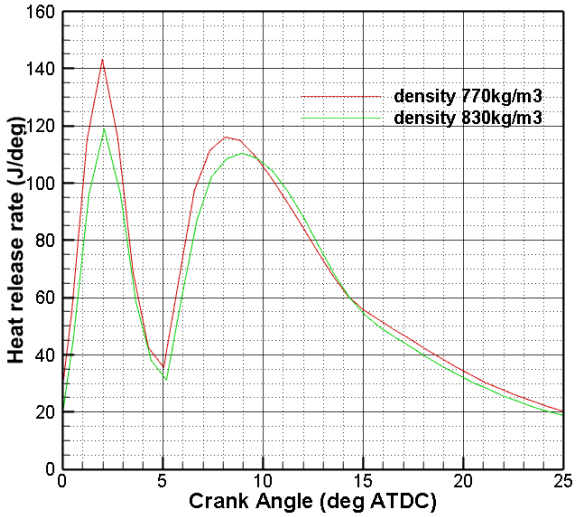

Figure 10 Heat release rate sensitivity to fuel density

Table 7 Engine output sensitivity to fuel density

	Density 770 kg/m3	Density 830 kg/m3
Torque (N-m)	212.4	196
BMEP (bar)	6	5.5
BSFC (g/kWh)	226.6	245.5
Burn Duration 10-90%(deg)	53.4	53
Ignition Delay (deg)	7.8	7.8

From Figure 9 and 12 and Table 7, the effect of lower heating value or higher density can be concluded as: higher density or lower heating value decreases pressure peak value and heat release rate. Due to lower rates of heat release, the torque output and BMEP decreases, but there is little influence on burn duration and ignition delay.

Entrainment Rate Multiplier

Entrainment Rate Multiplier is a very sensitive parameter in GT-Power simulations. It impacts the entrainment rate directly which mainly impacts air-fuel mixing condition, turbulence speed, and flame speed. Thus, the combustion characteristics change drastically when the parameter is changed. Those changing trends are shown in the Figure 11 and 12.

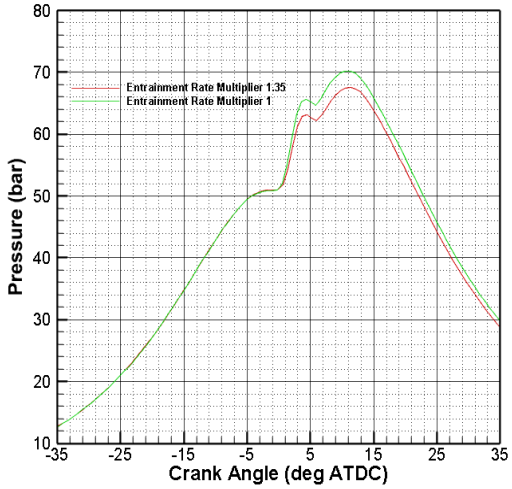

Figure 11 In-cylinder pressure sensitivity to entrainment rate multiplier

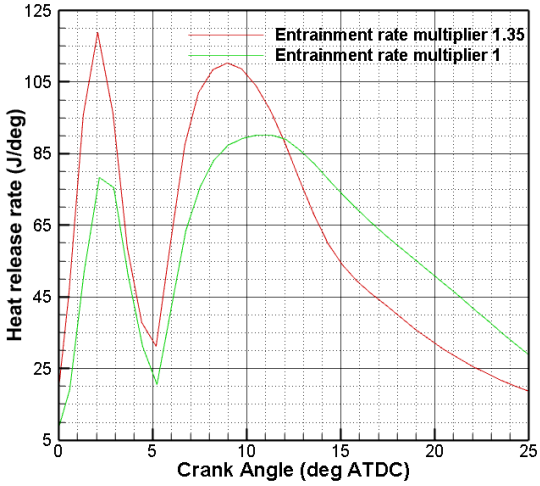

Figure 12 Heat release rate sensitivity to entrainment rate multiplier

Table 8 Engine output sensitivity to entrainment rate multiplier

	Entrainment Rate Multiplier 1.35	Entrainment Rate Multiplier 1
Torque (N-m)	196	191.78
BMEP (bar)	5.5	5.37
BSFC (g/kWh)	245.5	250.95
Burn Duration 10-90%(deg)	53	52.7
Ignition Delay (deg)	13.4	17

Increasing entrainment rate multiplier increases turbulence strength and improves fuel-air mixing. This causes an increase in peak pressure and heat release rate. Because of the higher heat release rate, BMEP and torque increase entrainment rate multiplier. Although entrainment rate multiplier has a significant influence on in-cylinder pressure and heat release rate, there is little net influence on burn duration and ignition delay; although increasing entrainment rate multiplier enhances mixing it also increases the heat convection rate between cylinder wall and mixture. Increasing entrainment rate multiplier, however, advances B50 location.

Ignition Delay Multiplier

The ignition delay in a diesel engine is defined as the time interval between the start of injection and the start of combustion. This parameter impacts ignition delay directly. **Figure 13** and 14 show the sensitivity with the ignition delay multiplier

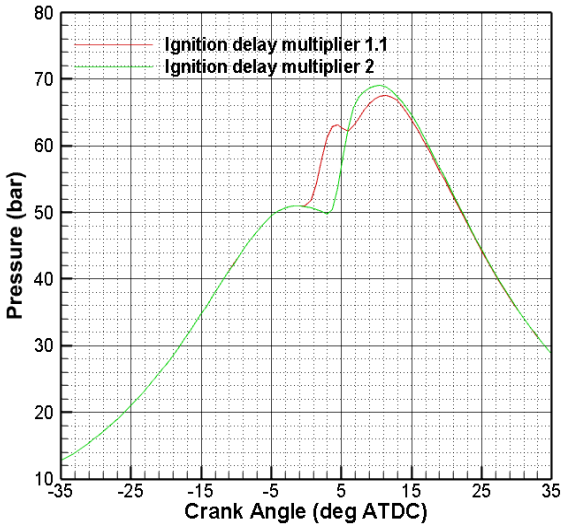

Figure 13 In-cylinder pressure sensitivity to ignition delay multiplier

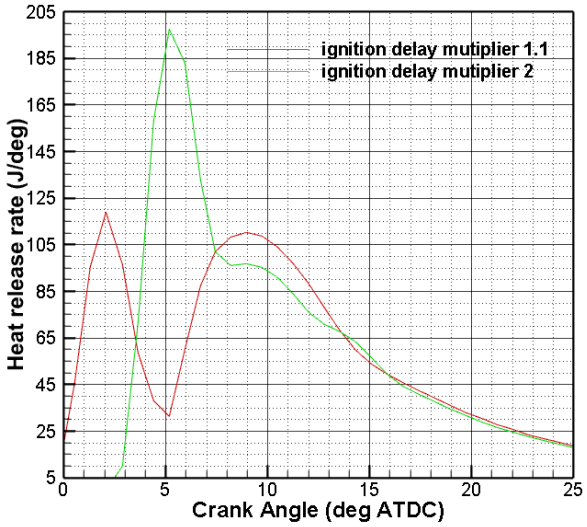

Figure 14 Heat release rate sensitivity to ignition delay multiplier

Table 9 Engine output sensitivity to ignition delay multiplier

	Ignition delay Multiplier 1.1	Ignition delay Multiplier 2
Torque (N-m)	196	196.2
BMEP (bar)	5.5	5.5
BSFC (g/kWh)	245.5	245.2
Burn Duration 10-90%(deg)	53	47
Ignition Delay (deg)	13.4	10.5

Increasing ignition delay multiplier increases the ignition delay. Thus, the fraction of premixed combustion Qpre/Qtotal is higher because more combustible mixture is formed during ignition delay period; accordingly, peak pressures are higher and a higher maximum heat release rate is attained. The longer ignition delay results in a shorter combustion duration Δθburn since a larger fraction of the fuel burns in a premixed fashion.

Premixed/Diffusion Combustion Rate Multiplier

Premixed/Diffusion Combustion Rate Multiplier is used to control the premixed and diffusion combustion rates. Figure 15 and 16 and Table 10 show with the sensitivity with the premixed/diffusion combustion rate multiplier.

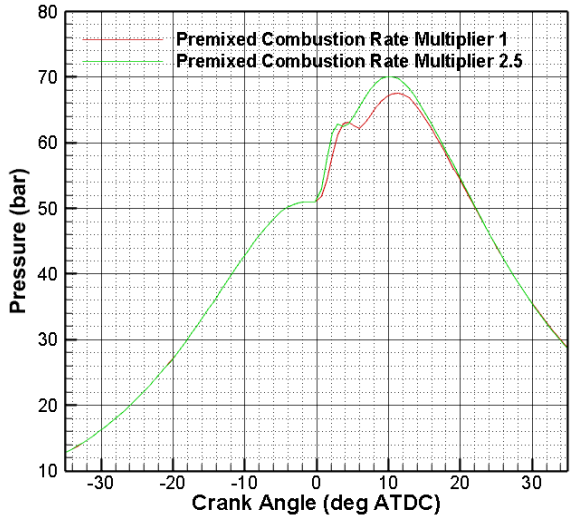

Figure 15 In-cylinder pressure sensitivity to premixed/diffusion combustion rate multiplier

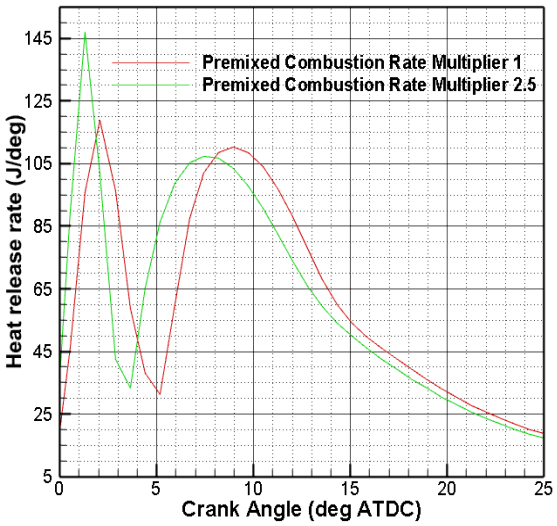

Figure 16 Heat release rate sensitivity to premixed/diffusion combustion rate multiplier

Table 10 Engine output sensitivity to premixed/diffusion combustion rate multiplier

	Premixed Combustion Rate Multiplier 1.1	Premixed Combustion Rate Multiplier 2.5
Torque (N-m)	196	196
BMEP (bar)	5.5	5.5
BSFC (g/kWh)	245.5	245.99
Burn Duration 10-90%(deg)	53	53
Ignition Delay (deg)	13.4	12

A larger Premixed Combustion Rate Multiplier leads to higher premixed combustion rate. Thus, the pressure rise rate is larger ultimately causing a higher peak pressure and advancement of the location of peak pressure. The location of combustion start is nearly unchanged, but the rise rate of premixed combustion heat release increases and location of first peak value advances causing an advance in the diffusion combustion period. In spite of the different rates of heat release curves, the combustion duration is unchanged but the B50 location advances nearly 1.5 degrees. Further, the BMEP and brake torque output is unchanged; the changes to heat release are small compared to those effected by the entrainment and ignition delay multipliers.

Convection Multiplier

Convection Multiplier is used for adjusting the convective heat transfer between cylinder wall and burned mixture. Figure 17 and 18 and Table 11: Summary of fuel property and GT-Power multiplier effects on various combustion phenomena. show the sensitivity of the convection heat transfer multiplier. A higher multiplier increases the rate of heat transfer between the cylinder gas and walls.

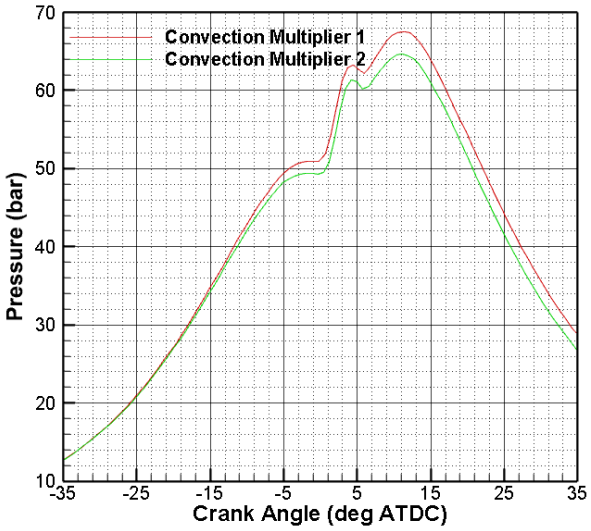

Figure 17 In-cylinder pressure sensitivity to convection multiplier

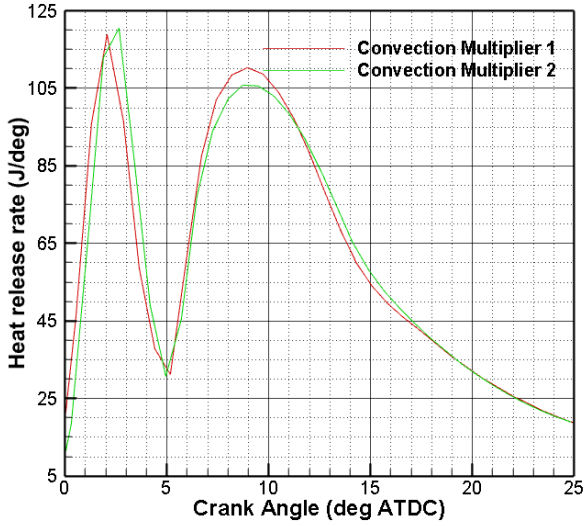

Figure 18 Heat release rate sensitivity to convection multiplier

Table 11 Engine output sensitivity to convection multiplier

	Convection Multiplier 1	Convection Multiplier 2
Torque (N-m)	196	166
BMEP (bar)	5.5	4.65
BSFC (g/kWh)	245.5	290
Burn Duration 10-90%(deg)	53	57
Ignition Delay (deg)	13.4	13.3

Both peak pressure and rate of heat release decrease only slightly as convection multiplier is increased. More dramatically, however, is the steep decrease in BMEP and brake torque with an increase in the convection multiplier. Even though combustion (heat release rate) is largely unaffected by the heat transfer, the increased heat transfer during expansion removes energy that otherwise could have been used for useful work. Also, increasing convection multiplier increases combustion duration as the heat release rate slows toward the later portions of combustion (not shown); location of B50 and ignition delay, however, do not change.

Combination Summary

It is necessary to relate the above discussion to how these parameters will materialize differences in the studied fuel properties, namely CN, AC, and T90. The table summarizes how the various GT-Power parameters can materialize a change in one of the fuel properties. For example, the effect of increasing ignition delay multiplier is nearly the same as decreasing CN. Additionally, changing premixed combustion multiplier is helpful for the effect of changing CN on pressure or heat release rate. AC plays little effect on combustion characteristics and the only part which it impact is flame temperature. Jeihouni, Y. et al [62] provide a relationship between AC and density. Thus, changing fuel density may appropriately capture the change in AC. Several parameters need to be adjusted to capture the effect of distillation temperature. Changing T90 seems to most substantially impact ignition delay, combustion duration, and flame temperature. Thus, it is possible to decrease ignition delay, increase entrainment rate multiplier and premixed multiplier to achieve the same effect of decreasing distillation temperature.

Table 12 Summary of fuel property and GT-Power multiplier effects on various combustion phenomena

Parameter ↑	Pressure	Heat release rate	Ignition Delay	Combustion duration	Location B50	Flame temperature
Cetane number	Decrease	Decrease in the premixed burn magnitude	Decrease	Increase	Postpone	
Aromatic content						Increase
Distillation temperature (T90)		Increase	Increase	Decrease	Advance	Decrease
Density	Decrease	Decrease				Decrease
Heat value	Increase	Increase				
Entrainment Rate Multiplier	Increase	Increase			Advance	Increase
Ignition Delay Multiplier	Increase	Increase in the premixed burn magnitude	Increase	Decrease	Advance	Increase
Premixed combustion Rate Multiplier	Increase	Increase in the premixed burn magnitude			Advance	
Diffusion combustion Rate Multiplier	Increase	Increase in the diffusion burn magnitude		Increase	Advance	
Convection Multiplier	Decrease	Decrease	Increase	Increase		Decrease

4. BASELINE TESTING

4.1 Overview

In order to get an idea of how engine size impacting combustion and emissions, and build a fundamental relationship between light duty engine and medium duty engine, the two engines are tested and simulated at 1500 RPM and nominally 1.88 bar BMEP with injection timing changing from 3° BTDC to 15° BTDC. This study investigates the effects of engine size on diesel engine performance and combustion characteristics (in-cylinder pressure, ignition delay, burn duration, and fuel conversion efficiency) using experiments between two differently sized diesel engines. The engine and combustion characteristics are investigated at various injection timings. Moreover, a 1-D model is used to calculate turbulence and reaction temperature with respect to geometric factors. The results are compared for the same brake mean effective pressure and show that engine size has a significant impact on indicated efficiency, with the larger displaced engine having a higher indicated efficiency than the smaller displaced engine. Although the larger sized engine has higher turbulence intensities, longer burn duration and higher exhaust temperature, the lower area to volume ratio and lower reaction temperature leads to lower heat loss to cylinder wall; the differences in heat loss to cylinder wall between the two engines increases with increasing engine load. In addition, due to smaller volume-normalized friction loss, the larger sized engine has higher mechanical efficiency. In the net, since the brake efficiency is a function of indicated efficiency and mechanical efficiency, the larger sized engine has higher brake efficiency and the

differences in brake efficiency between the two engines increase with increasing engine load.

4.2 Experimental Methodology

Test Engines

The different engines are used in the performance comparisons in this paper. The different engines are a four-cylinder 4.5 L diesel engine, and a four-cylinder 1.9L diesel engine. Some advanced engine technologies that enable the experimental study presented here include a high-pressure common rail fuel system coupled with electronically controlled direct-injection fuel injectors, a variable geometry turbocharger, and a cooled EGR system. Both engines have similar nominal compression ratios and similar combustion chambers. Some engine specifications and the properties of the fuel used in both engines are provided in Table 13 and 14, respectively. The fuel is commercially-available US diesel #2.

Table 13 Specification of the two engines under study

Engine	Medium Duty Engine	Light Duty Engine
Bore	106 mm	82 mm
Stroke	127 mm	90.4 mm
Number of Cylinders	4	4
Displacement Volume	4.7L	1.9L
Compression Ratio	18.3	18.3
IVC timing	-134.4°CA ATDC	-132 ATDC

Table 13 Continued

EVO timing	116 ATDC	106 ATDC
Area to volume ratio (at 0°CABTDC)	0.34 [1/cm]	0.465 [1/cm]
Combustion chamber	Toroidal	Toroidal

Table 14 Summary of the properties of the fuel used in this study

Density (kg/m3) (ASTM D4052s)	825.5
Net heat value (MJ/kg) (ASTM D240N)	43.008
Gross heat value (MJ/kg) (ASTM D240G)	45.853
Sulfur (ppm) (ASTM D5453)	5.3
Viscosity (cSt) (ASTM D445 40C)	2.247
Cetane number (ASTM D613)	51.3
Hydrogen (% mass) (SAE J1829)	13.41
Carbon (% mass) (SAE J1829)	85.81
Oxygen (% mass) (SAE J1829)	0.78
Initial boiling point (C) (ASTM D1160)	173.4
Final boiling point (C) (ASTM D1160)	340.5

The engines were studied at the operating conditions summarized in the following two tables. Notice that an injection timing sweep was studied, where the injection timings were the same for both engines. Recognizing the influence of geometrical features on combustion phasing, the engines were also evaluated at the same 50% mass fraction burned location (CA50) injection timing; these timings for each engine are also shown in the table. Engine speed was controlled by a DC electric motoring dynamometer; where load is controlled through adjustment of the fuel delivery rate.

Table 15 Studied Operating Conditions for low load

Engines	Medium duty (MD) engine conditions / Light duty (LD) engine conditions
Speed (RPM)	1500
Torque (Nm)	67.66 (MD) / 28.56 (LD)
BMEP (bar)	1.88
Fuel flow rates (g/s)	1.003 (MD) / 0.45 (LD)
Injection timings (deg BTDC)	Variable between 6 and 15, in 3 deg increments, for both engines
CA50 (deg BTDC) injection timings	Variable between 8.7 and11.5, depending on engine

Table 16 Studied Operating Conditions for medium load

Engine	Medium duty engine conditions / Light duty engine conditions
Speed (RPM)	1500
Torque (N-m)	203.3 (MD) / 85.85 (LD)
BMEP (BAR)	5.65
Fuel flow rates (g/s)	2.14 (MD) / 1.06 (LD)
Injection timing (deg BTDC)	Variable between 6 and 15, in 3 deg increments, for both engines
CA50 (deg BTDC) injection timing	Variable between 8.7 and11.5, depending on engine
Injection pressure (bar)	450 (MD) / 550 (LD)

The design specifications of the two engines' injectors are reported in Table 17. Both engines have the same number of holes per nozzle and similar spray cone angles. As described below, an engine simulation is used to help distinguish the differences between the two engines. The injection rate profiles which are used in the simulation are shown in Figure 19. Notice the two engines' injectors have similar mass flow rates for each respective load condition, with the exception of injection duration that reflects the different engine displacements. For matching the same BMEP, the fuel flow rates are different, as shown in Table 16. Thus, the needle lift currents, at the same BMEP, between the two engines are different.

Table 17 Summary of injectors' design specifications

Engine	Medium Duty Engine	Light Duty Engine
Injector Type	Denso G4	Bosch CRIP 2.2
Number of Holes per Nozzle	7	7
Spray Cone Angle	147°	149°

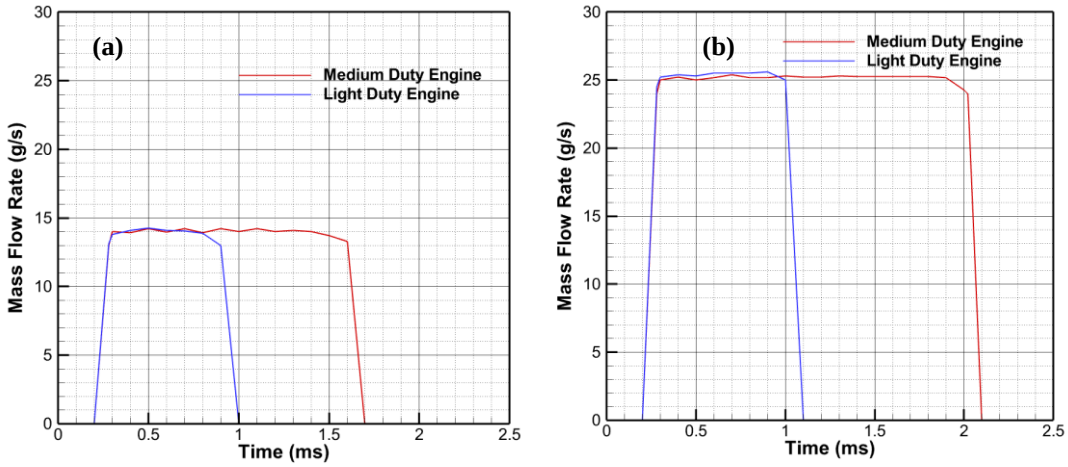

Figure 19: Injection profiles between the two engines at a) low-load and b) medium-load conditions. Each condition is at 1500 rev/min engine speed and injection timing = -9°ATDC

Several measurements are taken at each operating condition from both engines. A typical, commercially-available automotive emission analyzer system (Horiba MEXA 7000) is used to measure gaseous species of NOx, HC, CO, CO_2 and O_2 concentrations in the engine's exhaust and intake (intake CO_2 concentration is measured for calculation

of EGR level). The measuring techniques for the gaseous species are heated chemiluminescence for NOx, heated flame ionization detection (FID) for HC, nondispersive infrared (NDIR) for CO and CO_2, and magneto-pneumatic for O_2. Gas samples are delivered either through sample lines heated to 190°C (to NOx and HC analyzers, and smoke meter) or through sample lines cooled and dehumidified (CO, CO_2, and O_2 analyzers). Each analyzer is calibrated at the start of each test and checked routinely throughout the day's testing. Moreover, a commercially-available smokemeter (AVL 415S) is used to measure smoke concentration, reported as filter smoke number (FSN). Gaseous species, along with speed (optical dynamometer-mounted disk), torque (dynamometer-mounted load cell), fuel flow rate (using positive displacement flow meter), air flow rate (using laminar flow element), and several temperatures (thermocouples) and static pressures (strain-gage transducers) are measured at 1 Hertz.

All crank angle resolved measurements (rail pressure, needle lift, injection current, and in-cylinder pressure) are collected on a 0.2° crank angle basis for 300 consecutive cycles. The analysis is performed on the average of the 300 cycles to integrate cyclic variation and get a good measurement of the true steady-state operation.

In-cylinder pressure is measured from all 4 cylinders of each engine every 0.2º CA using commercially-available (Kistler 6056A) piezo-electric pressure transducers. The ordinary calibration and fidelity checks are carried out according to [63]. The reported pressure data are from a collection of 300 consecutive cycles. A low-pass zero-phase IIR (infinite impulse response) filter is used to remove high frequency reverberations so that relatively smooth heat release rate profiles can be obtained (it is

noted such pressure filtering is carefully monitored to prevent data shifting or excessive loss of signal). A filter order of three is used with a cutoff frequency of about 10% of the sampling frequency (1800 samples/revolution). The filter properties are determined so that the peak value and width of the pressure derivative maximums associated with combustion events are minimally affected.

The engines' in-cylinder pressure traces under a motored condition are shown in Figure 20. The maximum motored cylinder pressures are different. These features suggest the engines' compression ratios are slightly different, in spite of having the same nominal values of 18.3:1 (this is common for actual compression ratios to slightly differ from reported compression ratios). To create a basis of comparison, the effective compression ratio (defined as maximum motored pressure divided by IVC pressure, similar to an effective pressure ratio) is determined and reported as 14.7:1 for the light-duty engine and 14.3:1 for the medium-duty engine. The differences between geometric compression ratio and effective compression ratio are caused by various intake and exhaust valve events. Moreover, differences in in-cylinder pressure are related to different heat transfer during combustion, as described below.

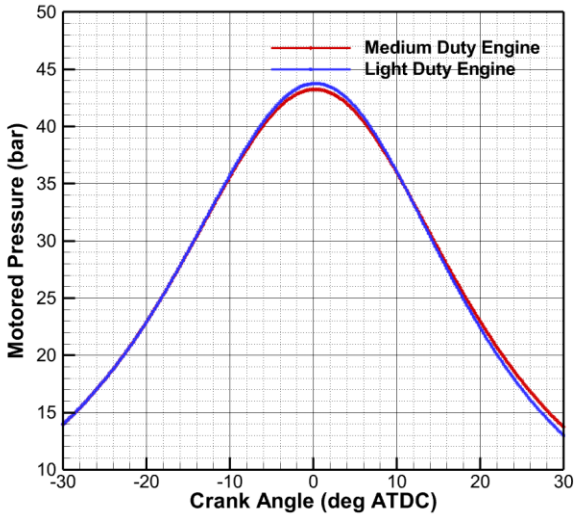

Figure 20: In-cylinder pressure for the two studied engines of different displacement and S/B ratio at a motored condition.

4.3 Results and discussion for effects of displacement and S/B on efficiency

The brake fuel conversion efficiency is a function of net indicated thermal efficiency, combustion efficiency, and mechanical efficiency. In this content, brake fuel conversion efficiency is brake work divided by delivered fuel energy. Net indicated thermal efficiency is net indicated work divided by released fuel energy. Combustion efficiency is released fuel energy divided by delivered fuel energy. Mechanical efficiency is brake work divided by net indicated work. Generally, a shorter burn duration (phased properly), lower heat losses, higher mixture ratios of specific heats, and lower pumping losses result in relatively higher indicated thermal efficiencies. Combustion efficiency tends to be very high in diesel engines (i.e., greater than 98%), but can be impacted by mixture over-leaning, poorly phased combustion, and some

piston ring crevice flow. Mechanical efficiency is impacted by friction losses from piston rings, bearings, and engine accessories. This section investigates all factors impacting the effects of engine size on brake efficiency by using experimental data and simulation for a sweeping injection timing (15° BTDC to 3° BTDC) and low load and medium load conditions (BMEP 1.88 and 5.65 bar, respectively). The uncertainty is calculated for the experimental data corresponding to 95% confidence.

Brake Fuel Conversion Efficiency

Figure 21 shows brake fuel conversion efficiency with different injection timings at the low and medium load conditions of the two engines. Over the range of studied injection timings, both engines show some sensitivity to injection timing but it is not dramatic. Of interest to this study is the difference in efficiency between the two engines. Medium duty engine has a slightly higher brake fuel conversion efficiency at low load condition but a much higher brake fuel conversion efficiency at medium load condition. As mentioned above, the brake fuel conversion efficiency is a function of net indicated thermal efficiency, combustion efficiency, and mechanical efficiency. In order to clarify engine size effect on brake efficiency, factors impacting the three efficiencies will be discussed.

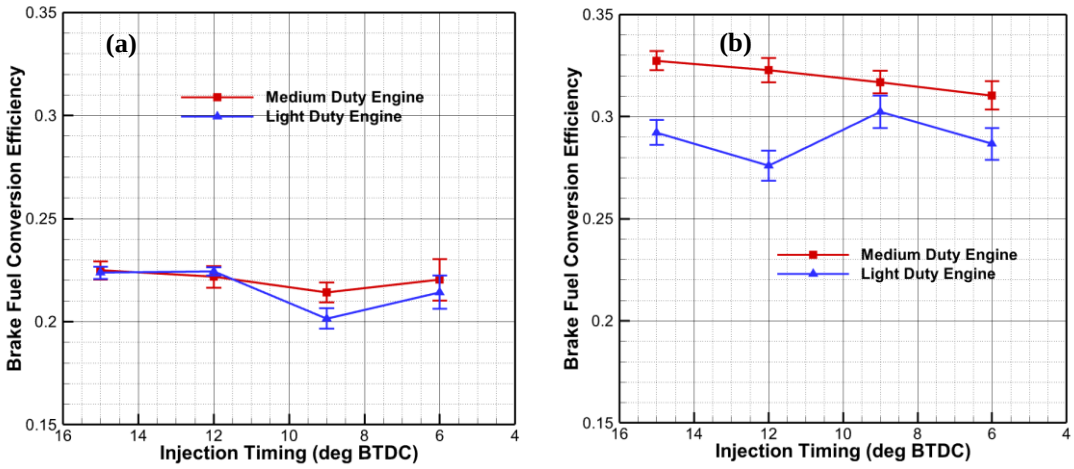

Figure 21: Comparison of brake fuel conversion efficiency between both engines at a) low-load and b) medium-load conditions as functions of injection timing corresponding to 95% confidence.

Net Indicated Thermal Efficiency

Generally, good combustion phasing, shorter burn duration (phased properly), high ratios of specific heats of the burned gas mixture, lower pumping losses (i.e. high pumping efficiency), and lower heat transfer losses result in relatively higher net indicated thermal efficiency. **Figure 22** shows net indicated thermal efficiency of both engines at various injection timings of the low load and medium load conditions. The light duty engine mostly has slightly higher indicated thermal efficiency among the studied injection timings at low load condition, but similar performance at medium load condition. The reason might be that at low load condition, due to shorter ignition delay, combustion of light duty engine is phased better. Thus, in order to isolate combustion phasing effects from engine size effects, the injection timing is adjusted independently

on each engine for matching 50% mass fraction burn locations (8.7°CA ATDC and 11.5° CA ATDC). The comparison of net indicated thermal efficiency at same MFB50 is shown in **Table 18**. Similarly, light duty engine has higher indicated thermal efficiency at low load condition, but similar efficiency at medium load condition. The various phenomena affecting combustion phasing, including ignition delay, combustion duration, and heat transfer are discussed further next.

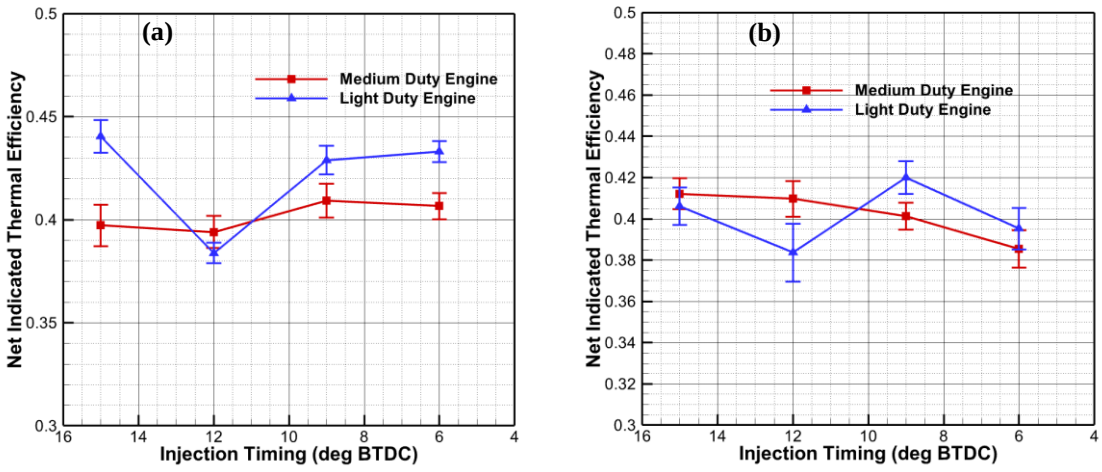

Figure 22: Comparison of net indicated thermal efficiency between the two engines at a) low-load and b) medium-load conditions as functions of injection timing corresponding to 95% confidence.

Table 18: Comparison of net indicated thermal efficiency between the two engines at a) low-load and b) medium-load conditions at the same CA50 location (effected through different injection timings)

Load Conditions	Low Load Condition		Medium Load Condition	
Engine	Medium Duty Engine	Light Duty Engine	Medium Duty Engine	Light Duty Engine
Indicated Thermal Efficiency at 8.7°CA ATDC 50%MFB	0.39	0.43	0.41	0.42
Indicated Thermal Efficiency at 11.5°CA ATDC 50%MFB	0.41	0.43	0.40	0.40

Combustion Efficiency

To continue the analysis of brake fuel conversion efficiency, combustion efficiency, shown in **Figure 23**, quantifies the extent of complete oxidation of fuel burned in the combustion process; combustion inefficiency is revealed by the presence of unburned hydrocarbons (HC) and carbon monoxide (CO) in the exhaust. Both engines at the low and medium load conditions exhibit high combustion efficiency (higher than 98 percent), which is typical of conventional diesel combustion. In detail, the two engines exhibit slightly different trends of combustion efficiency with increasing load;

these are very small and likely insignificant. Higher turbulence intensity on medium duty engine, shown in Figure 27, provides promotion of fuel-air mixture formation, which may contribute to this engine's higher combustion efficiency.

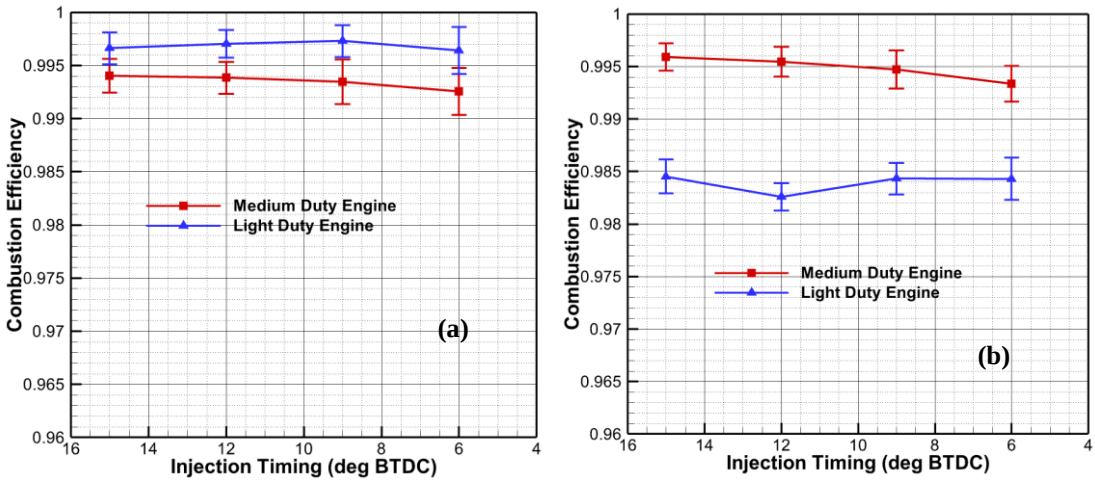

Figure 23: Comparison of combustion efficiency between both engines at a) low-load and b) medium-load conditions as functions of injection timing corresponding to 95% confidence.

Mechanical Efficiency

The final parameter for analysis in the comparison of brake fuel conversion efficiency is mechanical efficiency, which is shown in **Figure 24**a. Further, to assist the analysis, the friction losses of indicated power between both engines are shown in **Figure 24**b. The mechanical efficiency of the medium-duty engine is 6%-10% higher than the light-duty engine at the two load conditions. Generally, contributors to friction include that from piston rings and bearings, pumping losses, and engine accessories.

Although the long-stroke engine causes higher piston velocities and swept surfaces, increasing piston and piston ring losses [64], the higher cylinder pressure with higher effective compression ratio increases the friction from the piston rings and bearings. In balance, the impact of higher effective compression ratio is stronger, resulting in higher mechanical efficiency for the medium-duty engine.

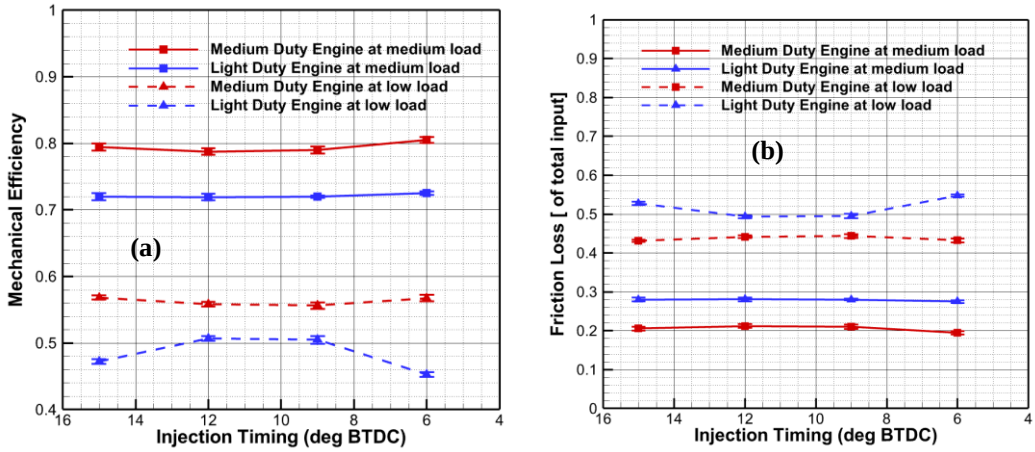

Figure 24 a) Mechanical efficiency and b) friction loss as a fraction of indicated power for both engines at low and medium load conditions as functions of injection timing corresponding to 95% confidence.

Ignition Delay

The variations in ignition delay with respect to injection timing at the two conditions of the two engines are compared in **Figure 25**a. Comparing to light-duty engine, ignition delay of medium-duty engine is higher, but the difference decreases with increasing engine load. Ignition delay is mainly impacted by mixture temperature

and air/fuel (A/F) ratio. Thus, the mixture temperature at injection timing and A/F ratio are shown in **Figure 25**. At the two load conditions, lower mixture temperature and higher A/F ratio (relatively leaner mixture) in medium duty engine seems to result in a longer ignition delay. With increasing engine load, due to increasing mixture temperature at time of injection and decreasing A/F ratio of both engines, ignition delay decreases further. Ignition delay will increase as timing is advanced from top dead center, because the fuel is injected into a lower-temperature environment, thus increasing the time it takes to prepare and ignite the fuel. Similar with net indicated thermal efficiency discussions, the comparison of ignition delay at same MFB50 is shown in Table 19. The light duty engine has shorter ignition delay and the ignition delay difference for the same CA50 is larger than the difference for the same injection timing. The reason is that the light duty engine has relative later injection timing for matching the same CA50 and the ignition delay decreases with injection timing delayed.

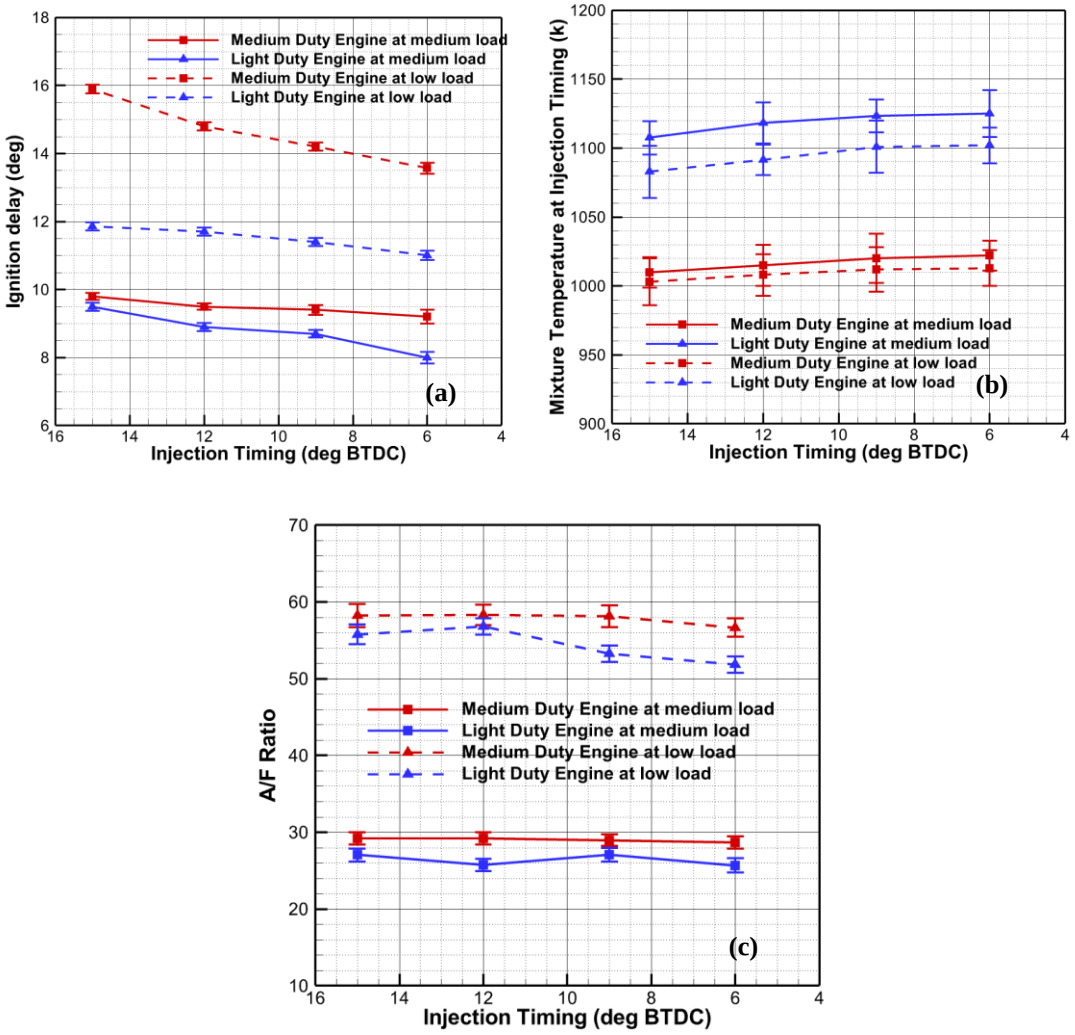

Figure 25 (a) Ignition delay, (b) mixture temperature at time of injection, and (c) air/fuel (A/F) ratio for the two studied engines at low and medium load conditions, as functions of injection timing corresponding to 95% confidence.

Table 19 Comparison of ignition delay between the two engines at a) low-load and b) medium-load conditions at the same CA50 location (effected through different injection timings)

Load Conditions	Low Load Condition		Medium Load Condition	
Engine	Medium Duty Engine	Light Duty Engine	Medium Duty Engine	Light Duty Engine
Ignition delay at 8.7°CA ATDC 50%MFB	14.7	11.3	9.5	8.8
Ignition delay at 11.5°CA ATDC 50%MFB	14.1	10.7	9.3	8.1

Burn Duration

Figure 26 shows the mass fraction burned calculated from measured in-cylinder pressure for the two engines at the same CA50 location ((8.7°CA ATDC and 11.5° CA ATDC), low and medium load conditions. For the two different CA50 locations, the mass fraction burned curves exhibit similar trend with engine size changing. Due to shorter ignition delay of light duty engine (as shown in Table 19), the injection timing is relatively delayed for matching the same CA50 location. Thus, although the light duty engine has shorter ignition delay, later injection timing along with the higher mixture

temperatures (due to higher compression ratio) has stronger impact on burn rate, requiring a slightly delayed combustion start location to achieve matched 50% burn fraction location. For the two load conditions, the mass fraction burned curves of the medium-duty engine are less steep than those of the light-duty engine. The burn rate is a balance result between fuel quantity and in-cylinder flow condition which is impacted by turbulence intensities (as shown in **Figure 27**). The turbulence intensity (u') is calculated using a zero-dimensional turbulence sub-model in the engine simulation. Turbulence intensity behavior through the engine cycles are similar between the engines for different load conditions, which has a rapid increase at the time of intake valve opening, then a gradual decrease due to compression. In the beginning of combustion, turbulence is increased again by the rapid compression of mixture ahead of reaction. Generally, turbulence intensity, especially the first turbulence intensity peak value is impacted by mean flow velocity, which is related to intake flow velocity and piston speed. Thus, at the same engine speed, the medium-duty engine with longer stroke has a higher piston speed which causes the larger first peak; meanwhile, because of more diesel burned in combustion duration, the compression condition of mixture ahead of flame is pronounced, leading to a larger second peak value. The higher turbulence intensity on medium duty engine would tend to result in higher burn rate and shorter burn duration, but the effect of injecting more fuel and higher mixture temperatures (due to higher compression ratio), shown in **Figure 28** in the light-duty engine seems to cause the light-duty engine to have a higher burn rate and thus relatively shorter burn duration.

The mixture gas temperatures of **Figure 28** are calculated assuming ideal gas behavior and using measured in-cylinder pressure and calculated cylinder volume (from measured crankshaft angular location). At low load, **Figure 28**a show that the medium duty engine has lower peak mixture gas temperatures, but maintains a more constant mixture gas temperature over the duration of the combustion event. This may be due to the slightly longer combustion duration and lower compression ratio. As discussed in previous section, the net indicated thermal efficiency is impacted by burn duration and heat transfer losses. In the study, although light duty engine has higher peak mixture gas temperature which tends to increase heat transfer, the effect of shorter burn duration seems to dominate and result in higher indicated efficiency. With engine load increasing, **Figure 28**b shows that the mixture gas temperature increases, but the temperature difference between the two engines decreases when operating at medium load. This would tend to cause the light-duty engine efficiency to increase even further above that of the medium-duty engine. The medium duty engine's burn rate more closely matches that of the light-duty engine, however, at medium load condition, thus making the combustion phasing nearly the same. These observations suggest combustion phasing has a stronger impact on indicated efficiency near the matched MFB50 location than heat transfer.

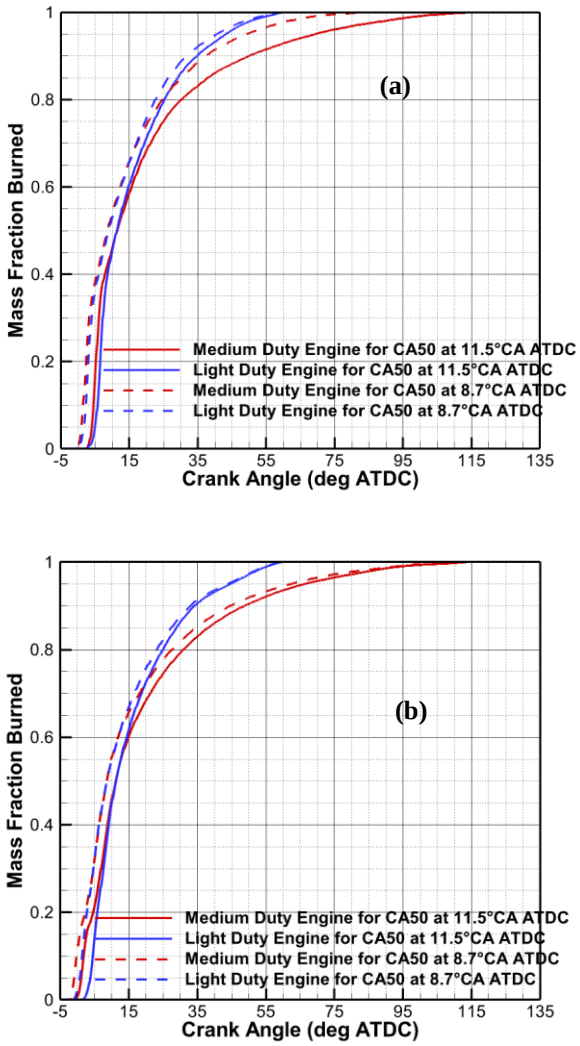

Figure 26 Burned mass faction profiles between the two engines at a) low-load and b) medium-load conditions at the same CA50 location (effected through different injection timings)

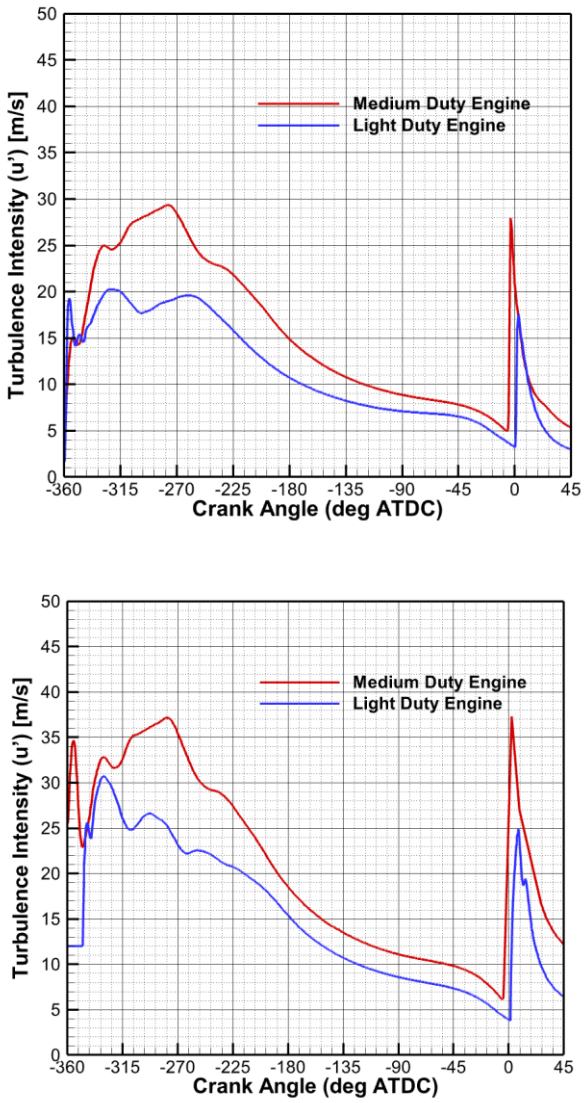

Figure 27 Simulated turbulence intensity for the two studied engines at a) low load and b) medium load conditions, 11.5° CA ATDC CA50 location**.**

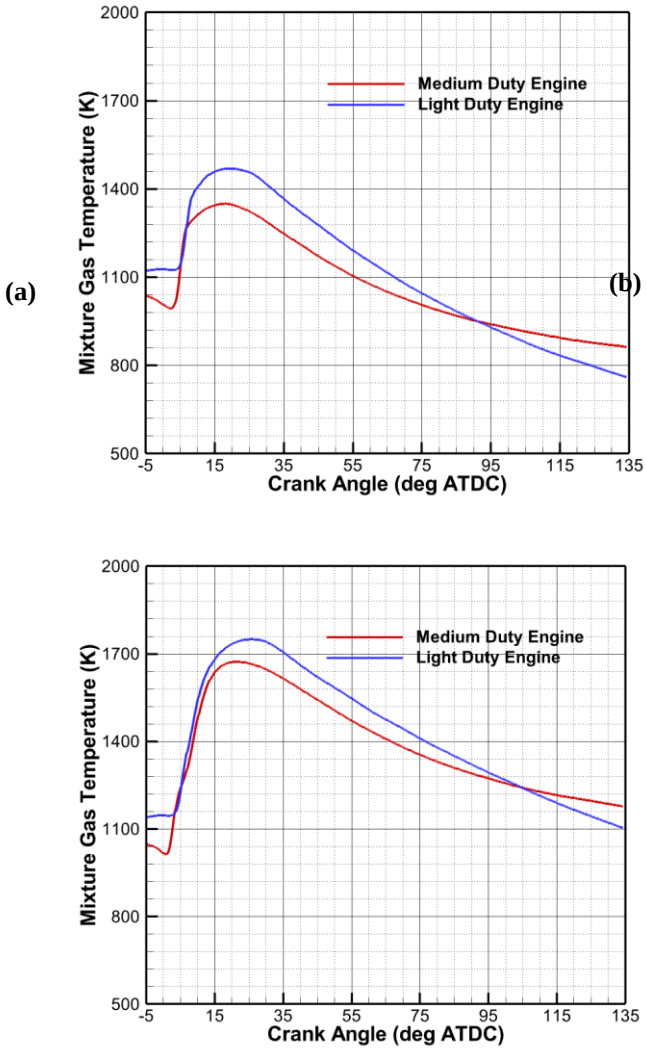

Figure 28 Mixture gas temperature between the two engines at a) low-load and b) medium-load conditions, 11.5° CA ATDC CA50 location (effected through different injection timings)

Heat Transfer to Cylinder Wall

The heat transfer to cylinder walls, as fraction of fuel energy, between the two engines for different load conditions are shown in **Figure 29**. As cylinder size increases,

the fractional heat transfer deceases and this difference increases as engine load increases. Moreover, the fractional heat transfer of light duty engine is more sensitive to injection timing. As explained in burn duration section, mixture gas temperature, as shown in **Figure 28**, impacts heat transfer to cylinder wall; on the other side, with engine size increasing, the ratio of surface area to volume decreases, as shown in Table 13. The final result is lower heat rejection to cylinder wall for the larger-sized engine. As engine load increases, the mixture gas temperature increases for both engines. The coolant fluid temperature of both engines are similar, maintaining at 90-92°C. Higher mixture temperatures mean larger temperature difference between bulk gas and cylinder wall, causing increased heat transfer to cylinder wall. Meanwhile, the proportion of the area-to-volume effect increases, resulting in a larger difference of heat transfer to cylinder wall between two engines. Moreover, the comparison of heat transfer to cylinder wall at same MFB50 is shown in Table 19. Similarly, the light duty engine has higher heat transfer to cylinder wall and the heat transfer differences between the two engines increase with the engine load increasing.

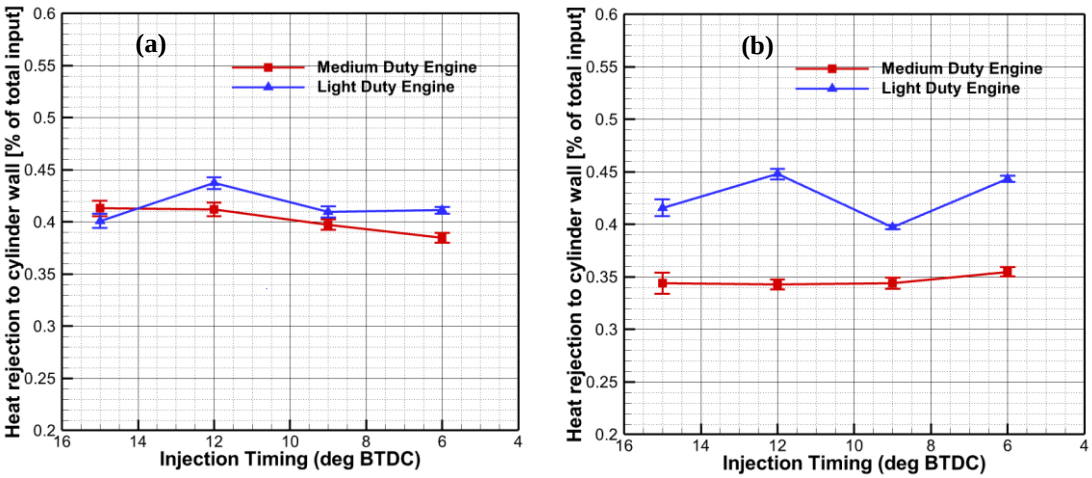

Figure 29 Comparison of heat rejection to cylinder wall between two engines at a) low load and b) medium-load conditions as functions of injection timing corresponding to 95% confidence.

Table 20 Comparison of ignition delay between the two engines at a) low-load and b) medium-load conditions at the same CA50 location (effected through different injection timings)

Load Conditions	Low Load Condition		Medium Load Condition	
Engine	Medium Duty Engine	Light Duty Engine	Medium Duty Engine	Light Duty Engine
Heat transfer to cylinder wall at 8.7°CA ATDC 50%MFB	0.413	0.425	0.343	0.397

Table 20 Continued

Heat transfer to cylinder wall at 11.5°CA ATDC 50%MFB	0.395	0.424	0.344	0.443

5. FACE FUELS TESTING*

5.1 Overview

In order to identify potential of fuel effects on combustion and engine behavior between light- and medium duty diesel engines, tests were performed with a single injection strategy, the timing of which was switched from 15 BTDC to 6 BTDC and controlled to maintain a constant combustion phasing (CA 50 –10deg ATDC) at all loads either. Injection quantity was adjusted for different duty engines, to match the same BMEP output. Boost pressure and injection pressure were kept the same value between two different duty engines.

5.2 Results and discussion for effect of cetane number on combustion and emissions between different duty engines

In order to discuss the potentially changing influence of CN on efficiency and emissions as engine size changes, it is best to first study the effects and potential differences of CN on combustion characteristics. To this end, the effects of CN on combustion characteristics are quantified using experimental data for a sweeping injection timing (15° before top dead center (BTDC) to 3° BTDC) at low load and medium load conditions (1.88 and 5.65 bar BMEP, respectively) between the MD and LD engines. As described above, combustion phasing effects are isolated from CN and engine size effects by matching the 50% burn location for both engines, loads, and fuels, to equal 10°ATD

*Section 5.3 is reprinted with permission from Li, J., Bera, T., Parkes, M., and Jacobs, T., "A Study on the Effects of Cetane Number on the Energy Balance between Differently Sized Engines," SAE Technical Paper 2017-01-0805, 2017

Heat Release Rate

As shown in Figure 30 increasing the CN advances combustion phasing of both engines, under both load conditions. Figure 30(a) shows heat release rate (HRR) with crank angle for both engines and fuels at low load (-12° after top dead center, or ATDC, injection timing) while Figure 30(b) shows the same at mid load (-9° ATDC injection timing). Increasing the CN decreases the magnitude of the peak HRR for the MD engine, and advances its location for both engines at both load conditions. The relative advance in heat release of the LD engine relative to the MD engine for both load points and fuels is attributed to the compression ratio being slightly higher for the LD engine. This caused the temperatures, and pressures (with the pressures shown in Figure 20) to be higher at start of injection. This effect appears amplified at the mid load condition, where injection timing is slightly later. Moreover, a clear dual-stage HRR in the MD engine at the medium load condition, operating on the high CN fuel (Figure 30 (b)) can be observed. This does not appear in the LD engine under the same load condition and fuel. In fact, this observation reveals the MD engine's higher sensitivity to CN than the LD engine. The reason may be due to a longer burn duration and lower heat transfer to the cylinder walls of the MD engine. This concept is explored in more detail below.

Figure 31 and Figure 32 show the HRR for the two studied fuels at the same 50% mass fraction burn location, at the low and medium load conditions for both engines. Contrary to the matched injection timing data of Figure 30, increasing the CN increases the magnitude of the HRR and advances its location for both engines at low load

conditions. This result is attributed to the nearly all-premixed burn taking place at low load; since both fuels' mixtures are nearly fully-premixed, the chemical component of ignition delay of the higher CN fuel causes it to ignite and burn more rapidly allowing a higher ROHR (compared to the low CN fuel). The opposite phenomenon is observed at medium load (Figure 32). Now, at the higher load condition requiring a longer injection duration, the short ignition delay of the high CN fuel causes a necessary fraction of diffusion burning, leading to less premixed burn and lower HRR magnitude.

Another noticeable difference resulting from the two different fuels is a low temperature heat release rate (LTHR) for the low CN fuel observed in both engines. This is particularly noticeable at the low load condition. LTHR is not observed for the high CN fuel under any test condition. The magnitude of the LTHR is larger in the MD engine and this could be due to both a longer lift-off length (made possible by the larger bore) and / or the compression ratio being slightly lower. Both factors will cause the resulting temperatures and pressures to be lower and increasing the magnitude of the LTHR. With increasing engine load the observable magnitude of the LTHR decreases, and indeed, cannot be observed in the LD engine under medium load. It should be noted that this result doesn't suggest that the LD engine, or indeed the high CN fuel do not have LTHR reactions, rather the transition to high temperature heat release, masks the appearance of LTHR in the ROHR profiles.

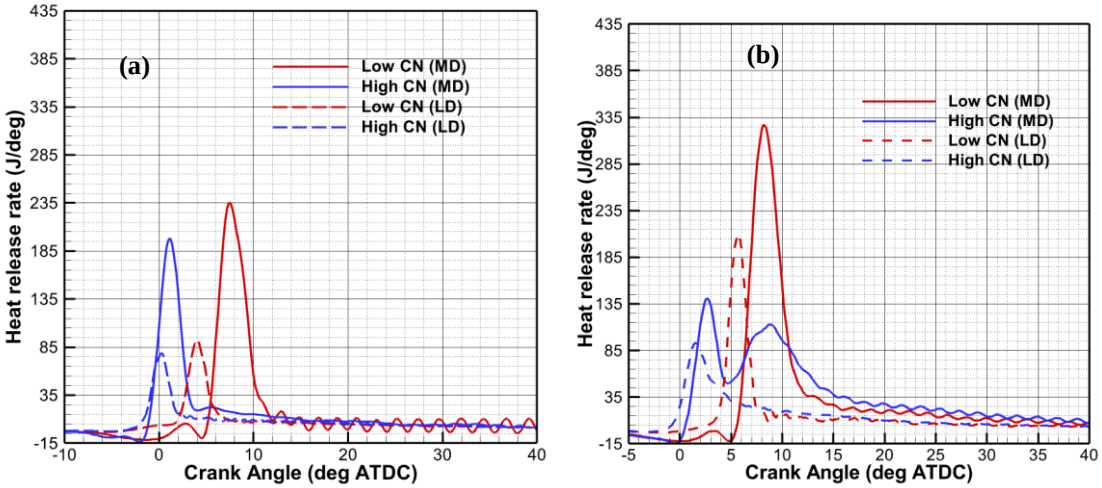

Figure 30 Heat release rate for the medium-duty (MD) and light-duty (LD) engines at a) low load (1500 RPM, nominally 1.88 bar BMEP, -12° after top dead center, or ATDC, injection timing) and b) medium load (1500 RPM, nominally 5.65 bar BMEP, -9° ATDC injection timing) conditions

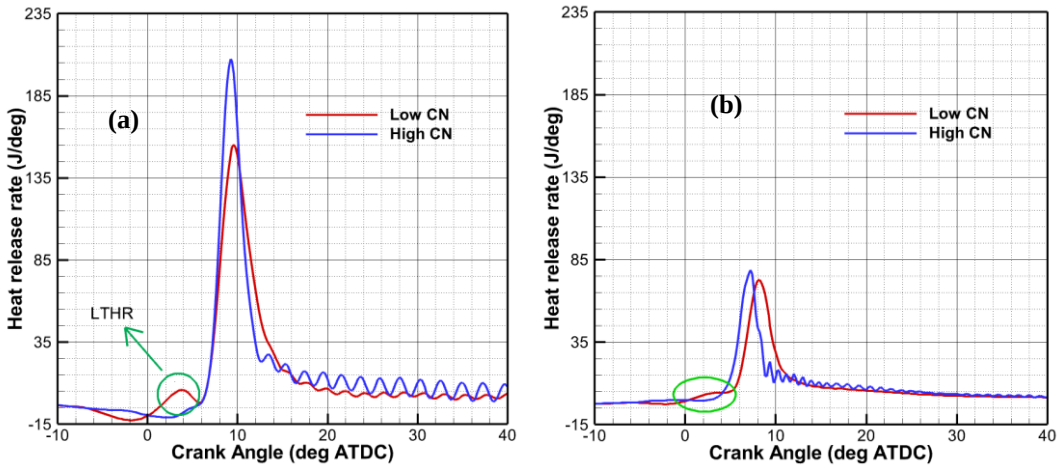

Figure 31 Heat release rate of the two studied CN fuels of a) MD engine and b) LD engine operating at the same CA50 location (effected through different injection timings) and low load condition

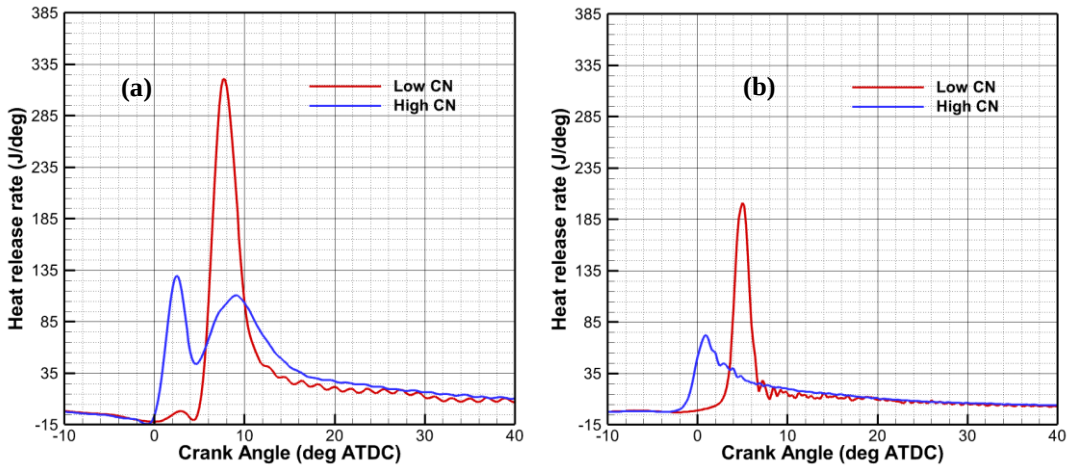

Figure 32 Heat release rate of the two studied CN fuels of a) MD engine and b) LD engine operating at the same CA50 location (effected through different injection timings) and medium load condition

Ignition Delay

The results of Figure 30 through Figure 32 are supported by the various ignition delays, shown in Figure 33. Again, as expected, increasing CN decreases ignition delay (defined as time between start of injection and 1% mass fraction burned location) for both engines at both load conditions. The ignition delay of the MD engine was relatively longer than the LD engine, which corresponds to the observed HRR trends discussed above. It was also noticed that the difference in the MD engine's ignition delay, due to changing CN, was larger than the LD engine's difference. This was true for most of the test conditions. Specifically, the ignition delay at the low load condition (12° BTDC injection timing) changed by over 4 crank angle degrees for the MD engine, while it changed by less than 2 crank angle degrees for the LD engine, as the fuel was changed from the low to high CN fuel. Similarly, ignition delay at the medium load condition (9° BTDC injection timing) changed by 5 crank angle degrees for the MD engine, while it changed by approximately 2 degrees for the LD engine, as the fuel changed from the low to high CN fuels. Moreover, it is worth noting that the MD engine misfired when injection timing was delayed further. This may have been due to a relatively longer ignition delay, and a lower in cylinder pressure and temperature.

One trend that may be interesting to note is the at-times increasing ignition delay with the MD engine at both low load and medium load conditions for the low CN fuel, and for the high CN fuel at late injection timings. It seems this increasing ignition delay

trend as injection timing retards is due to the MD engine's start of main combustion occurring later in the expansion stroke. This same behavior does not seem to happen with the LD engine, where start of main combustion occurs before or near TDC. Again, the difference in start of main combustion between the two engines, as described above, seems to be due to lower in-cylinder temperatures resulting from the small difference in compression ratio.

The variations in ignition delay of the two CN fuels under matched 50% MFB conditions are compared in Table 21. Similar to the observed behavior at same injection timings (Figure 33), increasing CN reduces the ignition delay (start of injection to 1% MFB). The magnitude of the change due to increasing CN in ignition delay increases with increasing engine load. It should be noted that for the matched 50% MFB location, injection timings are adjusted to different values. This result in different mixture temperatures of the studied conditions thus preventing a direct comparison in data presented between Table 21 and Figure 33.

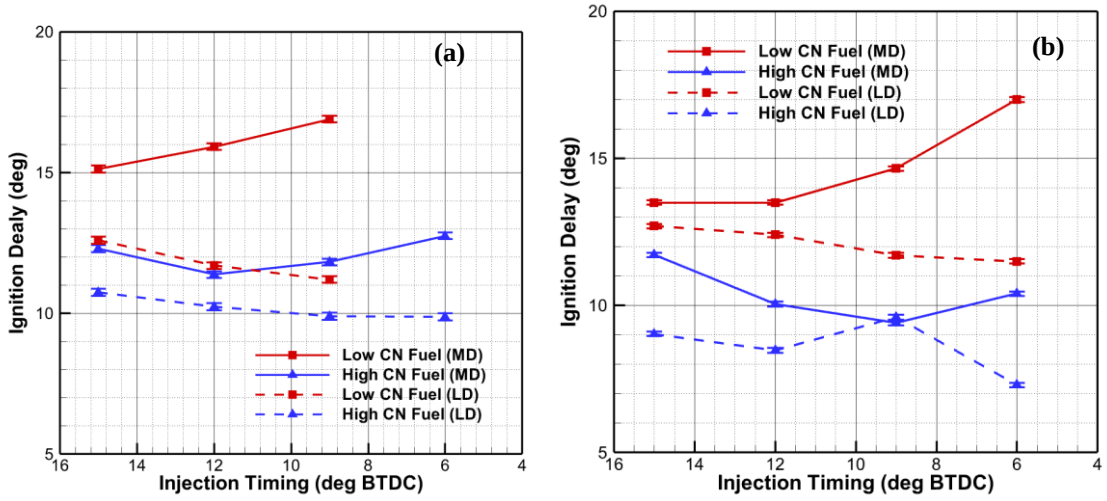

Figure 33 Ignition Delay for the MD and LD engines at a) low load and b) medium load conditions with the two studied CN fuels as functions of injection timing.

Table 21 Ignition delay for the two engines at the same CA50 location, low and mid load conditions (effected through different injection timings)

Ignition delay (degrees)	Low load	Medium load
MD engine	15 (low CN) 12.7 (high CN)	14.7 (low CN) 9.37 (high CN)
LD engine	11.2 (low CN) 9.3 (high CN)	12.1 (low CN) 6.7 (high CN)

Mass Fraction Burned

Figure 34(a) show the relationship between mass fraction burned (MFB) and crank angle for both engines and fuels at low load (12° BTDC, injection timing) while Figure 34(b) shows the same at mid load (9° BTDC injection timing). An increase in CN advances combustion phasing and increases the combustion duration of both engines at both load conditions. This agrees with HRR and ignition delay characteristics discussed above. Moreover, Figure 35 and 8 show the MFB curves with the two fuels at the matched 50% MFB location for both the low and medium load conditions and both engines. The MFB curves with the two fuels at the matched 50% MFB location are similar to the observed characteristics at the same injection timings.

It should be noted that the initial burn rate of low CN fuel at the low load condition (Figure 35) is very low. This corresponds to the LTHR period in the HRR plot shown in Figure 31. After the LTHR burn period, the two fuels have similar burn rates,

until the mass fraction burned reaches near 60 percent. In later phases of combustion, increasing the CN reduces the burn rate resulting in a longer burn duration.

At the mid load condition (Figure 36) the time taken for high CN fuel to ignite is relatively shorter. This reduces the burn rate and leads to a longer burn duration. The influence of LTHR does not appear at medium load on the MFB curve for either engine.

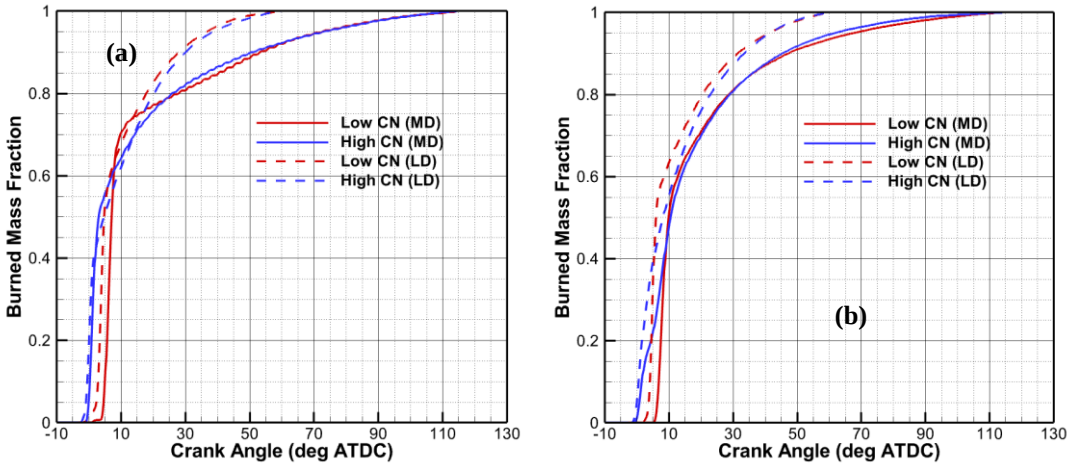

Figure 34 Mass fraction burned for the medium-duty (MD) and light-duty (LD) engines at a) low load (1500 RPM, nominally 1.88 bar BMEP, -12° after top dead center, or ATDC, injection timing) and b) medium load (1500 RPM, nominally 5.65 bar BMEP, -9° ATDC injection timing) conditions

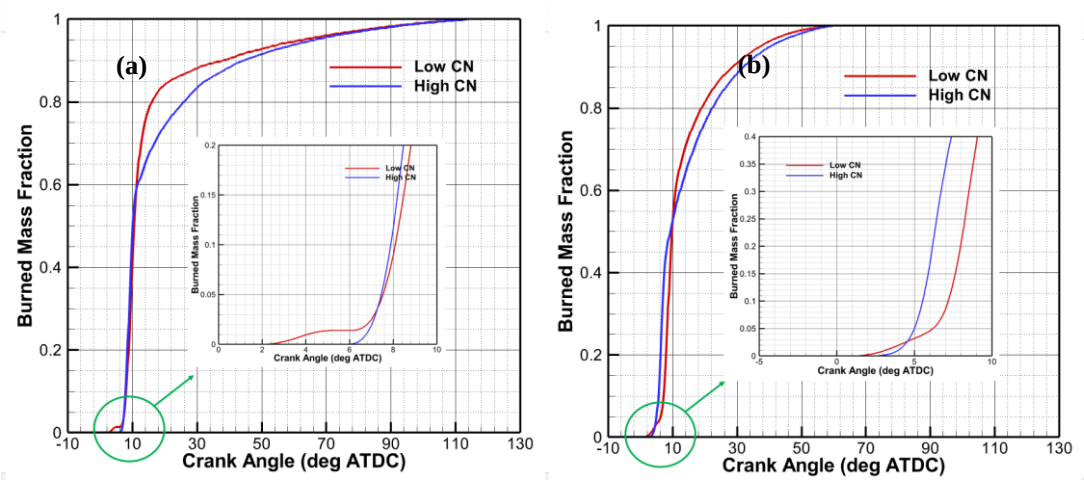

Figure 35 Mass fraction burned profiles of the two studied CN fuels of a) MD engine and b) LD engine operating at the same CA50 location (effected through different injection timings) and low load condition

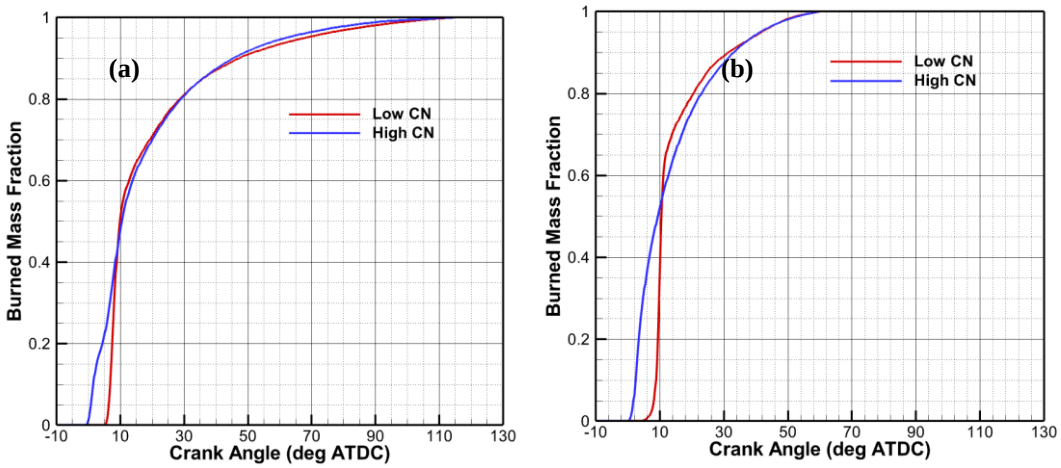

Figure 36 Mass fraction burned profiles of the two studied CN fuels of a) MD engine and b) LD engine operating at the same CA50 location (effected through different injection timings) and medium load condition

Net Indicated Fuel Conversion Efficiency

The results presented in the above section enable analysis of the net indicated fuel conversion efficiency (IFCE). The net IFCE is the product of net indicated thermal efficiency (ITE) and combustion efficiency (CE). It is essentially the net indicated work divided by the delivered fuel energy. It follows that the net ITE is the net indicated work divided by the released fuel energy. CE is the released fuel energy divided by the delivered fuel energy. This metric quantifies the extent of combustion from a heat release perspective.

Figure 37 shows net IFCE for the two different fuels at both the low and medium load conditions in both engines. For both engines, CN has a small and non-conclusive effect on the net IFCE at the low load condition. At the medium load condition, increasing CN generally decreases the net IFCE for the MD engine, and increases net IFCE for the LD engine. The net IFCE at same 50% MFB location, shown in Table 22, are similar to the observed performance at the same injection timings; there is, however, a dramatic increase in IFCE for the LD engine at medium load condition with increased CN.

Generally a shorter burn duration (phased correctly), lower heat losses, and better combustion results in relatively higher IFCE [6]. At the low load condition there appears to be a near-equal trade-off between the higher combustion efficiency of the high CN fuel (which can increase net IFCE and discussed more thoroughly in the below section),

and the longer burn duration of the high CN fuel (which can reduce net IFCE and as shown in Figure 36(b)).

The medium-load condition, however, first reveals the different sensitivity of the LD engine to CN effects than MD engine. As shown in Table 22, IFCE decreases a small amount for the MD engine at medium load, but increases by a large amount for the LD engine at medium load. A small part of this is different burn durations, as can be seen in Figure 36. More dominantly, however, seems to be combustion efficiency effects. These effects are discussed next.

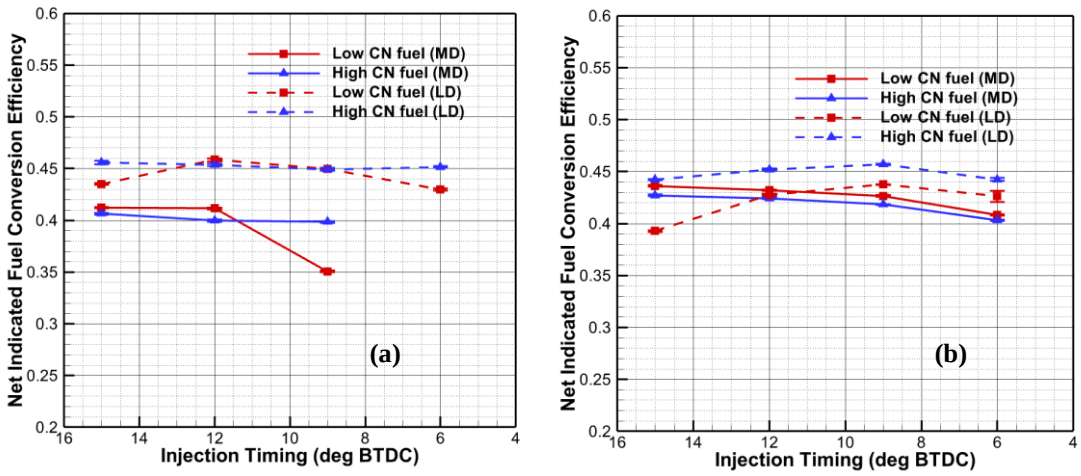

Figure 37 Net Indicated Fuel Conversion Efficiency for the MD and LD engines at a) low load and b) medium load conditions with the two studied CN fuels as functions of injection timing

Table 22 Net Indicated Fuel Conversion Efficiency for the two engines at the same CA50 location, low and mid load conditions (effected through different injection timings)

Net Indicated Fuel Conversion Efficiency	Low load	Medium load
MD engine	0.385 (low CN) 0.393 (high CN)	0.428 (low CN) 0.417(high CN)
LD engine	0.455 (low CN) 0.46 (high CN)	0.426 (low CN) 0.441 (high CN)

Combustion Efficiency

Continuing the discussion concerning differences in IFCE between the two fuels and engines, the variations in combustion efficiency with respect to the two fuels at the test conditions are compared in Figure 38. Increasing CN increases the combustion efficiency of both engines at both load conditions. It is worth noting that the MD engine's combustion efficiency drops dramatically when the injection timing was delayed to 9° BTDC; further retard in injection timing caused engine misfire. These behaviors support the ignition delay characteristics discussed above and in the context of Figure 33. The sensitivity of the combustion efficiency on the CN for different sized engines changes with engine load. At the medium load condition, the impact of CN on

the combustion efficiency of the MD engine is small; as discussed above, the longer burn duration of the high CN fuel resulted in a lower IFCE. The opposite, however, is true for the LD engine which seems to have a much higher sensitivity (at least in the context of CE, which is calculated from measurements of HC and CO emissions) to CN than the MD engine. Specifically, note the CE increases by around 2 percentage-points in the injection timing range used to achieve a 50% MFB location of 10° ATDC (i.e., the timing corresponding to those data shown in Table 22. This 2 percentage-point increase is nearly equal to the difference in IFCE for the LD engine at MD conditions. Thus, in spite of having a slightly longer combustion duration at medium load with the high CN fuel (Figure 36(b)), the substantially higher combustion efficiency at medium load with the high CN fuel causes the LD engine's efficiency to increase with higher CN. Although this is a rather nuanced result, it's important to note the differing sensitivity of an engine's combustion and efficiency behavior to CN based on its size. The discussion will now transition to evaluating potential differences in emissions between the two engines.

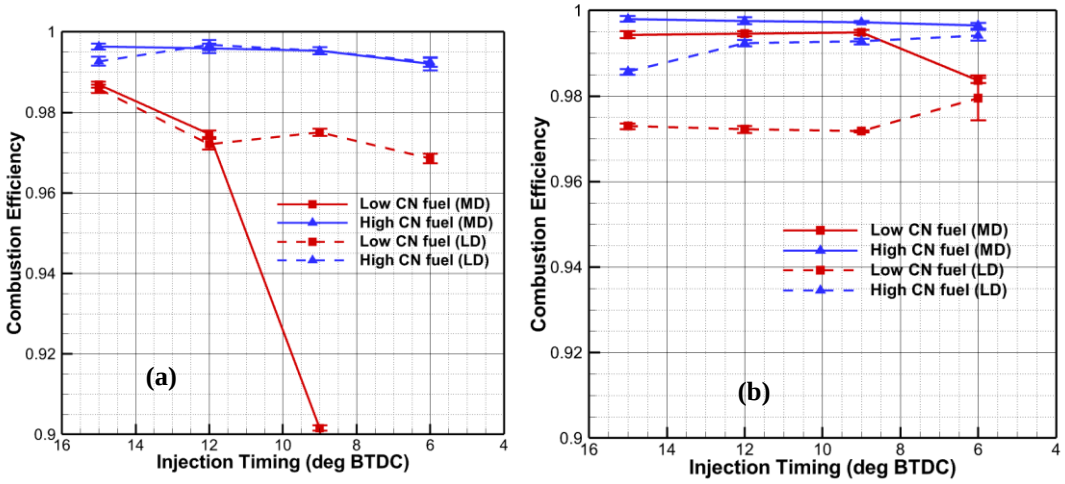

Figure 38 Combustion efficiency for the MD and LD engines at a) low load and b) medium load conditions with the two studied CN fuels as functions of injection timing

Brake Specific Nitrogen Oxides

Figure 39 shows the brake specific nitrogen oxides (BSNOx) emissions with respect to the two fuels, the two conditions, and the two engines at the same injection timing. At the low load condition, the high CN fuel resulted in lower NOx emissions on both engines for most test conditions. The low CN fuel appears to cause higher NOx emissions because the long ignition delay leads to a higher fraction of pre-mixed combustion. Pre-mixed combustion leads to a higher rate of heat release (ROHR) and thus higher reaction temperatures. It follows that high CN fuel (which give rise to lower ROHR, but has a longer combustion duration) leads to lower NOx emissions. As NOx emissions are linked to temperature [6] the higher fraction of premixed combustion and higher (ROHR) leads to higher NOx emissions.

At the medium load condition, ignition delay is shorter with the high CN fuel in the MD engine, and advances combustion. The resulting low premixed heat release and long diffusion heat release results in lower overall burn temperatures. In contrast, low CN fuel increases ignition delay and leads to relatively high percentage of premixed combustion, leading to a larger HRR. These factors tradeoff to a smaller extent with the LD engine, where the high CN fuel had slightly higher NOx emissions than the low CN fuel.

Table 23 shows the BSNOx emissions for the matched 50% MFB locations at the low and medium load conditions of both engines. Similar to the BSNOx emissions at the matched injection timings, the low CN fuel has higher BSNOx emissions for both engines at the low load condition. Correspondingly, the low CN fuel results in higher BSNOx emissions in the MD at medium load, but slightly lower BSNOx emissions for the LD engine at medium load. The differing trend of BSNOx for the LD engine at medium load is again believed to be attributed to the LD engine's different sensitivity to CN, in the context of hydrocarbons and combustion efficiency. Specifically, the higher BSNOx with low CN fuel at low load and medium load for MD engine all seem to be largely related to the CN effects on combustion. The LD engine at medium load, however, experiences a large difference in combustion efficiency; specifically, the higher CN fuel has a higher combustion efficiency. It is believed that the more complete burn perhaps contributes to higher NOx formation for the LD engine at medium load condition, in spite of the overall longer burn duration presumably at lower temperatures (i.e., in spite of the CN effects on combustion, which seem to dominate the NOx

behavior at other conditions for both engines). The same idea might explain why BSNOx for the MD engine using low CN fuel falls below that of the high CN fuel at the 9° BTDC injection timing (Figure 39); this point also corresponds to that where combustion efficiency is also low (Figure 38)

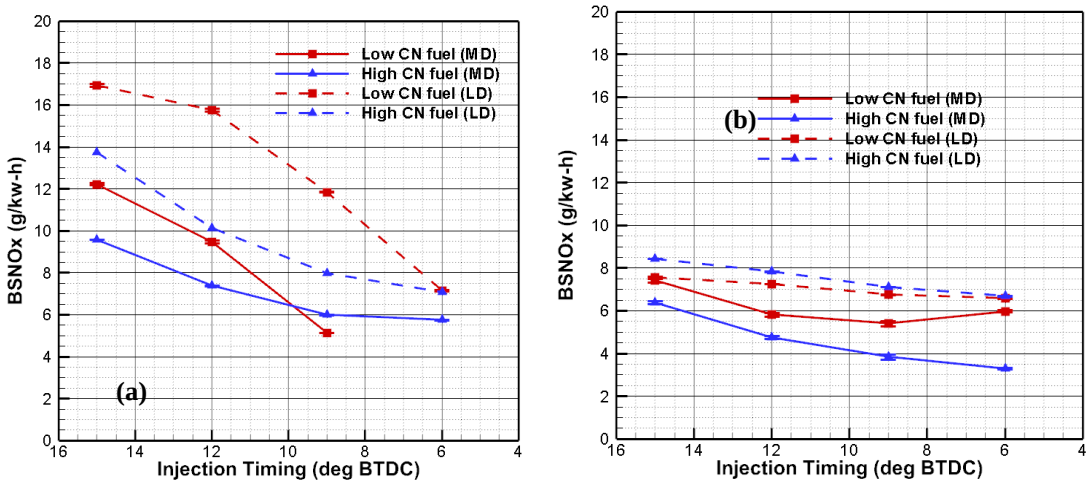

Figure 39 BSNOx for the MD and LD engines at a) low load and b) medium load conditions with the two studied CN fuels as functions of injection timing

Table 23 BSNOx for the two engines at the same CA50 location, low and mid load conditions (effected through different injection timings)

BSNOx (g/kW-h)	Low load	Medium load
MD engine	7.9 (low CN) 5.83 (high CN)	5.27 (low CN) 3.97 (high CN)
LD engine	11.06 (low CN) 7.32 (high CN)	6.58 (low CN) 6.68 (high CN)

Filter Smoke Number

In general, it would be expected that filter smoke number (a surrogate indication of soot and in some cases particulate matter) follows an opposite trend of BSNOx emissions, considering the common soot-NOx tradeoff of diesel combustion. A high combustion temperature will typically lead to a lower FSN, while a low combustion temperature will typically lead to a higher FSN. Figure 40 shows the filter smoke number (FSN) with respect to the two fuels at the low and medium load conditions for both engines at the same injection timing. As expected, FSN is effectively the opposite of NOx emissions. That is, the high CN fuel results in a higher FSN for both engines.

At low load, it should be noted that for all the test conditions, the FSN is very small (lower than 0.17). This implies that FSN is very sensitive to changing in-cylinder conditions, such as the local A/F ratio etc. This is also reflected in the large uncertainty bars for these data. At the medium load condition, increasing the CN increases FSN on both MD and LD engines. It appears that in the MD engine, as injection timing is swept from 15˚BTDC to 6˚BTDC, FSN number increases. This trend for the MD engine when using the low CN, however, is not as strong (and even changes direction at later injection timings). This result suggests that injection timing has a relatively smaller influence on the relative roles of premixed and diffusion burning with the low CN fuel. In other words, the low CN fuel is (for these studied timings) dominating the ignition delay behavior rather than in-cylinder conditions at the start of injection. This likely only

happens within the MD engine because of the size influence in mixture preparation for in-cylinder ignition.

Table 24 shows the FSN for the two studied fuels at the same 50% MFB location, at the low and medium load conditions of both engines. The FSN behavior with matched CA50 in general is similar to that for the same injection timing study. The high CN fuel generated a higher FSN for both engines at the low load condition and the MD engine at medium load condition. As discussed above, the medium load condition of the LD engine has an opposite trend to the other conditions, but consistent with the BSNOx behavior. In other words, the soot-NOx tradeoff is present at this condition, and is consistent with the suggestion that the high CN fuel causing a higher combustion efficiency is dominating the combustion phasing effects.

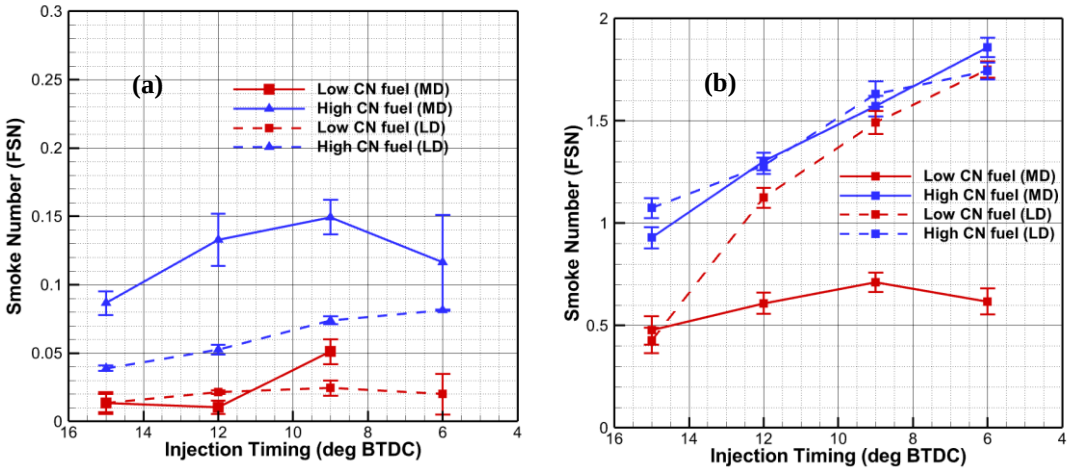

Figure 40 Smoke number for the MD and LD engines at a) low load and b) medium load conditions with the two studied CN fuels as functions of injection timing

Table 24 FSN for the two engines at the same CA50 location, low and mid load conditions (effected through different injection timings)

FSN	Low load	Medium load
MD engine	0.009 (low CN) 0.116 (high CN)	0.71 (low CN) 1.57 (high CN)
LD engine	0.0195 (low CN) 0.083 (high CN)	1.75 (low CN) 1.74 (high CN)

Brake Specific Hydrocarbon

Figure 41 shows brake specific hydrocarbon (BSHC) emissions with respect to the two fuels, at the low and medium load conditions, and for both engines. Generally, higher combustion efficiency results in lower HC emissions. As the high CN fuel yielded a higher combustion efficiency, BSHC emissions decreased with increasing CN for both engines (this matches the trends presented in Figure 6) Increasing CN has strong effect on reducing the HC emissions, and this is especially true for the late injection strategies at the low load condition (9˚ and 6˚ BTDC). At low load and 9˚ BTDC, BSHC decreased by 25 g/kWh for the MD engine, and 12 g/kWh for the LD engines, as CN increased from 30.3 to 56.2.

Table 25 shows BSHC emissions at the same CA50 location, at the low and medium load conditions of both engines. BSHC emissions decreased with increasing CN for both engines, which corresponds to the trends seen for combustion efficiency.

Table 25 BSHC for the two engines at the same CA50 location, low and mid load conditions (effected through different injection timings)

BSHC (g/kW-h)	Low load	Medium load
MD engine	9.55 (low CN) 0.718 (high CN)	0.56 (low CN) 0.075 (high CN)
LD engine	6.84 (low CN) 1.35 (high CN)	1.21 (low CN) 0.62 (high CN)

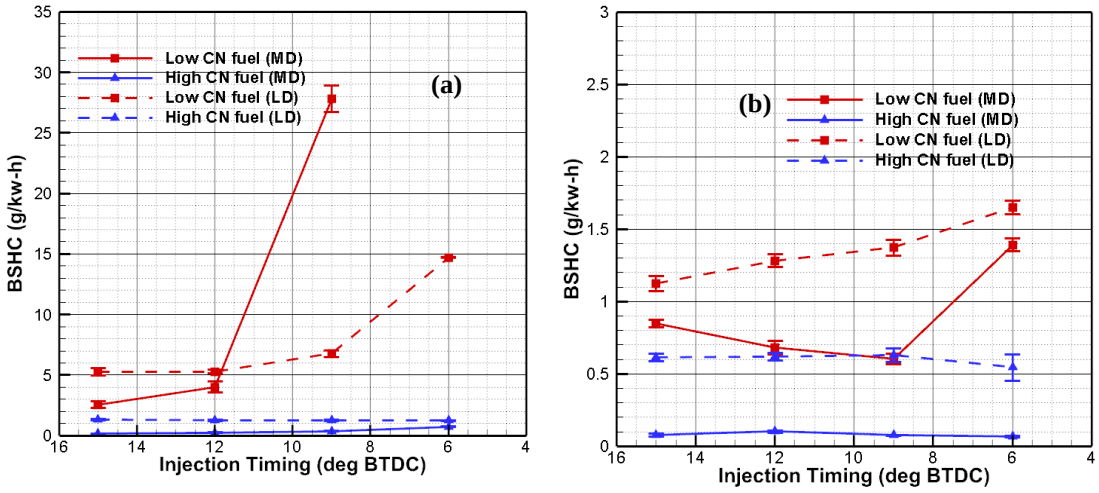

Figure 41 BSHC for the MD and LD engines at a) low load and b) medium load conditions with the two studied CN fuels as functions of injection timing

5.3 Results and discussion for effect of cetane number on energy balance between different duty engines

This section investigates the effect of the cetane number (CN) of a diesel fuel on the energy balance between a light duty (1.9L) and medium duty (4.5L) diesel engine. The two engines have a similar stroke to bore (S/B) ratio, and all other control parameters including: compression ratio, cylinder number, stroke, and combustion chamber, have been kept the same, meaning that only the displacement changes between the engine platforms. Two Coordinating Research Council (CRC) diesel fuels for advanced combustion engines (FACE) were studied. The two fuels were selected to have a similar distillation profile and aromatic content, but varying CN. The effects on the energy balance of the engines were hence recorded at two operating conditions; a "low load" condition of 1500 rev/min (RPM) and nominally 1.88 bar brake mean effective pressure (BMEP), and a "medium load" condition of 1500 RPM and 5.65 BMEP. Results were recorded at the same crank angle 50% burn (CA50) condition to decouple fuel effects from engine effects. The results show that the CN of the fuel impacts the distribution of supplied fuel energy in both engine systems. At the low load condition, a decrease in the fractional cylinder heat transfer is seen for the medium duty engine as CN increases. In general, the sensitivity of the engines to CN is found to increase as engine load increases. At the medium load condition, the observed differences in the fractional heat transfer are larger, and this is especially true for the medium duty engine.

This in turn balances the tradeoff between the changes in mixture temperatures and combustion durations. Moreover, as the CN increases, the energy lost to the exhaust increases for both engines at the medium load condition. This is in contrast to the low load condition, where increasing the CN increases the energy in the exhaust of the medium duty engine, but decreases the energy in the exhaust of the light duty engine. Finally, at the low load condition, a higher CN consistently increases the brake fuel efficiency of both engines. This is in contrast, to the medium load condition, where increasing the CN of the fuel increases the brake fuel efficiency of the light duty engine, but causes a slight decrease in the brake fuel efficiency of the medium duty engine.

Theory of energy balance

An internal combustion (IC) engine is an open thermodynamic system, thus enabling the tracking of mass, energy and entropy transfers between the system (i.e., the engine) and the surroundings. For the purposes of this study, the control system is assumed to be steady-state, thus not undergoing changes to mass, energy, or entropy. The control system and the associated energy transfer are shown in **Figure 42**.

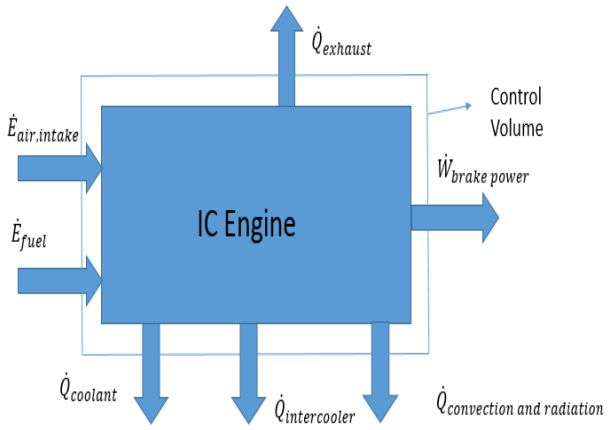

Figure 42 Control volume under study showing various energy transfers between the system (IC engine) and its surroundings. System is assumed to be in steady-state, thus not undergoing changes in mass, energy, or entropy.

The application of the first law of thermodynamics for the steady-state control system is given as Equation 1:

$$\dot{E}_{fuel} + \dot{E}_{air,intake} = \dot{W}_{brake\ power} + \dot{Q}_{coolant} + \dot{Q}_{exhaust} + \dot{Q}_{surf} + \dot{Q}_{intercooler} \quad (1)$$

where $\dot{E}_{fuel}$ is the energy supplied by the fuel, $\dot{E}_{air,intake}$is intake air energy, $\dot{W}_{brake\ power}$ is the output energy delivered by the engine, $\dot{Q}_{coolant}$ is heat rejected by coolant, $\dot{Q}_{exhaust}$ is energy removed as exhaust mass flow rate, and $\dot{Q}_{surf}$ is convection and radiation to the surroundings.

The energy supplied by the fuel is:

$$\dot{E}_{fuel} = \dot{m}_{fuel} * Q_{LHV} \quad (2)$$

where $\dot{m}_{fuel}$ is mass fuel flow rate and Q_{LHV} is the lower fuel heating value.

The intake air energy is:

$$\dot{E}_{air,intake} = \dot{m}_{air} * h_{air}(\mathrm{T}) \quad (3)$$

where $\dot{m}_{air}$ is mass air flow rate and h_{air} is the enthalpy of the air.

Since air is a mixture of numerous gases with disparate properties, the corresponding mixture enthalpy on a per mass basis must be calculated from the following:

$$h_{mix} = \frac{1}{MW_{mix}} * \sum_{i=1}^{mix} X_i \bar{h}_i \quad (4)$$

where MW_{mix} is the mixture's average is molecular weight, $X_i$is the mole fraction of a constitutive gas and $\bar{h}_i$ is the corresponding molar enthalpy.

The output energy delivered by the engine can be calculated directly from the measured dyno torque and engine speed:

$$\dot{W}_{brake\ power} = 2\pi * T_{dyn} * N \quad (5)$$

where T_{dyn} is the measured dyno torque and N is engine speed.

The heat rejected by coolant is:

$$\dot{Q}_{coolant} = \dot{m}_c * C_c * \Delta\ T_c \quad (6)$$

where $\dot{m}_c$ is the mass flow rate of coolant, C_c is the mass specific heat of the coolant and $\Delta\ T$ is the coolant temperature difference across the control system.

Similar to the intake air, the exhaust energy transfer rate is:

$$\dot{Q}_{exhaust} = \dot{m}_{exh} * h_{exh}(T) \tag{7}$$

where $\dot{m}_{exh}$ is the mass exhaust flow rate and h_{exh} is the enthalpy of the exhaust. With the steady state assumption, the mass exhaust flow rate is:

$$\dot{m}_{exh} = \dot{m}_{fuel} + \dot{m}_{air,intake} \tag{8}$$

The surface heat loss is assumed to the total of convective and radiative components:

$$\dot{Q}_{surf} = \dot{Q}_{conv} + \dot{Q}_{rad} \tag{9}$$

The radiative heat transfer is calculated using the Stefan Boltzmann equation [65]:

$$\dot{Q}_{rad} = \frac{\sigma}{\frac{1}{\varepsilon_{surf}} + \frac{1}{\varepsilon_{surr}} - 1} A_{surf}[\left(T_{surf}\right)^4 - (T_{surr})^4] \tag{10}$$

where σ is the Stefan-Botlzmann constant, ε is the emissivity of the surface or surroundings, A_{surf} is the estimated surface area, and all temperatures are in Kelvin.

The steady state convective heat transfer rate can be calculated using Newton's law of cooling [65]:

$$Q_{conv} = \bar{h}_{conv} A_{surf}(T_{surf} - T_{\infty}) \tag{11}$$

The intercooler heat transfer is:

$$\dot{Q}_{intercooler} = \dot{m}_{intercooler} * (h_{in} - h_{out}) \tag{12}$$

where $\dot{m}_{intercooler}$ is mass flow rate of air and h_{in} and h_{out} are enthalpies of air mixture at the inlet and outlet.

Moreover, the cylinder heat transfer is expressed as:

$$\frac{\delta Q}{d\varphi} = h_g * \mathrm{A} * (T_g - T_w) \quad (13)$$

And according to Woschni's correlation [66]:

$$h_g = C_0 * [B^{-0.2} * P^{0.8} \left(\left(C_1 * V_{mp} \right) + C_2 * \frac{V_d * T_1}{P_1 * V_1} (P - P_m) \right)^{0.8} * T^{-0.53} \quad (14)$$

where P_1, V_1 and T_1 are reference state properties, such as at intake valve closure (IVC); P_m is the motored in-cylinder pressure, B is the cylinder bore, P is the cylinder pressure, T is the cylinder temperature and $V_d$is the cylinder volume

Results and Discussions

The energy balance of the two engines is evaluated for the same combustion phasing. This isolates combustion phasing effects from engine size effects. One way to match the combustion phasing is to adjust the injection timing independently for each engine so that the crank angle 50% burn (CA50%) locations are the same. This methodology was applied in this study. The CA 50% locations were matched for both engines, for both load points (BMEP 1.88 and 5.65 bar), and for both fuels. CA 50% was reached at 10°ATDC. The uncertainty of the experimental data corresponds to 95% confidence and considers repeat measurements of the same conditions over different days.

Cylinder heat transfer and net indicated thermal efficiencies

As discussed, engine heat transfer is an important component of the overall engine energy balance. The heat transfer from the engine mostly emanates from the heat

transfer between the combustion gases and cylinder walls. Higher combustion and mixture gas temperatures result in a larger temperature gradient between the mixture gas and cylinder walls, which leads to an increase in cylinder heat transfer. Generally lower mixture temperatures and lower rates of heat release result in lower cylinder heat transfer.

Figure 43 and Figure 44 show the mixture gas temperature with respect to the 8 test conditions. Please note these temperatures are calculated assuming ideal gas behavior and using measured in-cylinder pressure and calculated cylinder volume (from measured crankshaft angular location). At low load, Figure 43 shows that the high CN fuel results in lower peak mixture gas temperatures, but maintains a more constant mixture gas temperature over the duration of the combustion event. This results in a slight reduction in the heat transfer to cylinder walls. Figure 4 shows that this effect is particularly significant for the medium duty engine when operating at medium load. The high CN fuel results in significantly cooler combustion and leads to lower cylinder heat transfer in the medium duty engine.

The overall rate of cylinder heat transfer, as a fraction of the total fuel energy for the 8 test conditions are shown in the left-hand panel of Figure 45. The LD engine transfers more fuel energy through cylinder heat transfer than the MD engine. Likewise, the fraction of fuel energy leaving as heat transfer through the cylinders decreases as load increases for both engines. With the exception of the MD engine operating under medium load, the overall fractional cylinder heat transfer is relatively insensitive to changes in CN. At the low load condition, the lower bulk gas temperature on high CN

fuel results in directionally lower cylinder heat transfer for both engines. In contrast, a statistically significant change is seen for the MD engine at the medium load condition, where heat transfer to the cylinders decreases by approximately 2.5%. This observation is likely due to the tradeoff between changes in mixture gas temperature, and burn duration.

The right-hand panel of Figure 45 shows the burn duration of the fuels at the 8 operating conditions. The burn duration of both fuels is always longer in the MD engine than in the LD engine, and the burn duration is always longer at the medium load condition, than at the light load condition. By increasing the CN, the burn duration of the fuels increases and this is true for both the LD and MD engines at both load points. This can be explained by a reduction in premixed burn.

The heat release rate (HRR) curves for the 8 test conditions, as shown in Figure 46, also demonstrate the changes in the cylinder heat transfer processes. At the medium load condition, the impact of increasing the CN on the HRR is larger than at the low load condition. Increasing CN leads to a dual-stage HRR in the MD engine, which results in a significant decrease in heat release magnitude.

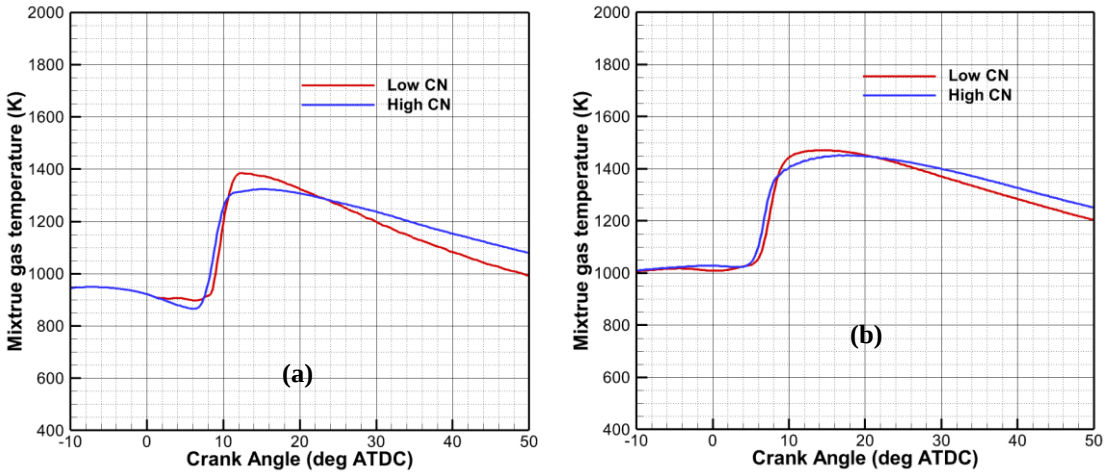

Figure 43 Mixture gas (i.e., bulk) temperature between the two different CN fuels with a) medium duty engine and b) light duty engine operating at the same CA50 location, and low load condition (effected through different injection timings)

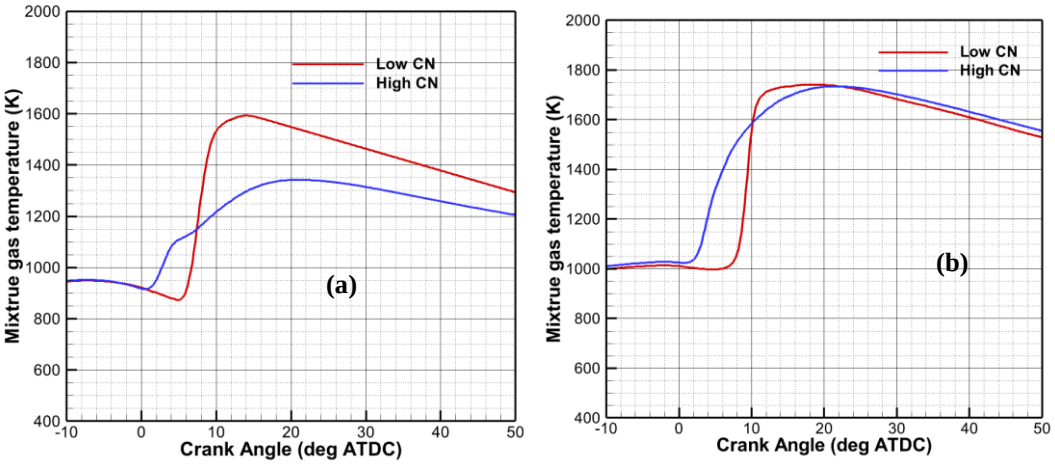

Figure 44 Mixture gas (i.e., bulk) temperature between the two different CN fuels with a) medium duty engine and b) light duty engine operating at the same CA50 location, and medium load condition (effected through different injection timings)

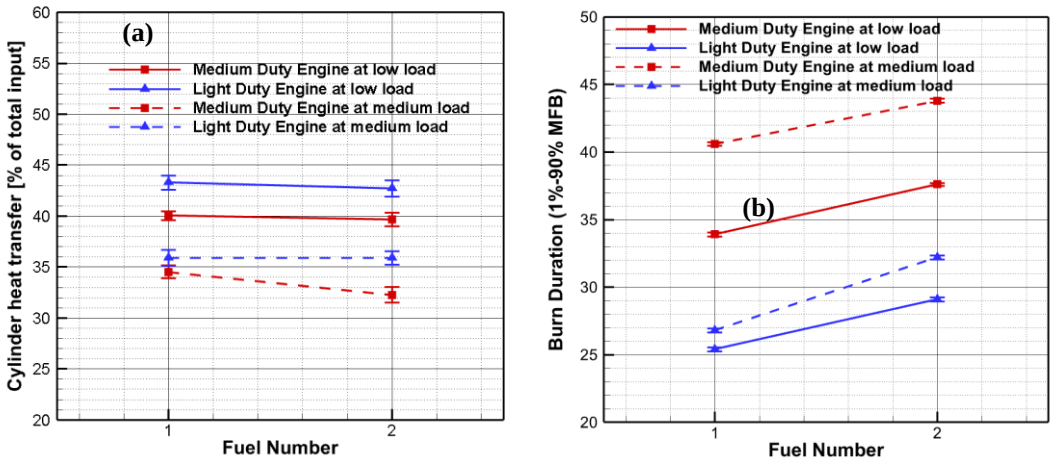

Figure 45 Comparison of a) cylinder heat transfer, and b) 1% - 90% burn duration between the two different CN fuels at the two load conditions operating with same CA50 location (effected through different injection timings).

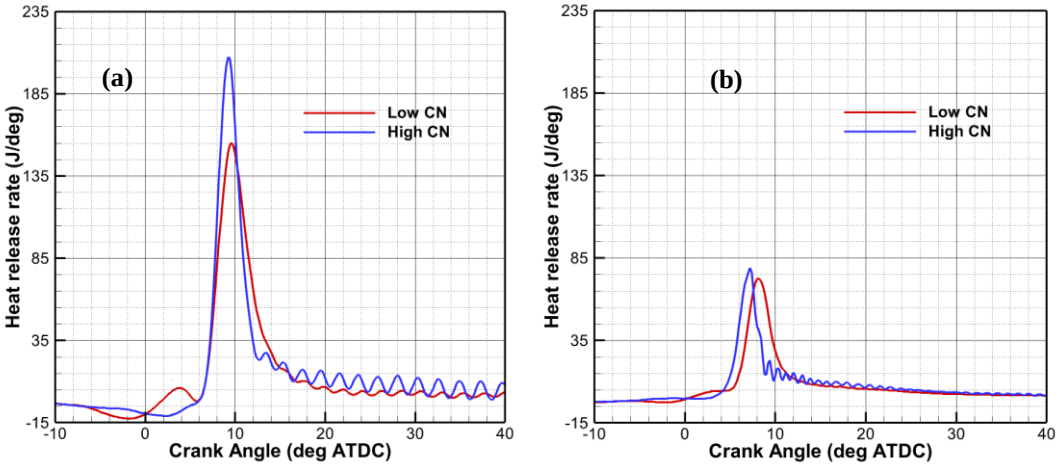

Figure 46 Heat release rate between the two different CN fuels with a) medium duty engine and b) light duty engine operating at the same CA50 location, and low load condition (effected through different injection timings)

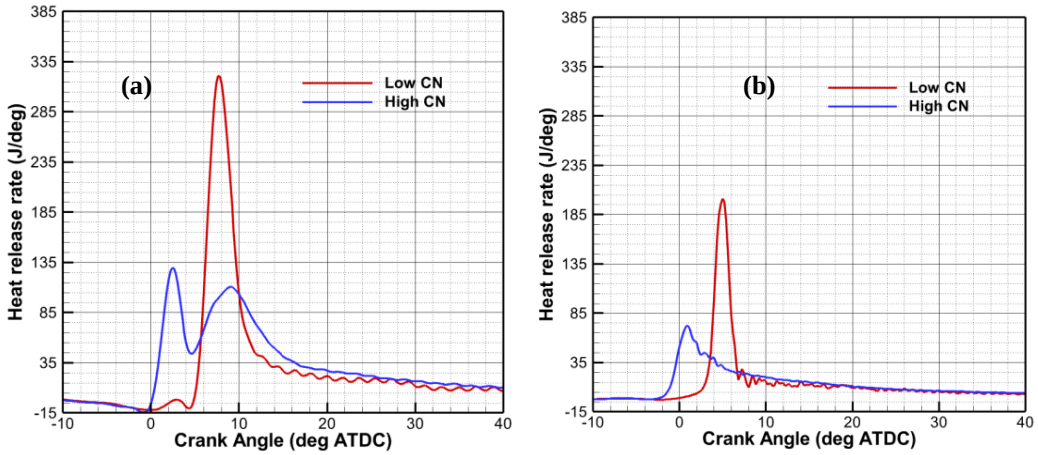

Figure 47 Heat release rate between the two different CN fuels with a) medium duty engine and b) light duty engine operating at the same CA50 location, and medium load condition (effected through different injection timings).

Coolant heat transfer

Figure 48 shows the coolant heat transfer for the 8 test conditions. Similar to the trends observed for the cylinder heat transfer, the LD engine transfers more fuel energy through coolant heat transfer than the MD engine. Similarly, the fraction of fuel energy leaving as coolant heat transfer decreases as the load increases for both engines. The heat transferred to the coolant in the LD engine appears to be insensitive to the change in CN. In contrast, the heat transferred to the coolant of the MD engine undergoes a significant decrease at both for the low and medium load conditions, as CN is increased.

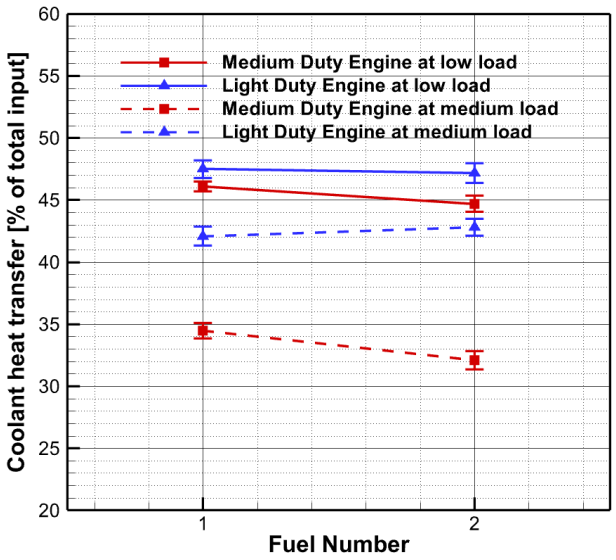

Figure 48 Comparison of coolant heat transfer between the two different CN fuels at the two load conditions operating with same CA50 location (effected through different injection timings)

Surface and intercooler heat transfer

The surface and intercooler heat transfer is calculated with respect to equations (9 – 11). The surface and intercooler heat transfer rates for the 8 test conditions are shown in Figure 49. The behavior of the surface heat transfer rate is similar to the trends observed for the cylinder and coolant heat transfer rates. Both the surface and intercooler heat transfer rates appear to be statistically insensitive to changes in CN. The exception to this is the surface heat transfer of the MD engine operating at medium load, where directionally, a decrease in heat transfer is seen as CN is increased.

Comparing the magnitude of the intercooler heat transfer rate to the other heat transfer processes reveals that it is smallest contributor to the overall energy balance.

Previous studies [67] have shown that the intercooler heat transfer rate is mainly impacted by the boost condition. As the boost pressure was kept constant at 1 bar for both engines, at both two load conditions, it is unsurprising that CN has no effect on the rate of intercooler heat exchange.

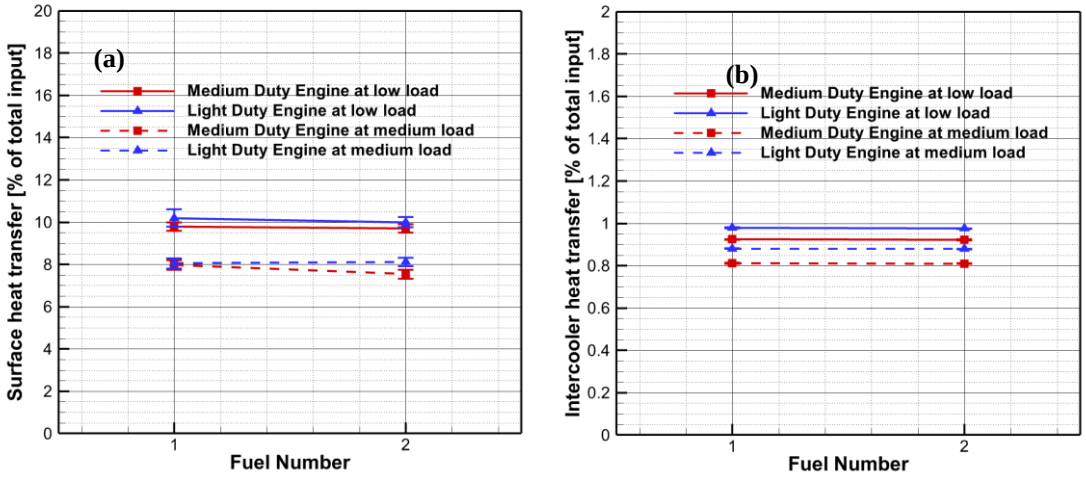

Figure 49 Comparison of a) surface heat transfer and b) intercooler heat transfer between the two different CN fuels at the two load conditions operating with same CA50 location (effected through different injection timings)

Exhaust Energy and Temperature

As described with Equation 6, exhaust energy transfer is calculated using the exhaust temperature, and knowledge of the exhaust species (i.e., thermal energy and chemical energy of the exhaust). The exhaust temperatures of the 8 test conditions are shown in (Figure 50).

Directionally, increasing the CN increases the exhaust temperature for both engines at the two loads. It should be noted that this effect is larger at medium load, and is only significant for the LD engine operating under medium load. The change in exhaust temperature can be partially explained by the results of Figure 2, where increasing the CN resulted in relatively higher mixture gas temperatures when the exhaust valves open. This appears correlated to higher exhaust energy transfer.

The calculated exhaust energy transfer rates as a fraction of total fuel energy for the 8 test conditions are shown in Figure 51. Directionally, increasing the CN slightly increases the exhaust energy transfer of both engines at the medium load condition. At the low load condition, increasing the CN directionally increases the exhaust energy transfer of the MD engine, but has no significant effect of the exhaust energy transfer of the LD engine. These trends appear correlated to the observations for the exhaust temperature.

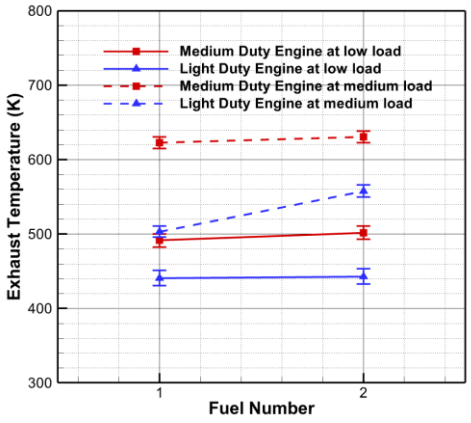

Figure 50 Exhaust temperatures of the two different CN fuels at the two load conditions operating with same CA50 location (effected through different injection timings)

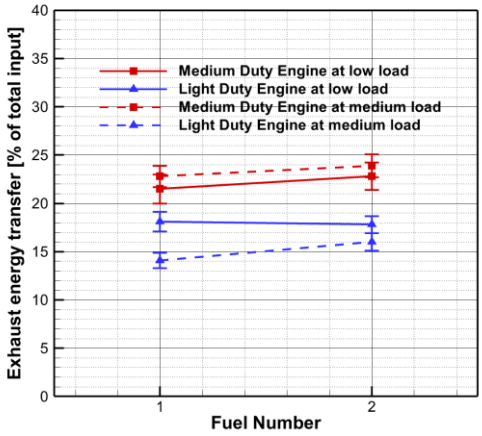

Figure 51 Comparison of exhaust energy fraction between the two different CN fuels at the two load conditions operating with same CA50 location (effected through different injection timings).

Brake Fuel Conversion Efficiency

The brake fuel conversion efficiency is a function of net indicated thermal efficiency, combustion efficiency, and mechanical efficiency, where each term is defined separately below:

- The net indicated thermal efficiency represents the efficiency of the collected thermodynamic processes, and additionally includes the pumping portion of the mechanical cycle. It is defined as the indicated power, divided by the released fuel energy

- The combustion efficiency quantifies the extent of heat release, and is defined as the released fuel energy divided by the delivered fuel energy.
- The mechanical efficiency indicates the mechanical translation of the thermodynamic indicated work to mechanical brake work, and is simply the brake power divided by the net indicated power.

Ultimately the brake fuel conversion efficiency is the power delivered by the engine divided by the delivered fuel energy.

The brake fuel conversion efficiencies for the 8 test conditions is shown in Figure 52.

At low load, increasing the CN of the fuel increases the brake fuel conversion efficiency for both engines. At medium load, increasing the CN increases brake fuel conversion efficiency of the LD engine, but causes a slight decrease in the brake fuel conversion efficiency of the MD engine.

As discussed, the overall brake fuel conversion efficiency is impacted by the indicated efficiency and the combustion efficiency. The indicated efficiencies of the engines were quantified through the cylinder heat transfer processes (Figure 2), while the combustion efficiencies for the 8 test conditions are compared in Figure 52(b).

At low load, increasing the CN of the fuel increases the combustion efficiency of both engines. At medium load, increasing the CN of the fuel increases the combustion efficiency of the LD engine, but has little impact on the combustion efficiency of the MD engine. The magnitude of the impact that CN has on the combustion efficiency as a function of load appears to be variable. CN appears to have a larger effect on the

combustion efficiency at low load conditions. At low load, combustion efficiency changes by over 4 percent for the MD engine, while it changes by just under 2 percent for the LD engine, as the CN of the fuel is increased. In contrast, combustion efficiency at the medium load condition changes by only 0.2 percent for the medium engine, while it changes by as little as 0.15 percent for the LD engine, as the CN of the fuel increases.

This performance can be attributed to various combustion characteristics with changing engine sizes. Specifically, the compression ratio for the MD engine, which is slightly lower which causes temperatures and pressures to be lower, resulting in a longer ignition delay. Hence, the ignition delay of low CN fuel when combusted in the MD engine at low load condition starts far away from TDC causing relatively lower combustion efficiency. With increasing engine load, the proportion of premixed combustion decreases, especially for MD engine with much longer burn duration [6]. Thus, the influence of CN on the combustion efficiency of the MD engine is less dependent on engine load.

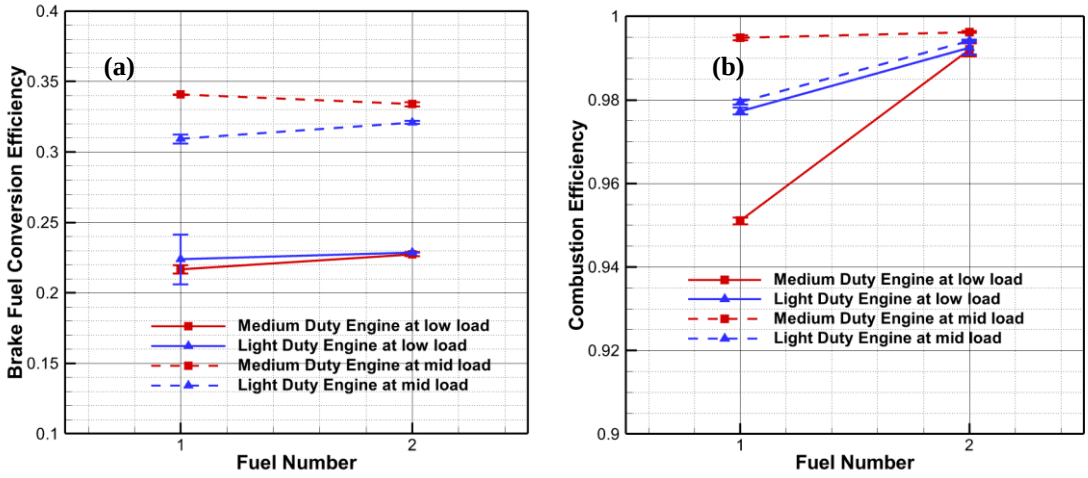

Figure 52 Comparison of a) brake fuel conversion efficiency and b) combustion efficiency between the two different CN fuels at the two load conditions operating with same CA50 location (effected through different injection timings)

Summary

The presented work has investigated the effects of CN on energy balance for both LD (1.9L) and MD (4.5L) compression ignition engines at both 1500 RPM and nominally 1.88 bar and 5.65 bar BMEP conditions. The two engines have similar a stroke to bore (S/B) ratio, and all other control parameters including: valve timing, injection timing, rail pressure and EGR rate, have been kept the same, meaning that only the displacement changes between the engine platforms. Two diesel fuels for advanced combustion engines (FACE) were studied. The two FACE fuels were selected to have a similar distillation profile and aromatic content, but varying CN. Results were recorded at the same crank angle 50% burn (CA50) condition to decouple fuel effects from engine

effects. The following conclusions were reached following the experimental results and analysis:

1. The fractional cylinder heat transfer is generally insensitive to changes in CN, except for the MD engine at medium load condition. This insensitivity appears to be caused by differing effects of CN on mixture gas temperature and combustion duration. Because of a decrease in heat release rate with in the high CN fuel being combusted in the MD engine at medium load, the mixture gas temperature drops more than combustion duration increases leading to a decrease in the heat transfer fraction.

2. The coolant and surface heat transfer also appear insensitive to CN aside from the MD engine at the medium-load condition.

3. The intercooler heat transfer does not change with increasing CN for both engines on the two load conditions.

4. Increasing CN increases exhaust energy transfer for both engines at medium load. At low load, increasing CN increases the exhaust energy loss of the MD engine, but decreases the exhaust energy loss of the LD engine. This performance appears to be caused by changing exhaust temperatures when CN changes. At medium load exhaust temperatures are larger, resulting in an increase of exhaust energy loss.

5. For both engines, increased CN consistently increases brake fuel conversion efficiency at low load. At medium load, increasing the CN of the fuel increases the brake fuel conversion efficiency of the LD engine at but causes a slight decrease in brake fuel conversion efficiency for the MD engine.

5.4 Results and discussion for effect of T90 on combustion and emissions between different duty engines

We investigate the effects of T90 on the combustion characteristics and emissions by using experimental data for a sweeping injection timing (15° before top dead center (BTDC) to 3° BTDC) at low load and medium load conditions (1.88 and 5.65 bar BMEP, respectively) between the MD and LD engines. Moreover, for isolating combustion phasing effects from engine size effects, matching the 50% burn location for both engines, loads, and fuels, to equal 10°ATDC are studied either. The uncertainty was calculated for the experimental data corresponding to 95% confidence and includes repeatability of the measurements of the same operating conditions on different days.

Heat Release Rate

Figure 53(a) shows heat release rate (HRR) with crank angle for both engines and fuels at low load while Figure 53(b) shows the same at mid load. Comparing with MD engine performance, increasing T90 shows relative stronger effects on HRR for LD engine, especially for low load condition. In details, at low load condition, high T90 fuel has earlier combustion start timing than low T90 fuel on LD engine, but has similar performance with low T90 fuel on MD engine. The reason is that with increasing T90, the injection timing of LD engine is advanced from 3° BTDC to 5.5° BTDC, but the injection timing of MD engine is kept at the same value—6° BTDC. At medium load condition, increasing T90 does not show obvious effect on MD engine, but slightly advances HRR on LD engine.

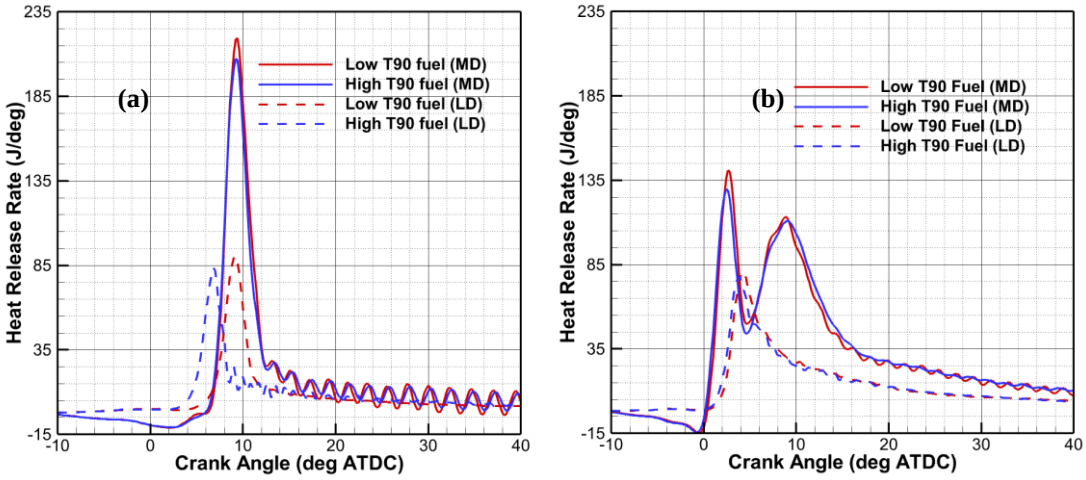

Figure 53 Heat release rate of the two studied T90 fuels of a) low load and b) medium load operating at the same CA50 location (effected through different injection timings)

Ignition Delay

Figure 54 plots the change in ignition delay with respect to changing T90 for both the low and medium load conditions of the two engines. Increasing T90 decreases ignition delay (defined as time between start of injection and 1% mass fraction burned location) for LD engine at both load conditions, but does not show any obvious effect on MD engine. It was also noticed that the difference in the LD engine's ignition delay at low load condition, due to changing T90, was larger than difference at medium load condition. In details, the ignition delay of LD engine at the low load condition (12° BTDC injection timing) changed by over 2 crank angle degrees, while it changed by less than 0.5 crank angle degrees at medium load condition, as the fuel was changed from the low to high T90 fuel.

The variations in ignition delay of the two T90 fuel under the 4 test conditions are compared in Table 21. Different with the observe performance at the same injection timings, increasing T90 does not impact the ignition delay strongly for both engines. The magnitude of the change due to increasing T90 in ignition delay decreases with increasing engine load for LD engine. It should be noted that for the matched MFB50% location, injection timings are adjusted to different values. This result in different mixture temperatures of the studied conditions, and mean that the ignition delays presented in Table 21 cannot be directly compared to those in Figure 54.

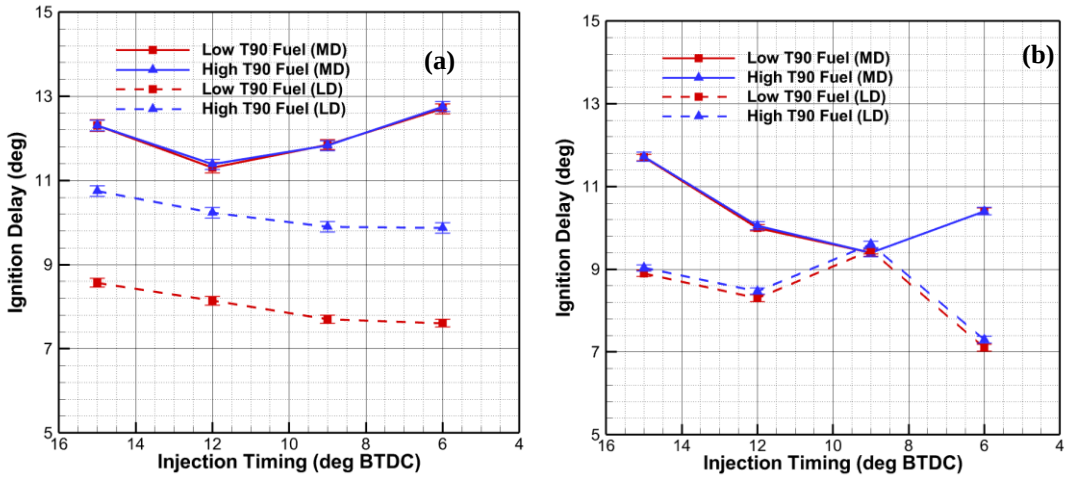

Figure 54 Ignition Delay for the MD and LD engines at a) low load and b) medium load conditions with the two studied T90 fuels as functions of injection timing.

Table 26 Ignition delay for the two engines at the same CA50 location, low and mid load conditions (effected through different injection timings)

	Low load	Medium load
MD engine	12.7/12.7 (low 90/high T90) (deg)	9.4/9.4 (low T90/high T90) (deg)
LD engine	9/9.7 (low T90/high T90) (deg)	9.45/9.6 (low T90/high T90) (deg)

Mass Fraction Burned

Figure 55 shows the MFB curves with the two fuels at the matched 50% MFB location for both the low and medium load conditions and both engines. Similar to the observe HRR performance, with the exception of the LD engine operating under low load, the MFB is relatively insensitive to changes in T90. For LD engine under low load condition, an increase in T90 advanced combustion phasing and increased the

combustion duration. This corresponds to the advanced injection timing of high T90 fuel for LD engine at low load, shown in Table 2.

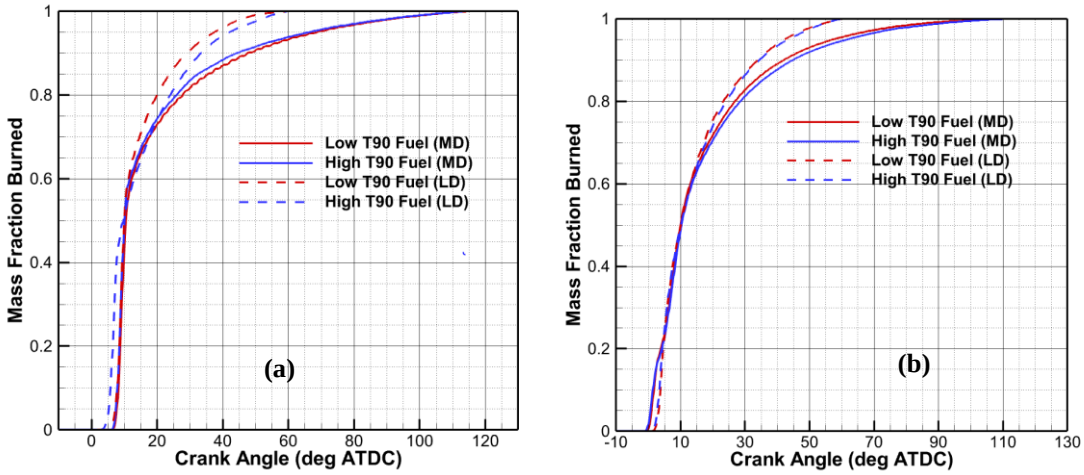

Figure 55 Mass fraction burned profiles for the MD and LD engines at a) low load and b) medium load conditions with the two studied T90 fuels.

Figure 56(a) shows 50% MFB location (CA50) with injection timings for both engines and fuels at low load while Figure 56(b) shows the same at mid load. Increasing T90 delays CA50 location for LD engine at both load conditions, but does not show any obvious effect on MD engine. Moreover, the influence of T90 on CA50 location for LD engine is also impacted by load conditions: increasing load decreases the effect of T90 on CA50 location. The reason is that although an increasing in T90 results shorter ignition delay, the burn rate is decreased either. Slower burn rate for high T90 fuel results relative delayed CA50 location on LD engine for both load conditions. With increasing engine load, the burn duration is longer and the proportion of premixed

combustion is decreased, which results smaller burn rate difference between two T90 fuels, finally resulting smaller difference of CA50 between two T90 fuels for LD engine.

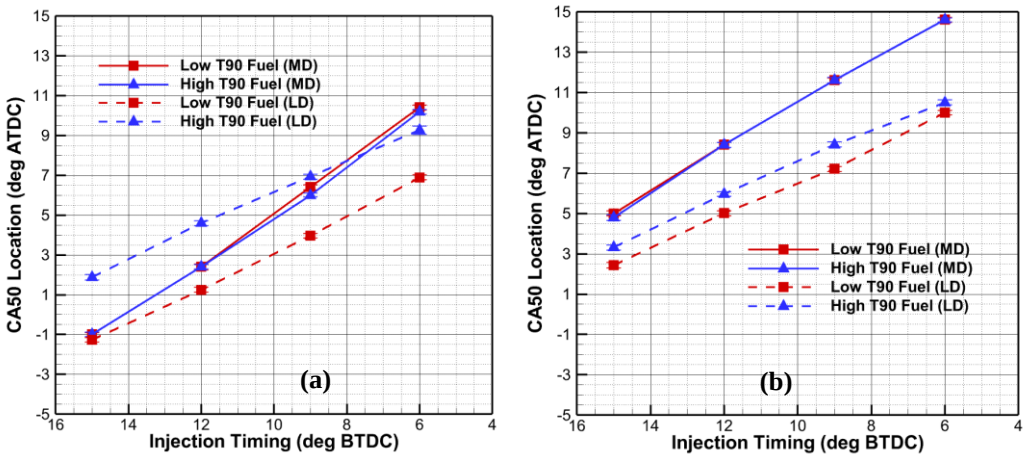

Figure 56 CA50 locations for the MD and LD engines at a) low load and b) medium load conditions with the two studied T90 fuels as functions of injection timing.

Combustion Efficiency

The variations in combustion efficiency with respect to the two fuels at the test conditions are compared in Figure 57. Increasing T90 shows different effects on combustion efficiency of the two engines at low load condition: higher T90 fuel has higher combustion efficiency on MD engine, but lower combustion efficiency on LD engine. At medium load condition, the combustion efficiency is relatively insensitive to changes in T90 for both engines.

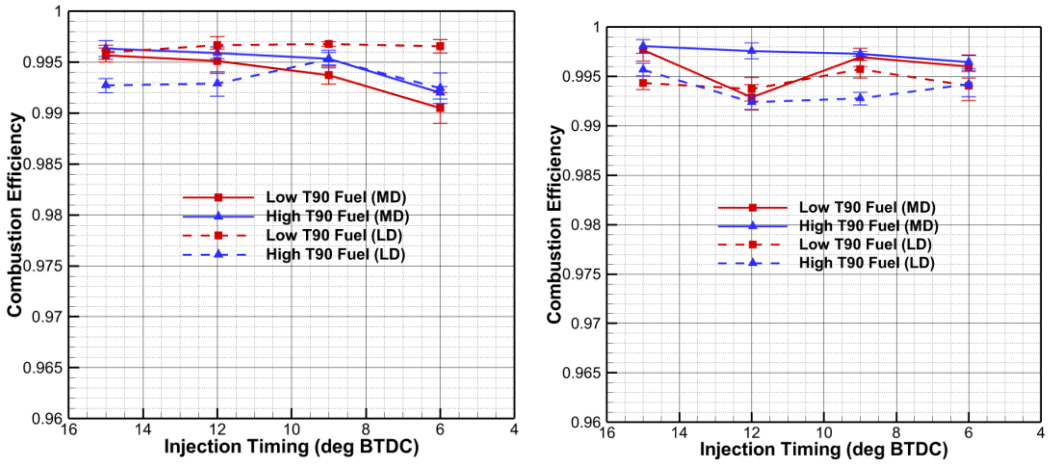

Figure 57 Combustion Efficiency for the MD and LD engines at a) low load and b) medium load conditions with the two studied T90 fuels as functions of injection timing

Brake Specific Nitrogen Oxides

Figure 58 shows the brake specific nitrogen oxides (BSNOx) emissions with respect to the two fuels, the two conditions, and the two engines at the same injection timing. Comparing with MD engine, the BSNOx of LD engine was more sensitive for changes in T90. In details, at low load condition, the high T90 fuel results in lower NOx emissions on LD engines, but similar performance of BSNOx on MD engines. At the medium load condition, the effect of T90 on BSNOx is smaller: an increasing in T90 increases BSNOx on LD engine for most test points, but decreases the BSNOx on MD engine slightly.

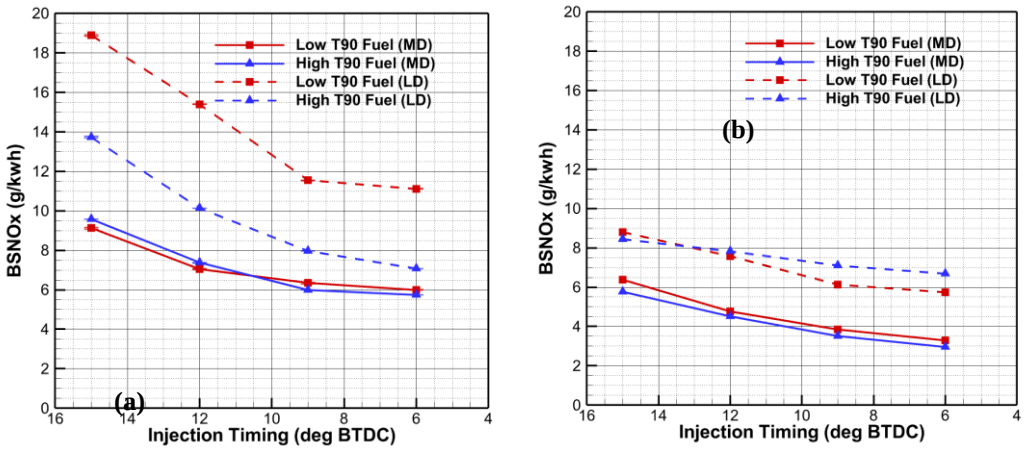

Figure 58 BSNOx for the MD and LD engines at a) low load and b) medium load conditions with the two studied T90 fuels as functions of injection timing

Filter Smoke Number

Figure 59 shows the filter smoke number (FSN) with respect to the two fuels at the low and medium load conditions for both engines at the same injection timing. At low load, high T90 results higher FSN for both engines. Another thing be noted that for all the test conditions, the FSN is very small (lower than 0.2). This implies that FSN is very sensitive to changing in-cylinder conditions, such as the local A/F ratio etc. At the medium load condition, increasing the T90 increases smoke number on both engines for most testing points and has stronger effects on LD engine. Moreover, FSN is effectively the opposite of NOx emissions. A high combustion temperature will lead to a lower FSN, while a low combustion temperature will lead to a higher FSN. It follows that the

advancing injection timing generated a higher FSN for both engines at medium load condition.

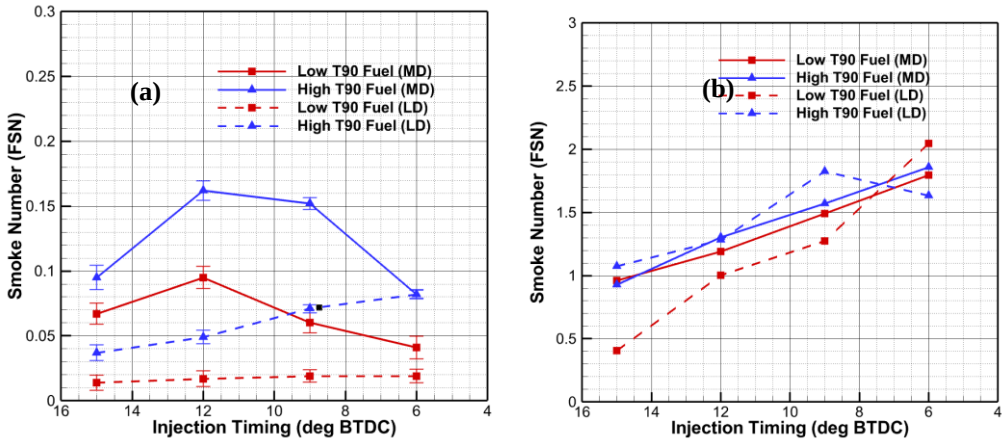

Figure 59 Smoke number for the MD and LD engines at a) low load and b) medium load conditions with the two studied T90 fuels as functions of injection timing

Brake Specific Hydrocarbon

Figure 60 shows brake specific hydrocarbon (BSHC) emissions with respect to the two fuels, at the low and medium load conditions, and for both engines. Generally, higher combustion efficiency results in lower HC emissions. As the high T90 had different performance on combustion efficiency, HC emissions are different either with increasing T90 between two engines at low load condition (this matches the trends presented in Figure 57). Increasing T90 increased HC emissions on LD engine, but decreased HC emissions on MD engine. At medium load condition, the effect of T90 on

HC was relative smaller. Different T90 fuels showed similar HC emissions results on the two engines.

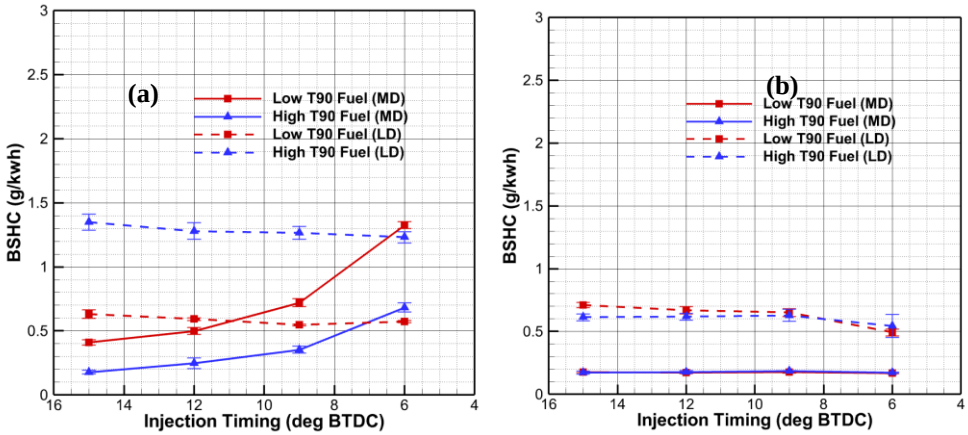

Figure 60 BSHC for the MD and LD engines at a) low load and b) medium load conditions with the two studied T90 fuels as functions of injection timing

5.5 Results and discussion for effect of Aromatic Content on combustion and emissions between different duty engines

We investigate the effects of aromatic content on the combustion characteristics and emissions by using experimental data for a sweeping injection timing (15° before top dead center (BTDC) to 3° BTDC) at low load and medium load conditions (1.88 and 5.65 bar BMEP, respectively) between the MD and LD engines. Moreover, for isolating combustion phasing effects from engine size effects, matching the 50% burn location for both engines, loads, and fuels, to equal 10°ATDC are studied either. The uncertainty was calculated for the experimental data corresponding to 95% confidence and includes repeatability of the measurements of the same operating conditions on different days.

Heat Release Rate

Figure 61 (a) shows heat release rate (HRR) with crank angle for both engines and fuels at the same injection timing, low load while Figure 61 (b) shows the same at mid load. Increasing aromatic content has similar influence on the two engines. In details, increasing aromatic content increases the magnitude of the peak HRR, and delays its location for both engines at low load condition. At medium load condition, increasing aromatic content has similar effect on LD engine, but does not show obvious effect on MD engines. Moreover, it is also noticed that the effect of aromatic content is impacted by load condition: increasing load decrease effect of aromatic content on HRR for both engines.

Figure 62 (a) and (b) show the HRR for the two studied fuels at the same 50% mass fraction burn location, at the low and medium load conditions for both engines. Contrary to the matched injection timing data of Figure 61, increasing the aromatic content does not show obvious effect on both engines at low load condition. At mid load condition, increasing aromatic content has relative stronger effect on LD engine, which increases the magnitude of the peak HRR, and delays its location.

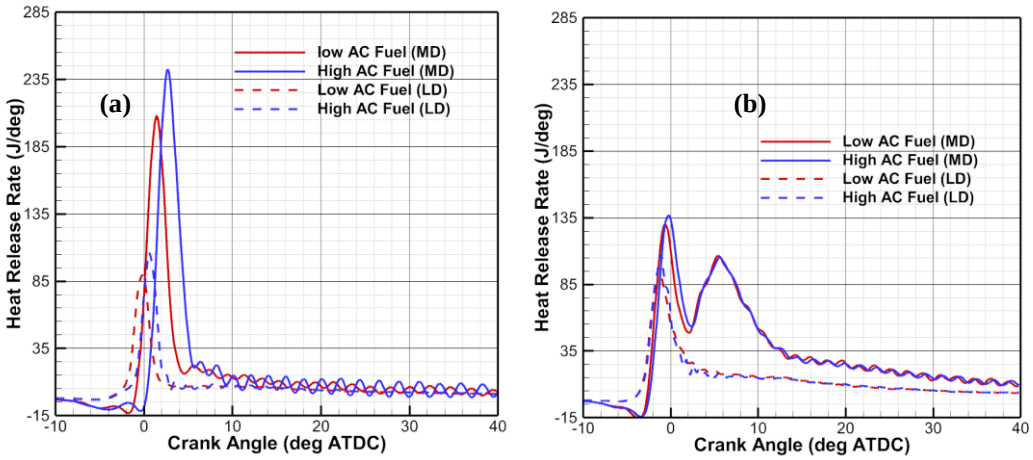

Figure 61 Heat release rate of the two studied AC fuels of a) low load and b) medium load operating at the same injection timing

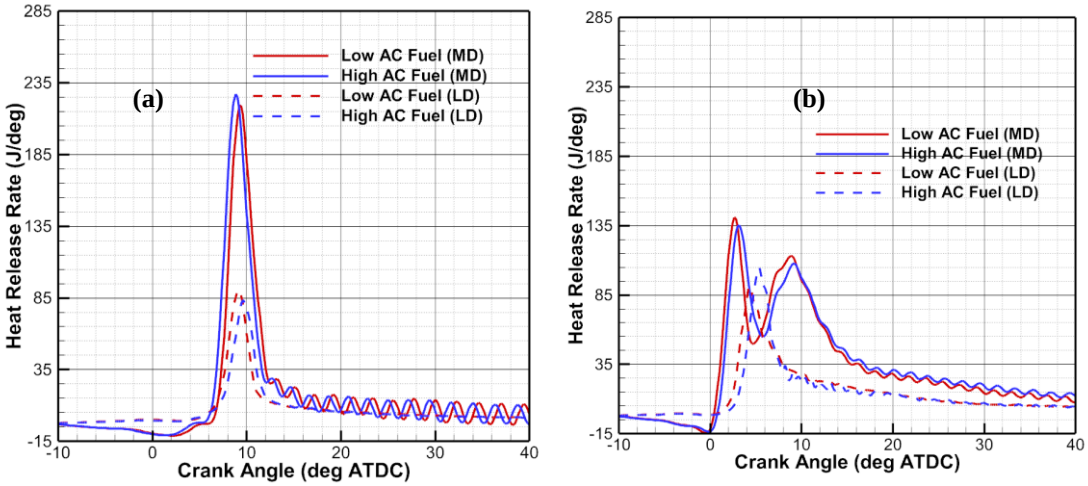

Figure 62 Heat release rate of the two studied AC fuels of a) low load and b) medium load operating at the same CA50 location (effected through different injection timings)

Ignition Delay

Figure 54 plots the change in ignition delay with respect to changing aromatic content for both the low and medium load conditions of the two engines. Increasing aromatic content increases ignition delay (defined as time between start of injection and 1% mass fraction burned location) for LD engine at the two load conditions, but just shows the same effect for MD engine at low load condition. It was also noticed that the difference in the LD engine's ignition delay at low load condition, due to changing aromatic content, was larger than difference at medium load condition. In details, the ignition delay of LD engine at the low load condition (12° BTDC injection timing) changed by over 2 crank angle degrees, while it changed by less than 0.2 crank angle degrees at medium load condition, as the fuel was changed from the low to high aromatic content fuel.

The variations in ignition delay of the two aromatic content fuels under the 4 test conditions are compared in Table 21. Different with the observe performance at the same injection timings, increasing aromatic content does not impact the ignition delay strongly for both engines.

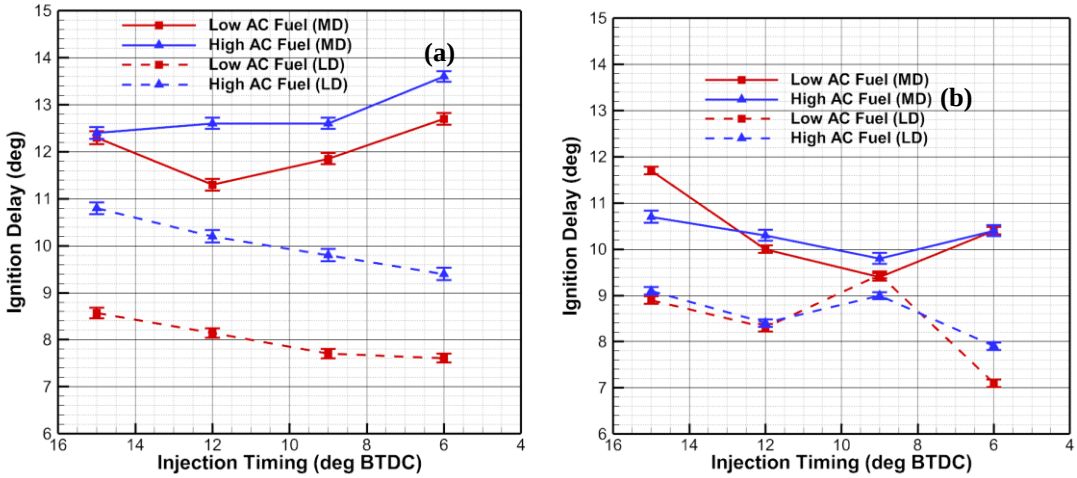

Figure 63 Ignition Delay for the MD and LD engines at a) low load and b) medium load conditions with the two studied AC fuels as functions of injection timing.

Table 27 Ignition delay for the two engines at the same CA50 location, low and mid load conditions (effected through different injection timings)

	Low load	Medium load
MD engine	12.7/12.5 (low AC/high AC) (deg)	9.4/9.3 (low AC/high AC) (deg)
LD engine	9/9.1 (low AC/high AC) (deg)	9.45/9.7 (low AC/high AC) (deg)

Mass Fraction Burned

Figure 55 shows the MFB curves with the two fuels at the same injection timing (12 deg BTDC) for both the low and medium load conditions and both engines. A decrease in aromatic content advances combustion phasing and increases the combustion duration of both engines at low load conditions, but does not show obvious effect at mid load condition. This agrees with HRR and ignition delay characteristics discussed above. Moreover, Figure 65 shows the MFB curves with the two fuels at the matched 50% MFB location for both the low and medium load conditions and both engines. The MFB curves with the two fuels at the matched 50% MFB location are very similar for both engines and loads.

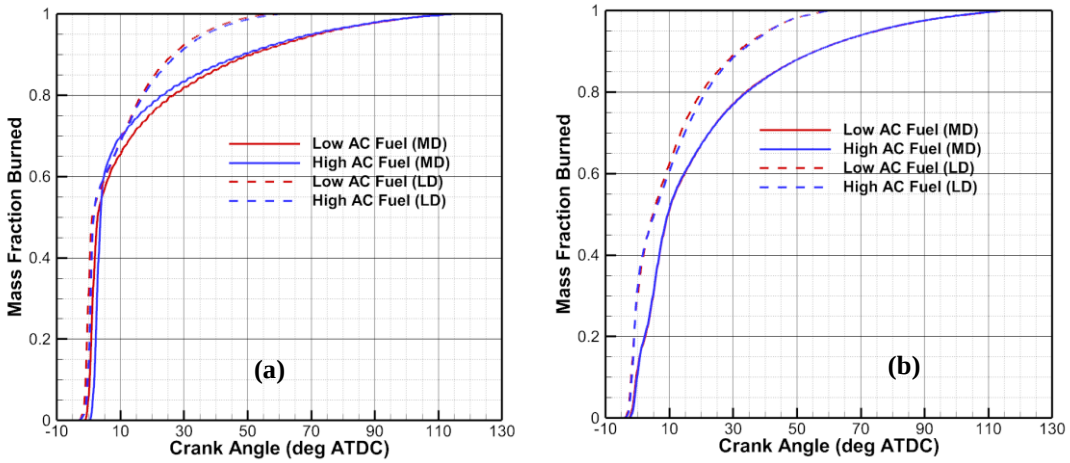

Figure 64 Mass fraction burned profiles for the MD and LD engines at a) low load and b) medium load conditions, the same injection timing with the two studied AC fuels.

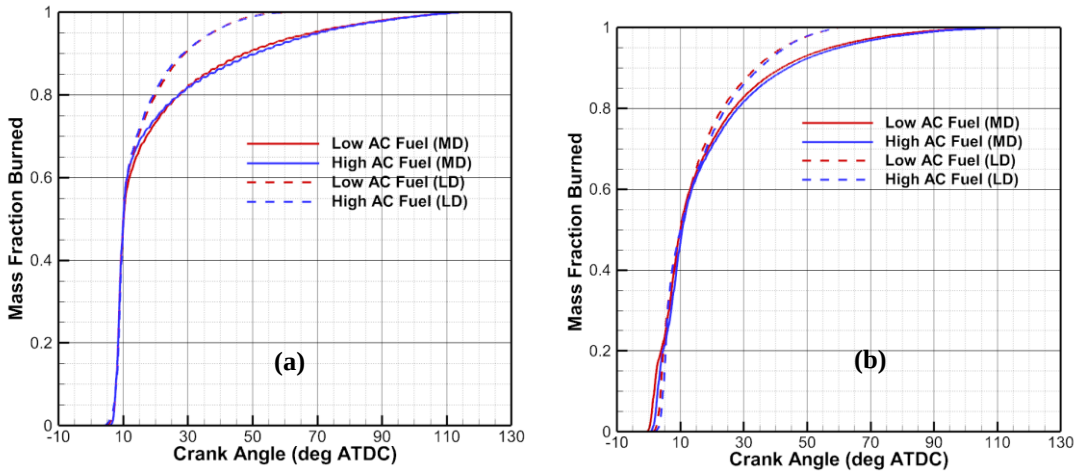

Figure 65 Mass fraction burned profiles for the MD and LD engines at a) low load and b) medium load conditions, the same CA50 location with the two studied AC fuels.

Figure 66(a) shows 50% MFB location (CA50) with injection timings for both engines and fuels at low load while Figure 66 (b) shows the same at mid load. Increasing aromatic content delays CA50 location for both engines at low load condition, but does not show any obvious effect for both engines at mid load condition. Moreover, the influence of aromatic content on CA50 location for MD engine is also impacted by injection timing: advancing injection timing increases the effect of aromatic content on CA50 location.

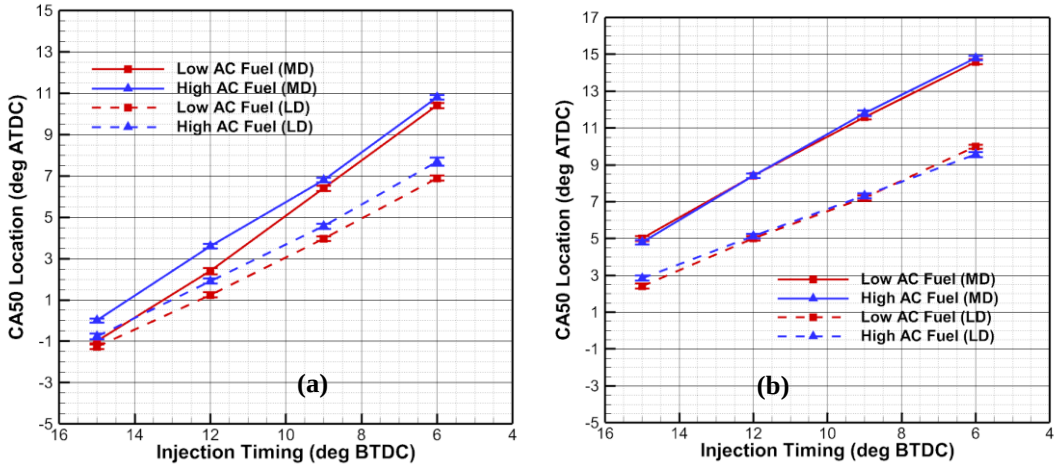

Figure 66 CA50 locations for the MD and LD engines at a) low load and b) medium load conditions with the two studied AC fuels as functions of injection timing.

Combustion Efficiency

The variations in combustion efficiency with respect to the two fuels at the test conditions are compared in Figure 67. Increasing aromatic content shows different effects on combustion efficiency for the two engines at the two load conditions: higher aromatic content decreases combustion efficiency for LD engine at the two load conditions, but does not show any obvious effect on MD engine.

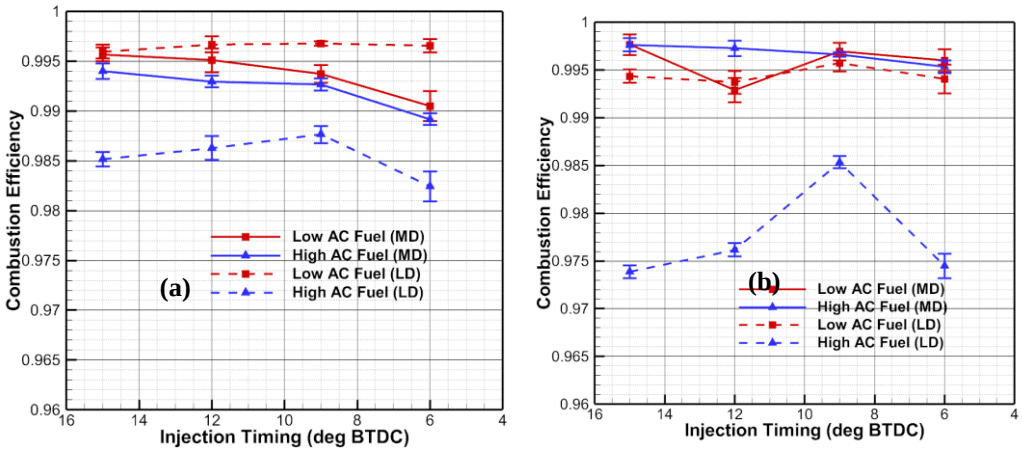

Figure 67 Combustion Efficiency for the MD and LD engines at a) low load and b) medium load conditions with the two studied AC fuels as functions of injection timing

Brake Specific Nitrogen Oxides

Figure 68 shows the brake specific nitrogen oxides (BSNOx) emissions with respect to the two fuels, the two conditions, and the two engines at the same injection timing. Increasing aromatic content increases BSNOx for both engines at low load condition, and shows similar performance on LD engine, but no obvious effect on MD engine at mid load condition, which with HRR, ignition delay and MFB characteristics discussed above. For high aromatic content fuel, longer ignition delay results higher HRR magnitude and faster burn rate, finally resulting higher reaction and bulk peak temperature. Higher bulk peak temperature is the reason of an increase in aromatic content. Moreover, the effect of aromatic content on HRR and ignition delay is

decreased by increasing engine load. Thus, the effect of aromatic content on BSNOx at mid load condition is relative smaller either.

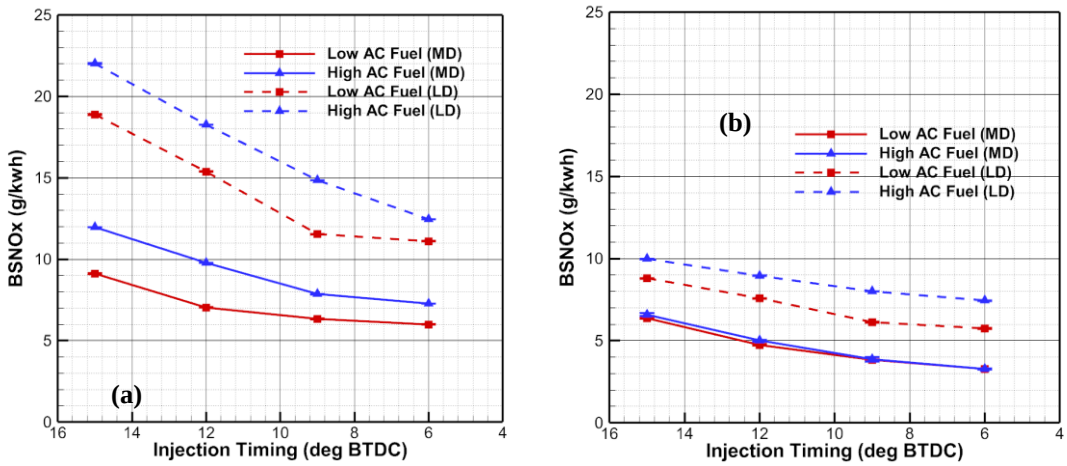

Figure 68 BSNOx for the MD and LD engines at a) low load and b) medium load conditions with the two studied AC fuels as functions of injection timing

Filter Smoke Number

Figure 69 shows the filter smoke number (FSN) with respect to the two fuels at the low and medium load conditions for both engines at the same injection timing. At low load, high aromatic content results higher FSN for LD engine, but lower FSN for MD engine. Another thing be noted that for all the test conditions, the FSN is very small (lower than 0.1). This implies that FSN is very sensitive to changing in-cylinder conditions, such as the local A/F ratio etc. At the medium load condition, increasing the aromatic content increases smoke number on MD engine, but decreases FSN on LD engine for most testing points. It is also noticed that the effect of aromatic content on

FSN is impacted by injection timing. Advancing injection timing decreases the effect of aromatic content on FSN. Moreover, FSN is effectively the opposite of NOx emissions. A high combustion temperature will lead to a lower FSN, while a low combustion temperature will lead to a higher FSN. It follows that the advancing injection timing generated a higher FSN for both engines at medium load condition.

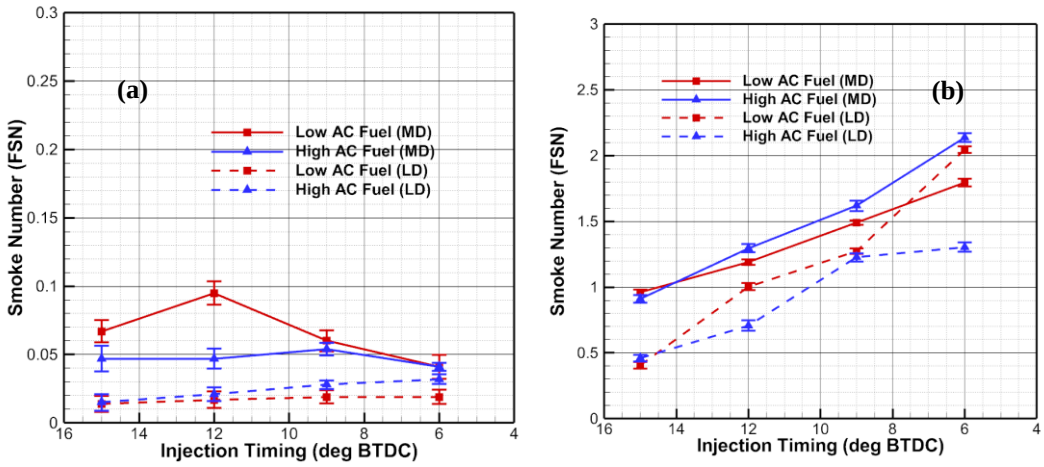

Figure 69 Smoke number for the MD and LD engines at a) low load and b) medium load conditions with the two studied AC fuels as functions of injection timing

Brake Specific Hydrocarbon

Figure 70 shows brake specific hydrocarbon (BSHC) emissions with respect to the two fuels, at the low and medium load conditions, and for both engines. Generally, higher combustion efficiency results in lower HC emissions. An increase in aromatic content increases BSHC for both engines, the two load conditions, and has relative

stronger effect on LD engine (this matches the trends presented in Figure 67). Moreover, the effect of aromatic content is impacted by engine load either. An increase in engine load decreases the effect of aromatic content on BSHC.

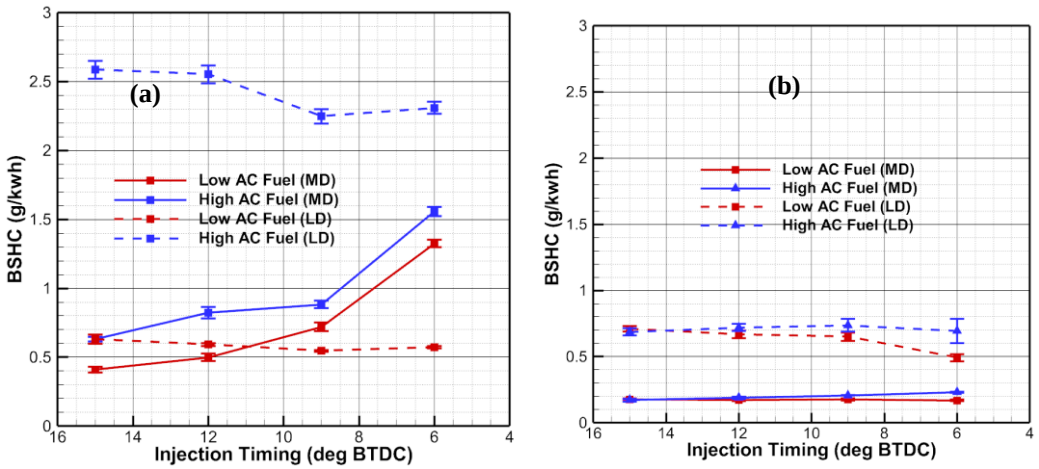

Figure 70 BSHC for the MD and LD engines at a) low load and b) medium load conditions with the two studied AC fuels as functions of injection timing

Brake Specific Carbon Monoxide

Figure 71 shows brake specific carbon monoxide (BSCO) emissions with respect to the two fuels, at the low and medium load conditions, and for both engines. Generally, BSCO is mainly impacted by air/fuel mixing conditions. Increasing aromatic content increases BSCO emissions for both engines at low load condition. At mid load condition, increasing aromatic content decreases BSCO emissions for LD engine, but does not show obvious effect for MD engine. Moreover, the effect of aromatic content

on BSCO is impacted by engine size either: LD engine has relative stronger aromatic content influence on BSCO.

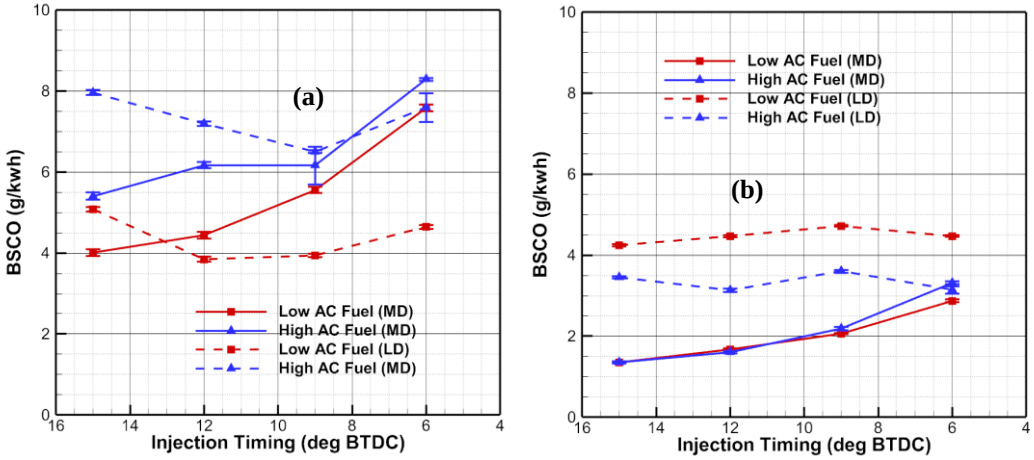

Figure 71 BSCO for the MD and LD engines at a) low load and b) medium load conditions with the two studied AC fuels as functions of injection timing

6. CONCLUSIONS

6.1 Cetane Number

1. For any given injection timing, the magnitude of HRR increases and its location advances as CN increases for both engines. This result is expected. In the context of different engine sizes, it is noted that a distinctive dual-stage HRR process was often observed at the mid load condition for the MD engine and high CN fuel resulting in longer combustion durations. This result did not, however, translate to observable effects in other portions of the study (i.e., effect on efficiency or emissions).

2. Although the HRR characteristics with matched 50% MFB locations follow those at low load when injection timing is the same, they are quite different at medium load. Specifically, HRR still tends to be advanced with high CN fuel, but much lower magnitude (hence, longer combustion duration). The reason being that ignition delay of the high CN fuel is shorter, establishing a smaller fraction of premixed heat release and larger fraction of diffusion heat release. These differences create different sensitivities of the engines to the fuels, as concluded below.

3. The LD engine's combustion efficiency (i.e., extent of heat release) demonstrates high sensitivity to CN. This high sensitivity causes the LD engine's indicated fuel conversion efficiency, BSNOx, and FSN to trend differently at medium load than at low load condition or as compared to the medium duty engine. Such behavior, along with the differing combustion characteristics, suggest the need for careful consideration of CN on engine efficiency and emissions depending on the engine size.

6.2 Distillation Temperature

1. Comparing with MD engine performance, increasing T90 shows relative stronger effects on HRR for LD engine, especially for low load condition. Similarly, increasing T90 decreases ignition delay for LD engine at both load conditions, but does not show any obvious effect on MD engine.

2. Increasing T90 delays CA50 location for LD engine at both load conditions, but does not show any obvious effect on MD engine. Moreover, the influence of T90 on CA50 location for LD engine is also impacted by load conditions: increasing load decreases the effect of T90 on CA50 location.

3. Comparing with MD engine, the BSNOx of LD engine was more sensitive for changes in T90. At the medium load condition, increasing the T90 increases smoke number on both engines for most testing points and has stronger effects on LD engine. At low load condition, increasing T90 increased HC emissions on LD engine, but decreased HC emissions on MD engine. At medium load condition, the effect of T90 on HC was relative smaller. Different T90 fuels showed similar HC emissions results on the two engines.

6.3 Aromatic Content

1. At low load condition, increasing aromatic content increases the magnitude of the peak HRR, and delays its location for both engines. At medium load condition, increasing aromatic content has similar effect on LD engine, but does not show obvious effect on MD engines.

2. A decrease in aromatic content advances combustion phasing and increases the combustion duration of both engines at low load conditions, but does not show obvious effect at mid load condition.

3. Increasing aromatic content shows different effects on combustion efficiency for the two engines at the two load conditions: higher aromatic content decreases combustion efficiency for LD engine at the two load conditions, but does not show any obvious effect on MD engine.

4. Increasing aromatic content increases BSNOx for both engines at low load condition, and shows similar performance on LD engine, but no obvious effect on MD engine at mid load condition. For smoke number, increasing the aromatic content increases smoke number on MD engine, but decreases FSN on LD engine for most testing points at mid load condition. For HC emissions, an increase in aromatic content increases BSHC for both engines, the two load conditions, and has relative stronger effect on LD engine.

7. FUTURE WORK

Based on the study of baseline testing, the effect of engine size on combustion and engine behavior are clarified. Moreover, the effect of cetane number on combustion, emissions and energy balance between different sized-engines are clarified either through FACE fuel matrix testing. According to objectives in section 3, the effect of distillation temperature (T90) and aromatic content on combustion and engine behavior between different sized-engines need to be analyzed.

Thus, the future work includes two main parts:

1) Explain the influence of multi-injection strategy on CN effect on medium duty engine efficiency and emissions.

2) With increasing engine size, explain the effect of CN additive on engine combustion and emissions.

REFERENCES

1. Amann, M., T.W. Ryan, and N. Kono, HCCI Fuels Evaluations-Gasoline Boiling Range Fuels, 2005, SAE International.
2. Zhong, S., et al., Experimental Investigation into HCCI Combustion Using Gasoline and Diesel Blended Fuels, 2005, SAE International.
3. Risberg, P., et al., Auto-ignition quality of Diesel-like fuels in HCCI engines, 2005, SAE International.
4. Szybist, J.P. and B.G. Bunting, Cetane Number and Engine Speed Effects on Diesel HCCI Performance and Emissions, 2005, SAE International.
5. Bunting, B.G., et al., Fuel chemistry and cetane effects on diesel homogeneous charge compression ignition performance, combustion, and emissions. International Journal of Engine Research, 2007. **8**(1): p. 15-27.
6. Heywood, J.B., Internal Combustion Engine Fundamentals1988: McGraw-Hill, Inc.
7. Benajes, J., et al., Influence of Boost Pressure and Injection Pressure on Combustion Process and Exhaust Emissions in a HD Diesel Engine, 2004, SAE International.
8. Tao, F., et al., Modeling the Effects of EGR and Injection Pressure on Soot Formation in a High-Speed Direct-Injection (HSDI) Diesel Engine Using a Multi-Step Phenomenological Soot Model, 2005, SAE International.
9. Ogawa, H., et al., Characteristics of Diesel Combustion in Low Oxygen Mixtures with Ultra-High EGR, 2006, SAE International.
10. Li, T., et al., Characterization of Low Temperature Diesel Combustion with Various Dilution Gases, 2007, SAE International.
11. Filipi, Z. and D. Assanis, The Effect of the Stroke-To-Bore Ratio on Combustion, Heat Transfer and Efficiency of a Homogeneous Charge Spark Ignition Engine of Given Displacement. International Journal of Engine Research, 2000. **1**(2): p. 191-208.

12. Yamin, J.A.A. and M.H. Dado, Performance simulation of a four-stroke engine with variable stroke-length and compression ratio. Applied Energy, 2004. **77**(4): p. 447-463.
13. Thornhill, D., et al., An Experimental Investigation into the Effect of Bore/Stroke Ratio on a Simple Two-Stroke Cycle Engine, 1999, SAE International.
14. Altin, İ., İ. Sezer, and A. Bilgin, Effects of the Stroke/Bore Ratio on the Performance Parameters of a Dual-Spark-Ignition (DSI) Engine†. Energy & fuels, 2008. **23**(4): p. 1825-1831.
15. Wittek, K., C. Tiemann, and S. Pischinger, Two-Stage Variable Compression Ratio with Eccentric Piston Pin and Exploitation of Crank Train Forces. SAE Int. J. Engines, 2009. **2**(1): p. 1304-1313.
16. Bilgin, A., Geometric features of the flame propagation process for an SI engine having dual-ignition system. International Journal of Energy Research, 2002. **26**(11): p. 987-1000.
17. Kleeberg, H., et al., Increasing Efficiency in Gasoline Powertrains with a Two-Stage Variable Compression Ratio (VCR) System, 2013, SAE International.
18. Aceves, S.M., et al., Piston-Liner Crevice Geometry Effect on HCCI Combustion by Multi-Zone Analysis, 2002, SAE International.
19. Dong, J., et al., Study on Variable Combustion Chamber (VCC) Engines, 2012, SAE International.
20. Dong, J., et al., Effect of Design Features on Dynamic Characteristics of VCC Piston for I. C. Engine. SAE Int. J. Engines, 2013. **6**(1): p. 209-216.
21. Hyvönen, J., C. Wilhelmsson, and B. Johansson, The Effect of Displacement on Air-Diluted Multi-Cylinder HCCI Engine Performance, 2006, SAE International.
22. Shi, Y. and R.D. Reitz, Study of Diesel Engine Size-Scaling Relationships Based on Turbulence and Chemistry Scales, 2008, SAE International.
23. Shi, Y. and R.D. Reitz, Assessment of Optimization Methodologies to Study the Effects of Bowl Geometry, Spray Targeting and Swirl Ratio for a Heavy-Duty

Diesel Engine Operated at High-Load. SAE Int. J. Engines, 2008. **1**(1): p. 537-557.

24. Staples, L.R., R.D. Reitz, and C. Hergart, An Experimental Investigation into Diesel Engine Size-Scaling Parameters. SAE Int. J. Engines, 2009. **2**(1): p. 1068-1084.
25. Ge, H.-W., et al., Coupling of Scaling Laws and Computational Optimization to Develop Guidelines for Diesel Engine Down-sizing, 2011, SAE International.
26. Shi, L., K. Deng, and Y. Cui, Study of diesel-fuelled homogeneous charge compression ignition combustion by in-cylinder early fuel injection and negative valve overlap. Proceedings of the Institution of Mechanical Engineers, Part D: Journal of Automobile Engineering, 2005. **219**(10): p. 1193-1201.
27. Nevin, R.M., et al., PCCI Investigation Using Variable Intake Valve Closing in a Heavy Duty Diesel Engine, 2007, SAE International.
28. Stager, L.A. and R.D. Reitz, Assessment of Diesel Engine Size-Scaling Relationships, 2007, SAE International.
29. Musculus, M., et al., End-of-injection over-mixing and unburned hydrocarbon emissions in low-temperature-combustion diesel engines. 2007.
30. Takahashi, K., et al., Effects of Cetane Number and Chemical Components on Diesel Emissions and Vehicle Performance, 2009, SAE International.
31. Kumar, S., et al., The Effect of Diesel Fuel Properties on Engine-out Emissions and Fuel Efficiency at Mid-Load Conditions, 2009, SAE International.
32. Gallant, T., et al., Fuels for Advanced Combustion Engines Research Diesel Fuels: Analysis of Physical and Chemical Properties. SAE Int. J. Fuels Lubr., 2009. **2**(2): p. 262-272.
33. Ryskamp, R., Thompson, G., Carder, D., and Nuszkowski, J., "The Influence of High Reactivity Fuel Properties on Reactivity Controlled Compression Ignition Combustion," SAE Technical Paper 2017-24-0080, 2017.

34. Waqas, M., Naser, N., Sarathy, M., Morganti, K. et al., "Blending Octane Number of Ethanol in HCCI, SI and CI Combustion Modes," SAE Int. J. Fuels Lubr. 9(3):659-682, 2016
35. Hosseini, V., et al., Effects of Cetane Number, Aromatic Content and 90% Distillation Temperature on HCCI Combustion of Diesel Fuels, 2010, SAE International.
36. De Ojeda, W., et al., Impact of Fuel Properties on Diesel Low Temperature Combustion. SAE Int. J. Engines, 2011. **4**(1): p. 188-201.
37. Bonsack, P., et al., Number Concentration and Size Distributions of Nanoparticle Emissions during Low Temperature Combustion using Fuels for Advanced Combustion Engines (FACE), 2014, SAE International.
38. Schweitzer, P.H., Penetration of Oil Sprays. Journal of Applied Physics, 1938. **9**(12): p. 735-741.
39. Wakuri, Y., et al., Studies on the Penetration of Fuel Spray in a Diesel Engine. Bulletin of JSME, 1960. **3**(9): p. 123-130.
40. DENT.J, SAE Int. J. Engines, 1971: p. SAE Paper No.710571.
41. Dent, J.C., P.S. Mehta, and J. Swan. A predictive model for automotive DI diesel engine performance and smoke emissions. in IMechE. 1982.
42. Hiroyasu, H. and M. Arai, Structures of Fuel Sprays in Diesel Engines, 1990, SAE International.
43. Bao, Y., et al., A Comparative Analysis on the Spray Penetration of Ethanol, Gasoline and Iso-Octane Fuel in a Spark-Ignition Direct-Injection Engine, 2014, SAE International.
44. Murphy, L. and D. Rothamer, Effects of Cetane Number on Jet Fuel Combustion in a Heavy-Duty Compression Ignition Engine at High Load, 2011, SAE International.
45. Aradi, A.A. and T.W. Ryan, Cetane Effect on Diesel Ignition Delay Times Measured in a Constant Volume Combustion Apparatus, 1995, SAE International.

46. Butts, R.T., et al., Investigation of the Effects of Cetane Number, Volatility, and Total Aromatic Content on Highly-Dilute Low Temperature Diesel Combustion, 2010, SAE International.
47. Azetsu, A., Y. Satao, and Y. Wakisaka, Effects of Aromatic Components in Fuel on Flame Temperature and Soot Formation in Intermittent Spray Combustion in International Spring Fuels & Lubricants Meeting, JSAE, Editor 2003, SAE International: Yokohama, Japan.
48. Rosenthal, M.L. and T. Bendinsky, The Effects of Fuel Properties and Chemistry on the Emissions and Heat Release of Low-Emission Heavy Duty Diesel Engines, 1993, SAE International.
49. Ullman, T.L., K.B. Spreen, and R.L. Mason, Effects of Cetane Number on Emissions From a Prototype 1998 Heavy-Duty Diesel Engine, 1995, SAE International.
50. Green, G.J., et al., Fuel Economy and Power Benefits of Cetane-Improved Fuels in Heavy-Duty Diesel Engines, 1997, SAE International.
51. Canaan, R.E., et al., The Influence of Fuel Volatility on the Liquid-Phase Fuel Penetration in a Heavy-Duty D.I. Diesel Engine, 1998, SAE International.
52. Ryan, T.W., et al., The Effects of Fuel Properties on Emissions from a 2.5gm NOx Heavy-Duty Diesel Engine, 1998, SAE International.
53. Tamanouchi, M., et al., Effects of fuel properties and oxidation catalyst on exhaust emissions for heavy-duty diesel engines and diesel passenger cars, in SAE International Congress and Exposition1998, SAE International: Detroit, Michigan.
54. Kidoguchi, Y., C. Yang, and K. Miwa, Effects of Fuel Properties on Combustion and Emission Characteristics of a Direct-Injection Diesel Engine, 2000, SAE International.
55. Kee, S.-S., et al., Effects of Aromatic Hydrocarbons on Fuel Decomposition and Oxidation Processes in Diesel Combustion, 2005, SAE International.

56. Sluder, C.S., et al., Fuel Property Effects on Emissions from High Efficiency Clean Combustion in a Diesel Engine, 2006, SAE International.
57. Eckerle, W.A., et al., Effects of methyl ester biodiesel blends on NOx emissions. SAE International Journal of Fuels and Lubricants, 2009. **1**(SAE Paper No. 2008-01-0078): p. 102-118.
58. Li, X., <Effects of fuel cetane number, density and aromatic content on diesel engine NOx emissions at different operating conditions.pdf>. 2008.
59. Warey, A., et al., Fuel Effects on Low Temperature Combustion in a Light-Duty Diesel Engine, 2010, SAE International.
60. Nishiumi, R., et al., Effects of Cetane Number and Distillation Characteristics of Paraffinic Diesel Fuels on PM Emission from a DI Diesel Engine, 2004, SAE International.
61. Technologies, G., GT- Suit Engine Performance Application Manual, 2012. p. 106.
62. Jeihouni, Y., et al., Relationship between Fuel Properties and Sensitivity Analysis of Non-Aromatic and Aromatic Fuels Used in a Single Cylinder Heavy Duty Diesel Engine, 2011, SAE International.
63. Lancaster, D.R., R.B. Krieger, and J.H. Lienesch, Measurement and analysis of engine pressure data. SAE Transactions, 1975. **84**(SAE Paper No. 750026): p. 155-172.
64. Patton, K.J., R.G. Nitschke, and J.B. Heywood, Development and evaluation of a friction model for spark-ignition engines1989. Medium: X; Size: Pages: (21 p).
65. Incropera, F.P., et al., Fundamentals of heat and mass transfer2011: Wiley.
66. Woschni, G., A universally applicable equation for the instantaneous heat transfer coefficient in the internal combustion engine. SAE paper 670931. SAE Trans, 1967. **76**: p. 3065.
67. Penny, M.A. and T.J. Jacobs, Efficiency improvements with low heat rejection concepts applied to diesel low temperature combustion. International Journal of Engine Research, 2015.